Developing a droplet microfluidic platform for making double emulsions towards manufacturing polymersomes

by

Sepehr Ghadami

A thesis

presented to the University of Waterloo

in fulfillment of the

thesis requirement for the degree of

Master of Applied Science

in

Mechanical and Mechatronics Engineering

Waterloo, Ontario, Canada, 2020

Author's Declaration

I hereby declare that I am the sole author of this thesis. This is a true copy of the thesis, including any required final revisions, as accepted by my examiners.

I understand that my thesis may be made electronically available to the public.

Abstract

In recent years, there has been growing interest in the use of double emulsions in various industries such as pharmaceutical, foods, and cosmetics. Polymersomes are one of the promising applications of double emulsions that are being increasingly used in drug delivery to carry and release a specific dose of the drug. The efficacy of using polymersomes for controlled release of drugs is significantly dependent on the monodispersity and size generated double emulsions. Over the past few years, microfluidics technology has been used to produce double emulsions with high throughput and precision. Single-step, two-step and tandem methods are among the most common techniques that are being used for generation of water/oil/water (w/o/w) or oil/water/oil (o/w/o) emulsions. However, the existing methods have not yet addressed the challenges in the field. In this work, we present a microfluidic design to produce double emulsions with high monodispersity in addition to high control over the thickness of the middle phase. The presented design also solves the challenge of surface modification of microchannels which usually adds complexity to the existing methods. Moreover, in this project, a thorough guideline is provided to design an optimized platform for producing double emulsions with different sizes. Finally, we successfully show how such double emulsions can be used for generation of polymersomes by extraction of the organic component.

Acknowledgments

Pursuing my MASc at the University of Waterloo in Canada was a true privilege for me. I would like to thank my supervisor, Professor Carolyn Ren, an exceptional individual both in academic and life matters. I learned a lot from her and owe her a great deal of my professional development in that past two years. She made me believe in myself and have confidence in the work I do, something I will never forget.

I would also like to acknowledge all my friends and colleagues; I've worked with at the University of Waterloo. The opportunities I had to share ideas and knowledge with them were critical for making the progress and outcomes. I would like to thank Dr. Anna (Anna) Hoang Anh Thu Nguyen for her support and help. During last year, she helped me a lot to learn and improve my knowledge in microfluidics and experimental fluid mechanics. Moreover, I would like to thank Mr. Matt Courtney for his suggestions and helps.

I would also like to thank Professor Juewen Liu for his support of my work and his grateful advises. I would also say thank you to the examining committee, Professor Sushanta Mitra and Professor Juewen Liu for their time and contributions.

In the end I would like to thank my Parents and friends, for their support.

TABLE OF CONTENTS

Author's Declaration ii

Abstract iii

Acknowledgments iv

List of Figures vii

Chapter 1: Introduction: 1

Chapter 2: Literature review 5

2.1 Polymersome: 5

2.1.1 Mechanism of Polymersome Formation: 6

2.1.2 Polymersome morphology: 7

2.1.3 Conventional techniques for polymersome formation 7

2.1.4 Microfluidics approach for polymersome formation: 11

2.2 Droplet Microfluidics: 13

2.2.1 Physics at droplets microfluidics: 14

2.2.2 Passive methods for droplet formation: 15

2.2.3 Breakup modes 19

2.2.4 Active methods for droplet formation: 21

2.2.5 Fluid instabilities: 23

2.3 Multiple emulsions: 24

2.3.1 Double emulsion formation using Microfluidics: 25

Chapter 3: Materials and fabrication 36

3.1 Microfabrication 36

3.2 Materials 37

3.2.1 Oil phase 38
3.2.2 Aqueous phase 38
3.3 Experimental setup 38
Chapter 4: Methodology and circuit analysis 40
4.1 Methodology 40
4.2 Design criteria 44
Chapter 5: Experimental design and results 53
5.1 Experimental procedure 53
5.2 Experimental data 58
5.3 Experimental Results and discussions 61
5.3.1 Characterizing chip I: 61
5.3.2 Investigating decoupling effect: 64
5.3.3 Characterizing chip II: 66
5.3.4 Dewetting and polymersome formation 75
Chapter 6: Conclusion and recommendations for future works: 78
6.1 Conclusion 78
6.2 Recommendations and future works 79
References: 81

List of Figures

Figure 1 – Number of published papers on microfluidics during past years**[1]** 1

Figure 2: Structure of a polymersome **[6]**..... 5

Figure 3 Two mechanisms of polymersome formation **[8]** 6

Figure 4 Different possible morphology of assembled diblock copolymers based on packing parameter**[11]**..... 7

Figure 5 Procedure of polymersome formation with controlled size using photolithography**[18]** 9

Figure 6 Polymersome and liposome formation using inkjet**[19]** 10

Figure 7 Polymersome formation using micromixer**[20]** 10

Figure 8 Polymersome formation after extraction of organic phase from double emulsions generated using microfluidics**[22]** 12

Figure 9 W/O/W Double emulsion formation using microfluidics**[23]**..... 12

Figure 10 Three different geometries utilized for droplet generation a) co-flow b) cross-flow c) flow-focusing**[24]** 16

Figure 11 Flow map of different regimes in a flow focusing based on capillary number a) threading b) jetting c) dripping d) tubing e) viscous displacement**[30]**..... 18

Figure 12 Different regimes in a flow-focusing a) squeezing b) Thread formation c) dripping d) jetting**[31]**..... 18

Figure 13 different droplet regimes in cross flow geometry**[34]**..... 19

Figure 14 Different breakup modes for different geometry of the droplet generator. breakup modes: a) squeezing b) dripping c) jetting d) tip-streaming e) tip-multi-breaking **[35]** 20

Figure 15 Three stages of droplet formation in squeezing regime**[36]**..... 20

Figure 16 Double (a), triple(b), quadruple(c), and quintuple(d) emulsions**[51]**..... 24

Figure 17 Multi-cored emulsions**[51]**..... 24

Figure 18 Janus emulsions**[51]** 25

Figure 19 Glass capillary microfluidics for double emulsion formation in two steps**[51][52]** 26

Figure 20 Glass capillary microfluidics for double emulsion formation in a single step**[51][52]** 26

Figure 21 Controlling the wettability of microchannels for double emulsion formation**[54]** 28

Figure 22 Using lithography-based microfluidics for double emulsion formation in two steps**[51][60]** 29

Figure 23 Using two T-junction for double emulsion formation**[51][56]** 29

Figure 24 Using two flow focusing for W/O/W double emulsion formation**[51][60]** 30

Figure 25 Using lithography-based microfluidics for double emulsion formation in a single step**[62][51]**..... 30

Figure 26 Using lithography-based microfluidics for double emulsion formation in single step**[61]** 31

Figure 27 Using tandem microfluidics for double emulsion formation**[63]**..... 31

Figure 28 Extraction of middle phase for formation of double emulsion**[64]**..... 32

Figure 29 Three possible morphology**[61]** 33

Figure 30 The process of liposome formation using surfactant **[66]**..... 34

Figure 31 On-chip dewetting using octane as the organic phase**[54]** 35

Figure 32 Procedure of microfabrication using soft lithography method [69] 37

Figure 33 Laboratory facilities**[69]**..... 39

Figure 34 Schematic of the design including first chip, tubing and the second chip 41

Figure 35 Schematic showing droplet generation in the first chip 42

Figure 36 Schematic showing double emulsion generation in the second chip 43

Figure 37 Electric circuit for the first and second chips 45

Figure 38 Schematic of the first chip..... 48

Figure 39 Schematic of single emulsions in the BJ channel..... 49

Figure 40 a) first chip and the second chip are mounted on a glass b) first and the second chip are connected via a tubing 54

Figure 41 Droplet splitting in the junction of the second chip due to high shear stress 55

Figure 42 Schematic of droplet generation in chip I..... 59

Figure 43 Schematic of double emulsion generation in chip II..... 60

Figure 44 Electric circuit of the first chip..... 62

Figure 45 Droplet generation with different sizes in the first chip..... 63

Figure 46 Volume ratio of generated inner droplet vs flow rate ratio in the first chip..... 63

Figure 47 Electric circuit of the first chip..... 64

Figure 48 Volume ratio of generated inner droplets versus flow rate ratio for two different sets of applied pressure in the second chip 66

Figure 49 a) single emulsions coming from the first chip with large and non-uniform spacing b) packing single emulsion using extraction channel to improve double emulsion formation..... 67

Figure 50 Single emulsions passing pillars when the applied pressure to the extraction channel is very low 68

Figure 51 Droplet generation in the first chip..... 69

Figure 52 Outlet of the first chip during droplet generation..... 70

Figure 53 Double emulsion generation with different thickness of the middle phase by changing the applied pressure to the extraction channel 70

Figure 54 The effect of flow rate ratio on the thickness of the middle phase in generated double emulsions 71

Figure 55 Extraction of single emulsions when the flow rate of the extraction channel is high b) Single emulsions are lined up, and the extraction of single emulsions are eliminated for a low flow rate of the extraction channel..... 72

Figure 56 Single emulsions coming from the first chip..... 73

Figure 57 Droplet generation in the first chip..... 73

Figure 58 Outlet of the first chip during droplet generation 74

Figure 59 Double emulsion generation with different thickness of the middle phase by changing the applied pressure to the extraction channel 74

Figure 60 The effect of flow rate ratio on the thickness of the middle phase in generated double emulsions 75

Figure 61 Partially dewetted double emulsions b) complete dewetted double emulsion [82] 76

Figure 62 Generated double emulsions in the outlet of the second chip 76

Figure 63 a) and b) generated double emulsions after dewetting c) enlarged image of generated double emulsions after dewetting 77

Chapter 1: Introduction:

Microfluidics is the science of manipulating small amount of fluids for a specific application. Over the past two decades, there has been growing interest in microfluidic technology. This can be confirmed by the increase in the number of publications from 2000 to 2013 **[1]**.

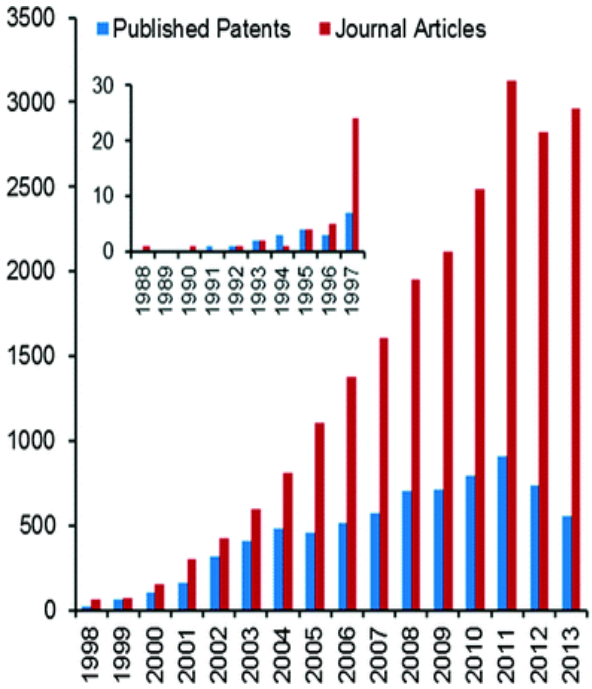

Figure 1 – Number of published papers on microfluidics during past years**[1]**

Nowadays, the focus of the field is to industrialize the microfluidic designs that are developed in the labs. Microfluidics has a lot of applications in biology and biomedical engineering (e.g. drug delivery and DNA analysis), industry and chemistry. Reduced environmental impact, better safety control, and low power consumption are some of the most crucial benefits of running experiments in microscale. Miniaturization of devices has another advantage of reducing the volume consumption of regents for running chemical and biological reactions. Moreover, in a microfluidics platform, all chemical or biological reactions can be done in series by the integration of microfluidic chips that are each responsible for one specific step. This integration is called Lab-on-a-chip (LOC) or Micro-Total-Analysis Systems (μTAS). Reducing the time required for running a specific chemical reaction or transporting a concentration dose, increasing the heat dissipation rate due to high surface area to volume ratio are two other advantages of microscale devices. In general, microfluidic systems can be divided into two different categories: single-phase

microfluidics and multiphase microfluidics, including two or more immiscible fluidic phases in contact such as aqueous-fluorous or liquid-gas phases.

Multiphase microfluidics advances the performance of single-phase microfluidics in different aspects. Due to the slow diffusion and Taylor dispersion limitation in single-phase flow, an immiscible fluid is added to single-phase microfluidics to improve mixing and transverse channel transport by generating vortices in the microchannel. Moreover, in some cases that the fluids in the single-phase microfluidics deposit on the microchannel wall, another immiscible fluid stream is added to surround the first phase fluid to prevent it from contacting the surface and eliminate clogging of the microchannel. Multiphase microfluidics facilitates mixing, mass transfer, and it has the advantage of large interfacial areas in comparison with conventional microscale systems. Depending on the dimensionless numbers of Reynolds (Re), Capillary, Weber, Bond, viscosity and flow rate ratios, the output of multiphase microfluidics can be one of the following forms: droplets suspending a carrier flow, channel spanning slugs and wall wetting films. In 2001, Thorsen et al. designed the first microfluidic channel for producing monodisperse droplets [2]. In droplet microfluidics, each droplet has the potential to work individually as a reactor and allow chemical species to react with each other while they are insulated by the outer phase. Droplets, by having the functionality of merging, splitting, sorting and mixing, can be used as a platform for chemical and biological reactions. These special features plus high throughput analysis expand the utilization of droplet microfluidics for different applications in biology and chemistry [3][4].

Polymersome formation is one of the research areas that, in 2005, microfluidics started to contribute to advance control over their morphology and monodispersity [5]. Polymersomes are artificial vesicles consisting of diblock copolymer bilayer and an aqueous phase core to encapsulate and protect sensitive material such as drugs and enzymes. The membrane of polymersome acts as a barrier to protect the encapsulated materials and provide the capability to release them at the desired target. Different conventional methods have been used for polymersome formation like film rehydration, cosolvent, Meng, and electroformation methods. However, the produced polymersomes using these methods are not monodispersed, and their encapsulation efficiency is quite low. Weitz et al. proposed a microfluidics approach to address the drawback of conventional methods **[5]**. In this approach, a microfluidic chip for generating

double emulsion droplets is designed. Diblock copolymers dissolved in an organic solvent are pumped through the channel to form the middle phase or bilayer of the double emulsion. Then, to form the vesicle polymersome, they were collected, dissolved in a solution such as acetone to remove the organic solvent in the bilayer of polymersomes to form vesicle polymersomes. Generally, the advantages of using microfluidics for producing polymersome include having high encapsulation efficiency, size monodispersity, and precise control over bilayer thickness, permeability, the thermal and mechanical stability of created polymersomes.

In this thesis, we present a platform to produce polymersomes in different sizes. Producing polymersomes in a microfluidic chip consists of two steps: 1- double emulsion formation 2- extraction of the organic component, which is the middle phase of the double emulsion, to form polymersome. Currently, there are many challenges in the existing droplet microfluidic techniques, limiting their broad applicability in making double emulsions. The need of partial surface modification of microchannels and the lack of thorough guideline to control the size or the thickness of the middle phases are two main challenges of producing double emulsions with the desired size in microfluidics. In this work, an optimized microfluidic design is provided that allows researchers to generate high monodisperse double emulsions (w/o/w) and flexibly manipulate the thickness of the middle phase in a highly controlled manner. The thickness of the middle phase in the double emulsion is important as it significantly affects the extraction of the middle phase and, consequently, production of polymersomes. Therefore, an extraction channel is embedded in the second chip to control the thickness of the middle phase in the double emulsion. In addition, a selective surface treatment, and coupling effect between the first and second drop maker are avoided using a tandem microfluidic technique.

This thesis includes six chapters. In this chapter, the project and its motivation are explained briefly. In the second chapter, a literature review on droplet microfluidics, polymersome formation and different methods for extraction of the middle phase is provided. In the third chapter, the microfabrication process, facilities and experimental methods that are going to be used for achieving the goal of each project is elaborated. In the fourth chapter, the methodology and circuit analysis for designing the chip is provided. Moreover, a thorough guideline for designing a platform to generate double emulsions with different sizes is provided. Chapter five provided the

experimental results and some discussion about the presented results. In Chapter six, more discussion about the results and how the results can be improved is provided. Moreover, recommendations and suggestions for future research on this topic are provided.

Chapter 2: Literature review

2.1 Polymersome:

Polymersomes are artificial spherical vesicles which encapsulate a solution in their core or membrane. The core radius of polymersomes is in the range of 50 nm to 50um. The membrane of polymersomes is made of amphiphilic synthetic copolymers. Copolymers are two or more different monomers united together to generate a polymer. Monomers can be united in linear or branches formation. Polymersomes have extensive applications in industry, biology, medicine, and in the environmental sciences. They are being used for protecting sensitive materials such as drugs, chemical species, protein, DNA and other related materials. Materials having the hydrophilic property are encapsulated in the vesicle core and those having the hydrophobic properties are protected in the membrane of the vesicle. Moreover, polymersomes have the ability to release a specific material in the desired site as their membrane can be designed to be sensitive to temperature or acidity amount of environment. In Fig 2, a polymersome vesicle is shown.

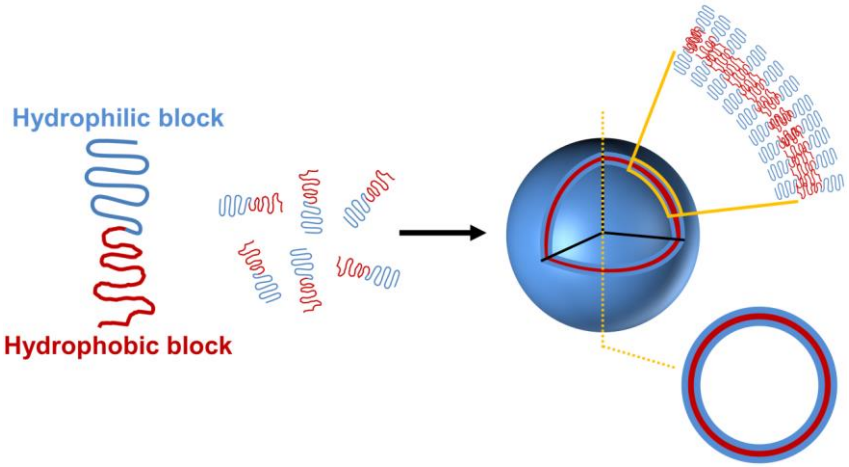

Figure 2: Structure of a polymersome **[6]**

During the last decades, lipid vesicles were being used in encapsulating drugs for delivery and protection; however, due to some limitations such as having a short life, limited structural variation since they are obtained from natural sources and inconsistent composition, they are being replaced by polymersomes. A comparison between liposomes and polymersomes regarding the structure of their membrane was first done by Discher and co-workers**[7].** As it was discussed before, polymersomes are self-assembled diblock copolymer vesicles created from a bilayer consist of

diblock copolymers and aqueous core. The bilayer can be created from different copolymers including AB, ABA, ABABA, ABC and ABCA copolymers. Therefore, polymersomes created from diblock copolymers have the advantages of having controllable structures and membranes with different physiochemical properties which enable their created vesicles to be thicker and highly entangled membrane. Consequently, polymersomes can be designed in order to be tougher, more permeable and stable in the physically harsh environmental conditions in comparison with liposomes.

2.1.1 Mechanism of Polymersome Formation:

As it is illustrated in Fig 3, two mechanisms have been predicted for the formation of vesicle in diblock copolymer solution by dynamic simulation based on the density functional theory**[8].** Moreover, these mechanisms have been supported by Monte Carlo simulations **[9]** and experiments of lipid systems **[10].** At the first step, as diblock copolymers are dissolved in a hydrophobic solution, hydrophilic tail of diblock copolymers escapes from the hydrophobic solution resulting in the aggregation of diblock copolymers and the formation of spherical micelles. Afterwards, collision of spherical micelles forms large cylindrical or open disklike micelles (mechanism I) or large spherical micelles (mechanism II). In the mechanism I, cylindrical or open disklike micelles close up to minimize the interfacial tension energy of the system and form the vesicles. In the other mechanism, the solvent diffuses inside the large spherical vesicles resulting in the formation of vesicles.

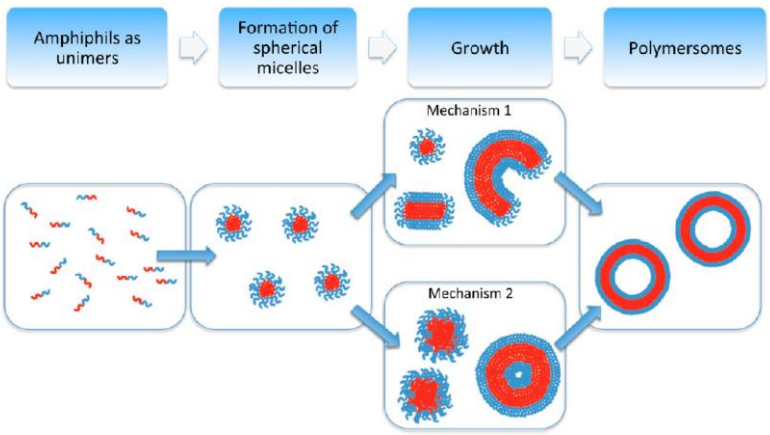

Figure 3 Two mechanisms of polymersome formation **[8]**

2.1.2 Polymersome morphology:

When diblock copolymers are dissolved in a hydrophobic or hydrophilic solution, depending on the volume ratio between hydrophobic and hydrophilic part of the diblock copolymer, different morphology such as spherical, cylindrical, micelles or vesicular structure are formed. Different possible morphology for the assembled diblock copolymers is presented in Fig 4. In 1976, Israelachvilli et al. introduced the critical packing parameter for predicting the morphology of the assembled diblock copolymers**[11]**. The critical packing parameter is defined as follows:

$$P_c = \frac{v}{a_0 l_c}$$

Where v represents the volume of the hydrophobic chain, a_0 is the area of hydrophilic-hydrophobic interfacial and l_c is the length of hydrophobic block perpendicular to the hydrophilic-hydrophobic interfacial. As it is illustrated in the Fig 4, the morphology of the assembled diblock copolymer is sphere, and cylinder.

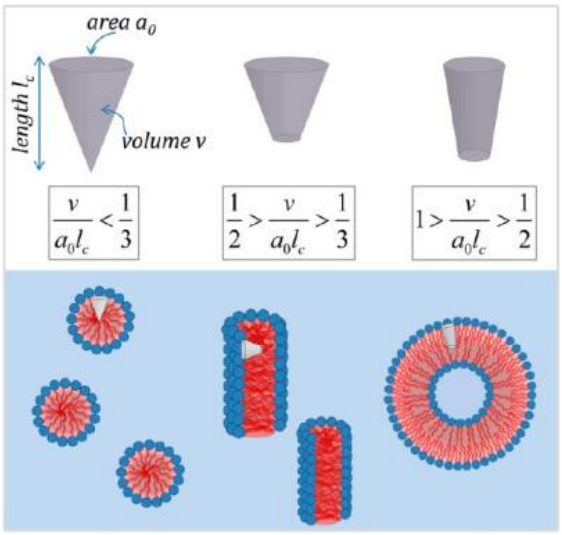

Figure 4 Different possible morphology of assembled diblock copolymers based on packing parameter**[11]**

2.1.3 Conventional techniques for polymersome formation

Common traditional methods for polymersome formation are categorized into two methods, namely, hydration (such as film rehydration, acetone cosolvent and meng) and electroformation. The procedure of vesicle formation for both of these methods is nearly the same. The diblock copolymers are dissolved in an organic solvent. Subsequently, the solution is left on a solid

substrate to remove the organic solvent via evaporation. After the evaporation of the organic solvent, a film of diblock copolymer is formed on the surface. The next step is to place a drop containing the solution, going to be encapsulated in the polymersome, on the film of polymer and is gently stirred. Subsequently, the dry film is soaked and injected into the solution. The size and structure of vesicles generated in the hydration method cannot be tuned precisely**[12]**. In the electroformation method, as an electric field is applied to the solution to induce the aggregation process, by changing the electric field parameters, the process of vesicle formation can be controlled **[13]**. However, this method is still suffered from the lack of control on producing monodisperse droplets. Moreover, both of these problems have the drawbacks of low and uncontrolled encapsulation efficiency. The encapsulation efficiency in these methods is around 35%**[14]**.

In general, conventional methods such as film rehydration and electroformation produce a broad range of vesicle sizes. Thus, a great deal of efforts has been made to improve the monodispersity of produced vesicles by doing some post preparation treatments such as extrusion, sonication and freeze thaw cycle **[15][16][17].** In the freeze thaw cycle method, the produced vesicles are suspended in a liquid nitrogen container. Afterwards, the solution is spontaneously bubbled to apply a shock to divide larger vesicles to smaller ones. By using this technique, the maximum size of vesicles can be reduced to decrease the range of vesicle size and improve the monodispersity. Sonication method utilizes vibration to divide large vesicles to eliminate the size range of generated vesicles and improve monodispersity. Extrusion method increases the monodispersity of vesicles by pushing the solution through a polycarbonate filter. Therefore, the size range of produced vesicles can be controlled by choosing an appropriate filter. These methods were proposed to improve the size distribution of vesicle by post processing methods while there are several methods used during the formation for improving monodispersity which some of them are explained briefly in the following section.

Photolithography method:

To improve the size distribution of vesicles, as it is illustrated in Fig 5, a patterned hydrophilic/fluorocarbon surface with the desired size for vesicles is generated and the polymer solution is spun and coated on the patterned surface. The rehydration from the grids yields polymeric vesicles having the desired size which depends on the size of patterned grids.**[18]**

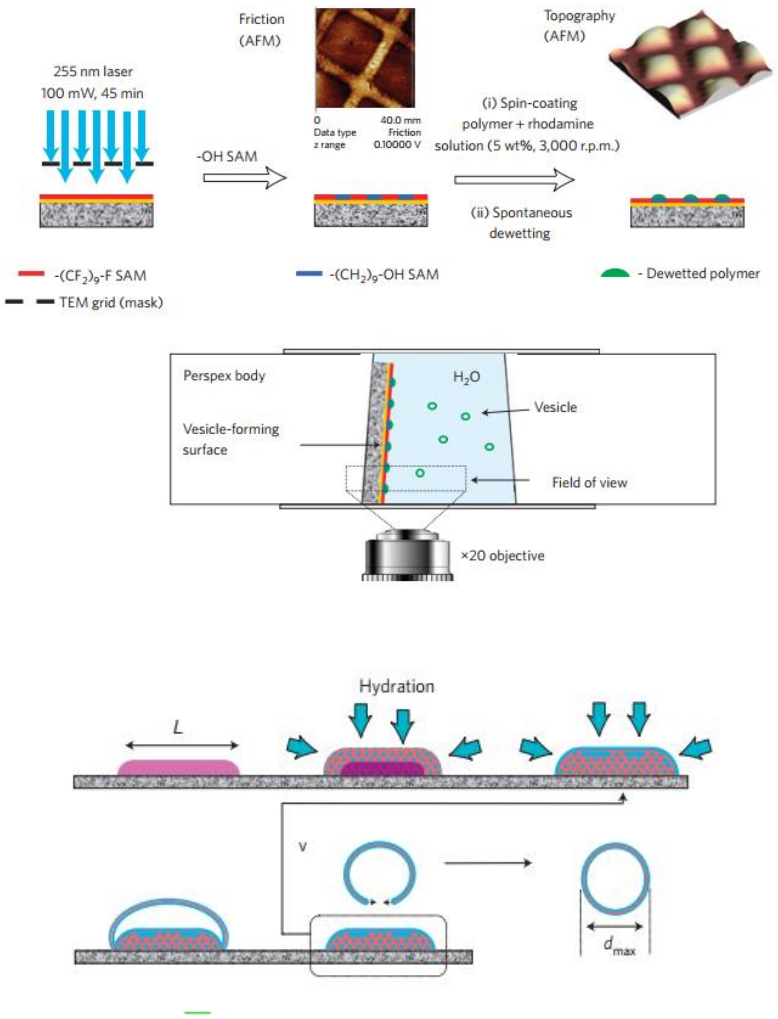

Figure 5 Procedure of polymersome formation with controlled size using photolithography**[18]**

Inkjet:

The inkjet technique is a developing version of rehydration method for narrowing the size distribution. In this technique, the solution containing amphiphilic is filled into a cartridge and printed into a stirred aqueous solution resulting formation of polymeric vesicles having size distribution characterized by the cartridge and the angular velocity of the stirred solution. A schematic of the techniques is presented in Fig 6.

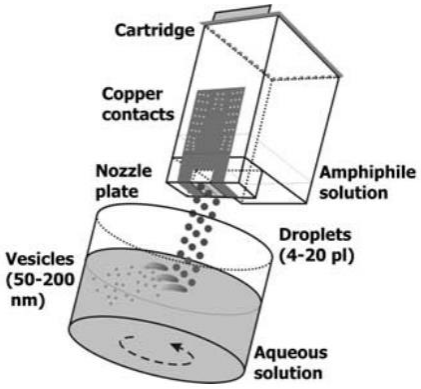

Figure 6 Polymersome and liposome formation using inkjet**[19]**

Micromixer:

This method similar to inkjet is a further development of the cosolvent method. As it is illustrated in Fig 7, two containers are filled with block copolymer and organic solvent; moreover, the hydrophobic and hydrophilic cargos needed to be encapsulated in the membrane and core of polymersome are dissolved, respectively. Afterwards, the content of these two containers are pumped to the micromixer and after mixing, they are dissolved in an aqueous solution resulting in the formation of polymersomes. The size and morphology of the polymersomes can be tuned via the initial polymer concentration, water content of the common, mixing ratio and speed and the flow rate.

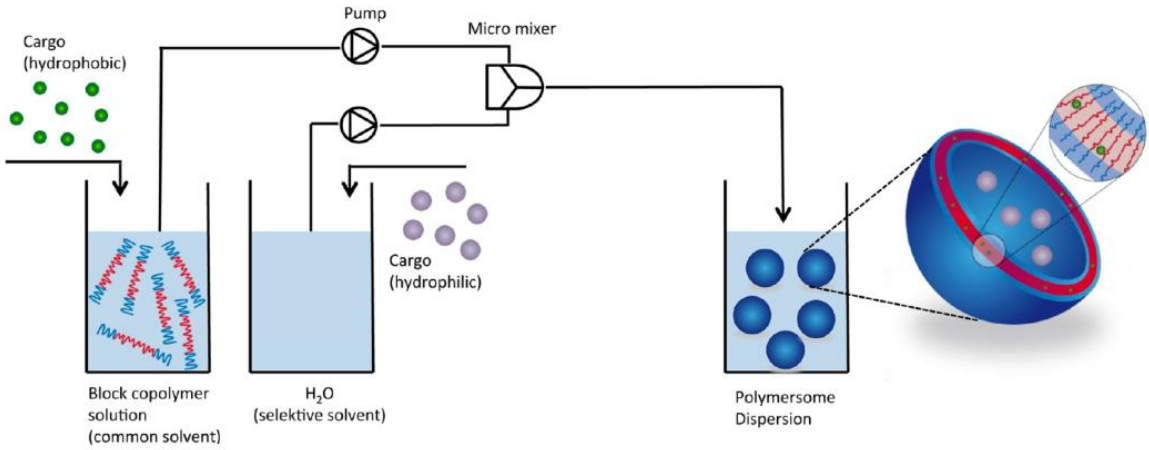

Figure 7 Polymersome formation using micromixer**[20]**

Despite all these advancements in vesicle formation techniques for improving the encapsulation efficiency, the monodispersity of produced polymersomes is still restricted. Microfluidics techniques offer an alternative technique for improving the monodispersity and encapsulation efficiency of the produced polymersomes. Moreover, further advantages for microfluidic approach for polymersome formation can be enumerated including having precise control over size, bilayer thickness, mechanical**,** permeability and thermal properties and stability of created polymersomes.

2.1.4 Microfluidics approach for polymersome formation:

High polydispersity and low encapsulation efficiency of bulk methods for producing polymersomes are the main drawbacks of majority of conventional methods such as film rehydration and electroformation methods. Different post preparation methods such as extrusion, sonication and freeze thaw cycle were proposed to improve the monodispersity and encapsulation efficiency of these methods. In 2005, the group of D. Weitz developed a new method that generated monodispersed polymersome having high encapsulation efficiency **[21]**. The first step for polymersome fabrication in this method is to produce water/organic solvent/water (W/O/W) droplets with dissolved copolymer in the middle phase. After formation of the double emulsion, copolymer migrates to the W/O and O/W interface and due to its surfactant like feature, it stabilizes the produced double emulsion. As illustrated in Fig 8, since diblock copolymers consist of a hydrophilic tail dissolved in a hydrophobic solution in the middle phase, the hydrophilic tail of diblock copolymers intends to migrate to the outer or inner phase while their hydrophobic tail is still inside the hydrophobic part. The final stage of polymersome formation is dewetting of the organic solvent from the middle phase. The Organic solvent is extracted from the middle phase using a different method such as dissolving in acetone and using a surfactant (explained in more detail in the next section). Hence, as shown in Fig 8, the hydrophobic tail of two diblock copolymers are merged together to form the bilayer of vesicles.

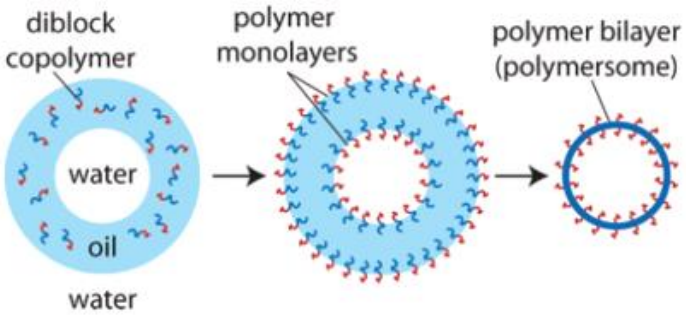

Figure 8 Polymersome formation after extraction of organic phase from double emulsions generated using microfluidics**[22]**

In this method, the size and morphology of the polymersome can be tuned precisely by changing the flow rate of phases. Moreover, this method provides the possibility of encapsulating hydrophobic and hydrophilic cargos inside the polymersome having extremely high efficiency since the formation of double emulsion can be precisely controlled in the microfluidics. To encapsulate cargos inside core or shell of the double emulsion, before pumping the inner, middle and through the microchannel, hydrophilic and hydrophobic cargos are dissolved in the inner and middle phases, respectively. A schematic of one of the designed microfluidics by the group of

D. Weitz for producing W/O/W double emulsion is shown in Fig 9 **[23].** In this design, a glass capillary microfluidic is used to generate monodisperse W/O/W droplets. Middle phase containing an organic solvent and diblock copolymers are pumped into the channel to squeeze the inner phase containing the aqueous phase and hydrophilic compartment while the second aqueous phase is pumped to apply the desired shear stress in order to pinch off the inner and middle phases to form double emulsions droplets.

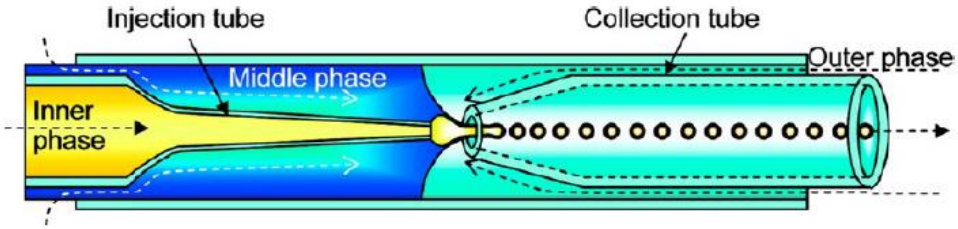

Figure 9 W/O/W Double emulsion formation using microfluidics**[23]**

The process of polymersome formation using microfluidics consists of two steps: 1-double emulsion formation 2- organic phase extraction from the double emulsion. Thorough literature is done on each of these steps in order to have a better vision about the process of polymersome formation using microfluidics.

2.2 Droplet Microfluidics:

Multiphase microfluidics advances the performance of single microfluidics in some different aspects. Due to the slow diffusion and Taylor dispersion limitation in a single-phase flow, an immiscible flow is added to single phase microfluidics to improve mixing and transverse channel transport by generating some vortices in the microchannel. Moreover, in some cases that the liquid in the single-phase microfluidics is deposited on the microchannel wall, another immiscible fluid stream is added to the liquid to surround the first phase in order to prevent liquid from contacting the surface and eliminate clogging of the microchannel. Multiphase microfluidics facilitates mixing, mass transfer and it has the advantage of large interfacial areas in comparison with conventional microscale systems.

Depending on the dimensionless numbers of Reynolds (Re), Capillary, Weber, bond numbers, viscosity and flow rate ratios, the output of multiphase microfluidics can be in one of the following forms: droplets suspending a carrier flow, channel spanning slugs and wall wetting films. Among different multiphase microfluidics, droplet microfluidics has been popular because of their application in micro-reactors for μTAS studies and fabricating droplets for material research.

Numerous advantages can be enumerated for droplet generation which facilitates the bio/chemical reactions and analysis. The first advantage is miniaturization which makes the single cell or subnonoliter analysis possible. The second one is fast mass transfer and mixing in a short diffusion distance which causes fast analyses and reactions. The third one is compartmentalization: droplets are analyzed independently; therefore, each droplet works as an individual unit and reactor. The final one is having a high throughput analysis since each droplet works as an individual compartment and their work does not overlap to reduce the speed of the overall process.

Generally, microfluidic droplet generators can be categorized into two groups: Passive Microfluidics and Active Microfluidics. To design a microfluidic device for generating and manipulating droplets having various behaviors and extensive applications, it is important to understand their unique fluid dynamics.

2.2.1 Physics at droplets microfluidics:

Since there is laminar flow condition in microfluidic devices which is the result of its microscale size, the mixing is a very slow process. To address this issue, droplet microfluidics has emerged to speed up the mixing process in microscale. Studies conducted on droplet microfluidics shows convective flow profile created inside the droplet to facilitate the mixing process in droplet microfluidics. Therefore, understanding the physics of fluid flow inside the droplet is very crucial for designing a very efficient microfluidic device. The dynamics of droplet generated in microfluidics is governed by stokes equation; however, due to having a deformable interface between droplet and carrier fluid, nonlinear behavior is observed in droplet microfluidics.

The process of droplet generation occurs due to the interfacial instability in the fluid dynamic. In this process, the interface of the continuous and dispersed phase is deformed which leads to interfacial instability and pinching off the dispersed phase and droplet formation. Generally, there are two methods for droplet generation: active and passive methods. In the passive method, the droplet is generated due to interfacial instability in the interface of continuous and dispersed phases; however, in active methods, external forces are added to the system in order to control pinching off process.

To analyze the droplet formation in microchannel more effectively, dimensionless numbers are defined to characterize the droplet formation in microfluidics. Generally, there are four forces exerted on a particle carried by a fluid in a microchannel: inertia, viscous, interfacial and gravity. Four dimensionless numbers are defined by combining the aforementioned forces to see which force dominates in a specific situation in comparison with other forces. The dimensionless numbers characterizing droplet microfluidics are listed as: Reynolds (Re), Capillary, Weber, bond numbers and viscosity, flow rate ratios. In table 1, the dimensionless parameters characterize the droplet microfluidics are defined. In most cases, the capillary number, viscosity and flow rate ratios are the most important dimensionless parameters for analyzing what happens in droplet microfluidics including mixing, breakup, coalescence and transport of droplets.

Symbol	Name	Formula	Physical

Re	Reynolds number	$\frac{\rho v l}{\mu}$	$\frac{Inertia\ force}{viscous\ force}$
Ca	Capillary number	$\frac{\mu v}{\sigma}$	$\frac{viscous\ force}{interfacial\ force}$
Bo	Bond number	$\frac{\rho v^2 l}{\sigma}$	$\frac{Inertia\ force}{interfacial\ force}$
We	Weber number	$\frac{\Delta \rho g l^2}{\sigma}$	$\frac{bouyancy\ force}{interfacial\ force}$
λ	Viscosity ratio	$\frac{\mu_d}{\mu_c}$	$\frac{dispersed\ viscosity}{continious\ viscosity}$
φ	Flow rate ratio	$\frac{Q_d}{Q_c}$	$\frac{dispersed\ flow\ rate}{continious\ flow\ rate}$

Table 1 Dimensionless numbers characterize the droplet microfluidics

2.2.2 Passive methods for droplet formation:

The geometry plays the most important role in passive droplet generators. There are three fundamental methods for generating droplet in microfluidics: co-flowing, flow focusing and cross flow designs. **[24]**

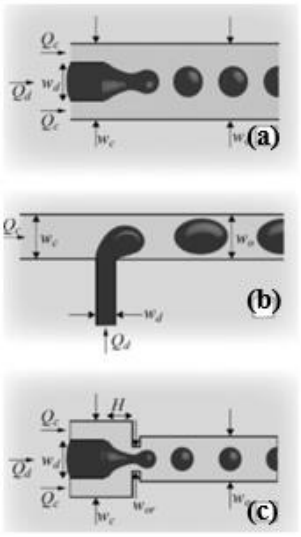

Figure 10 Three different geometries utilized for droplet generation a) co-flow b) cross-flow c) flow-focusing**[24]**

Co-flow

The most straightforward method for generating a droplet is two concentric microchannels which the continuous phase flows inside of the inner channel, and the outer channel carries the dispersed phase Fig 10. The first design for producing droplet in a co-flow geometry was designed by Fischer et al. in 2004 **[25]**.The size of droplet generated in Co-flow method highly depends on the flow rates and fluid properties. The size of droplets decreases as the continuous phase flow rate increases because of higher viscous shear stress which accelerates the pinching off process. On the other hand, the flow rate of dispersed phase affects the size of droplets as by increasing the flow rate, the volume of liquid encapsulated in one droplet before breaking up increases. Moreover, the size of the generated droplet increases by adding surfactant to the droplet generator microfluidic. Using a surfactant, as reduces the interfacial tension between phases resulting in a decrease in the resistance of droplet from pinching off and retardation of dispersed phase pinching off.

In this method, two regimes of droplets are observed: dripping regime and jetting regime. In the dripping regime, the droplet is generated next to the capillary tip. To generate droplets in the dripping regime, the flow rate of continuous and dispersed phases should be kept low. The transition between the dripping regime to the jetting regime occurs by increasing the flow rate of continuous or dispersed phases. In the jetting regime, droplets are generated far away from the capillary tip. By increasing the continuous phase, the width of jet is decreased, and the narrowing

jetting regime is created. In this transition, the balance between the viscous stress and interfacial tension is dominant and the capillary number of continuous phase determines the transition of dripping regime to narrowing jetting regime. Conversely, increasing the flow rate of dispersed phase, widen the jet of dispersed phase before pinching off resultant in the transition between dripping regime to wide jetting regimes. The transition between dripping and wide jetting regime is dominated by the weber number of the dispersed phase due to the high flow rate of dispersed phase and dominant role of inertial in this transition. More detailed investigations on the process of transition between dripping regime to jetting regime in co-flow geometry have been conducted by Cramer, C. et al. in 2004 **[26].** The monodispersity of generated droplets in co-flow geometry is highly dependent on the flow conditions. Droplets generated in dripping regime have a higher monodispersity**[27].** in comparison with jetting regime**[28]**

Flow-focusing:

The first flow focusing geometry was designed by Anna et al.**[29].** Considering this design, two immiscible fluids flow coaxially at a contraction region in which the continuous phase and dispersed phase flow through the outer and inner channel, respectively. In the contraction region, due to higher shear forces, the dispersed phase narrows and uniform droplets are generated. The size of the produced droplets in this geometry is highly dependent on the size of the orifice. Moreover, as the continuous phase flows symmetrically from both side of the dispersed phase, symmetrical shear stress creates the resultant formation of more controllable and stable droplets in comparison with other methods. In flow focusing geometry, fluids experience three different regimes: jetting, dripping and squeezing. In this geometry, at low continuous phase capillary number, due to low shear stress, the dispersed phase grows until the orifice is blocked; subsequently, pinching off occurs because of increasing hydrodynamic pressure. Increasing the capillary number results in producing droplets in dripping regime in which droplets with smaller diameter comparing with orifice size are generated due to high shear stress in the orifice. Further increasing of the value of capillary number results in formation of droplets in jetting regime in which pinching off occurs beyond the orifice. The droplets created in jetting regime are less monodisperse comparing with squeezing and dripping regimes. Cubaud et al. draw a map for different flow regimes in a flow focusing geometry based on the capillary number of continuous and dispersed phases**[30].**

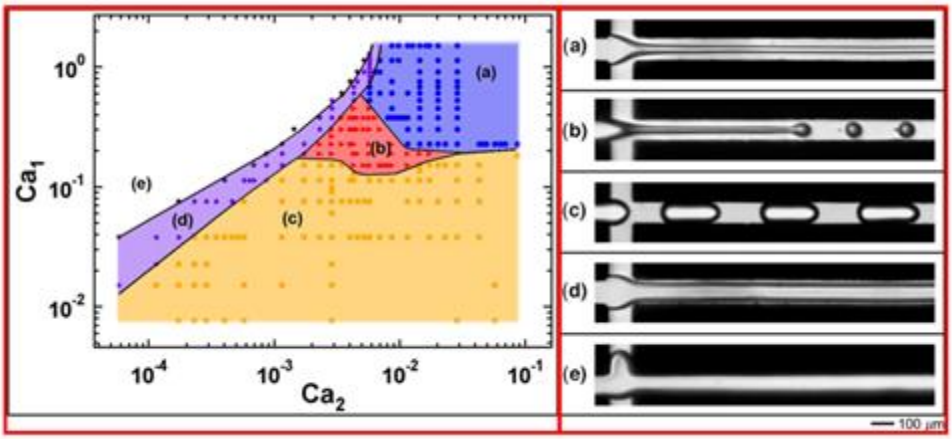

Figure 11 Flow map of different regimes in a flow focusing based on capillary number a) threading b) jetting c) dripping d) tubing e) viscous displacement**[30]**

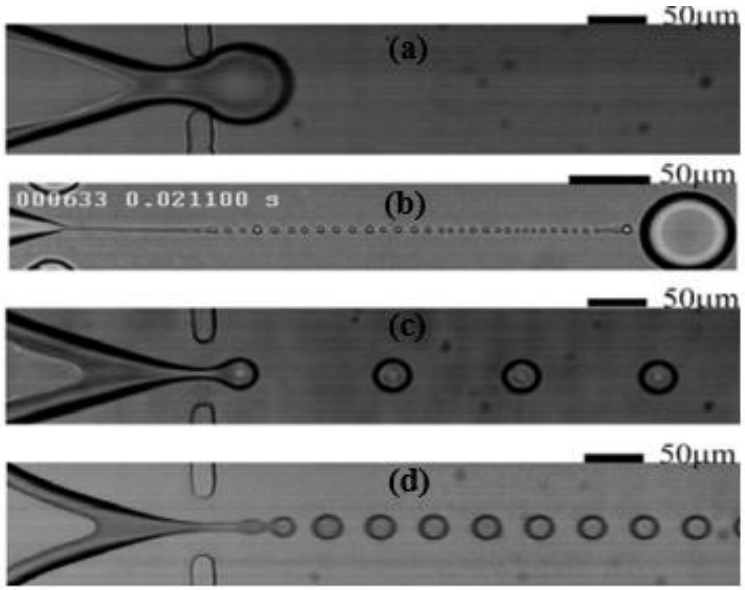

Figure 12 Different regimes in a flow-focusing a) squeezing b) Thread formation c) dripping d) jetting**[31]**

Cross-flow

In cross-flow geometry, droplets are generated in a geometry where continuous and dispersed phases meet at an angle ($0 \leq \theta \leq 180$) **[32].** In this geometry, similar to the aforementioned methods, droplets experience three different breakup modes: squeezing, dripping and jetting. The droplet generated in squeezing and dripping regimes are more monodisperse comparing with the

jetting regime. In squeezing regime, the capillary number of continuous phases is low resulting in lower shear stress. Therefore, droplets do not break up until the main channel is blocked and the hydrodynamics pressure is increased. The formation of droplets in squeezing regime is only dependent on the geometry and the flow rate ratio of continuous and dispersed phases**[33]**. Increasing the hydrodynamics pressure causes squeezing the interface of phases and eventually pinching off of the dispersed phase. Increasing the capillary number results in domination of shear stress over surface tension. Consequently, droplets are produced in dripping regime by pinching off before blocking the channel. Continued increasing the capillary number results in the formation of droplets in the jetting regime. Droplet generated in jetting regime is highly polydisperse while in the other two regimes, monodisperse droplets are mostly generated. As shown in Fig 13, based on experiments done by Guillot, in this geometry, the transition point between every two regimes is a function of flow rate ratio and capillary number**[34]**

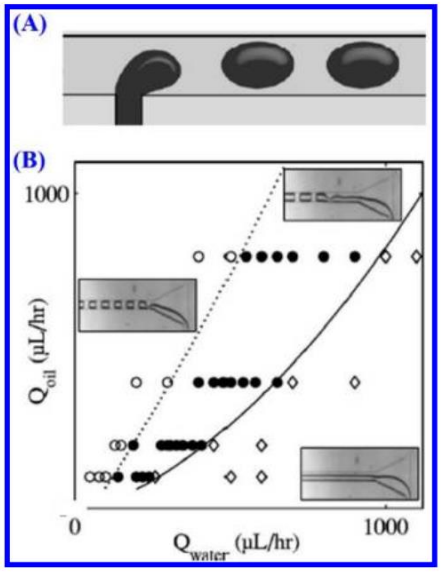

Figure 13 different droplet regimes in cross flow geometry**[34]**

2.2.3 Breakup modes

Squeezing:

In squeezing regime, the capillary number is low which means the value of interfacial force dominates viscous force. In this mode, as the shear stress is not sufficiently high to pinch off the dispersed phase, the interface grows until it obstructs the junction region. After obstructing the

junction, the pressure increases significantly and by excessing the pressure inside the dispersed phase, the interface starts squeezing and eventually breaks up. The generated droplet shape is mostly similar to a slug rather than a sphere. In Fig 14.a, an image of squeezing regime for different geometry is presented. As it is shown in Fig 14.a**,** the droplets generated in this mode consist of three stages: the filling, squeezing, necking and pinch off**[36]**. The droplets generated in this regime, are highly monodisperse and larger than the size of the main channel.

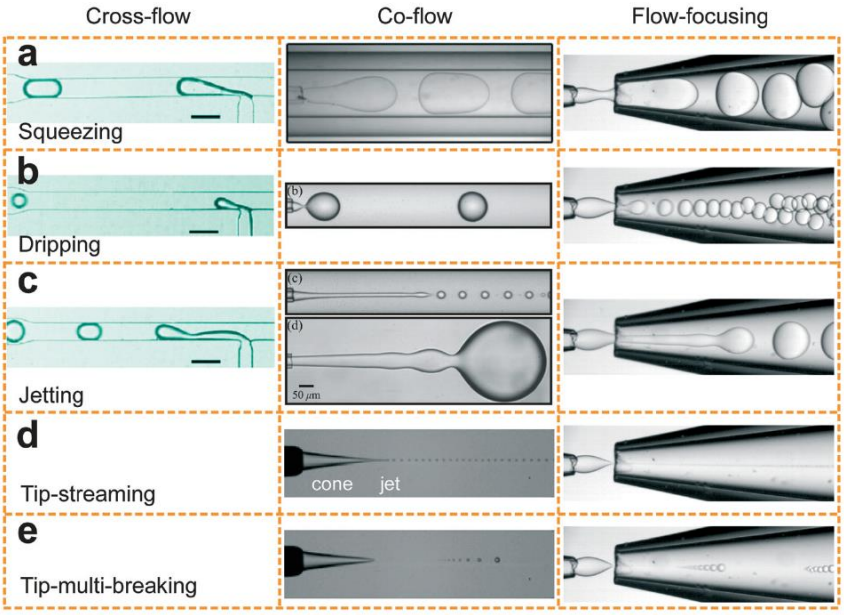

Figure 14 Different breakup modes for different geometry of the droplet generator. breakup modes: a) squeezing b) dripping c) jetting d) tip-streaming e) tip-multi-breaking **[35]**

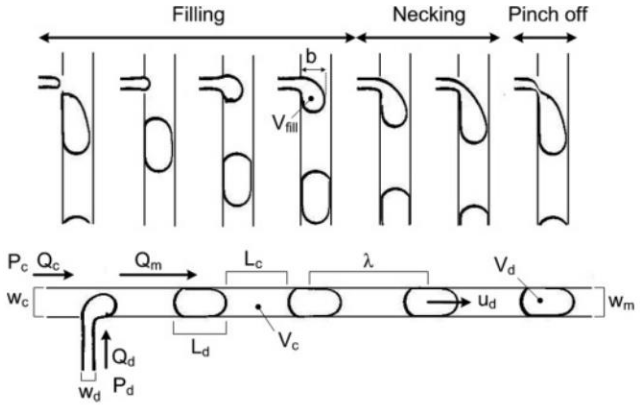

Figure 15 Three stages of droplet formation in squeezing regime**[36]**

Dripping:

A continued increase of capillary number results in transformation from squeezing regime to dripping. By increasing the capillary number, a viscous force which is responsible for dragging the interface and breakup, dominates interfacial force stabilizing the interface of dispersed and continuous phases. Therefore, the droplet is pinched off at the dispersed nozzle in the cross-flow and co-flow geometries, or at the focusing orifice in flow-focusing structures before blocking the junction region. Hence, as it is shown in Fig 14.b, the generated droplet is spherical. The produced droplets are monodispersed in this regime. J.K Nunes et al did a thorough investigation of the dimensionless numbers of dispersed and continuous phases at the moment of transition from squeezing to the dripping regime. He showed that there is no specific threshold for capillary or weber number for regime transition from squeezing to dripping and it is highly dependent on the geometry and fluid properties in each experiment**[37]**.

Jetting:

The transition from dripping to jetting occurs by increasing the flow rate of continuous or dispersed phases. In this regime, the dispersed phase is extended and squeezed, and the droplet is generated at the end of this jet due to Rayleigh–Plateau instability. Because of capillary perturbation in this specific regime, polydisperse droplets are mostly generated in comparison with dripping and squeezing regimes. For co-flowing geometry, the condition which should be satisfied for occurring jetting regime is as follows: **[38]**

$$Ca_c + We_d \geq O(1) \quad (1)$$

In other words, the jetting regime occurs when the inertia and viscous forces dominate interfacial tension. Generally, there are two different kinds of the jetting regime: narrowing jet and widening jet. The narrowing jet occurs when the value of drag viscous force exceeds the interfacial tension since in this condition, the high value of drag viscous force squeezes the dispersed phase and causes the thickness of jet to decrease significantly. However, if the velocity of dispersed phase exceeds the continuous phase, the shear stress of continuous phase cannot squeeze the interface resulting in an increase in the width of the jet and formation of the widened jetting regime.

2.2.4 Active methods for droplet formation:

As the main focus of this thesis is on passive methods for droplet formation, in what follows, a brief description of most common active methods for droplet formation is presented. In active

methods, external forces are applied to the system in order to facilitate droplet formation. Generally, active methods are categorized into electrical, magnetic, thermal, and mechanical methods.

Electrical method:

In this category, direct current (DC) or alternating current (AC) is applied to the microchannel to assist other forces such as viscous and interfacial forces for droplet breaking up. Moreover, the electric field can be used for the purpose of changing the physical properties of fluids such as wettability which can contribute to the process of droplet formation.

In electrical methods, by using DC, the water plays the role of conductor and the oil acts as the insulator. Therefore, the water-oil stream is similar to a capacitor. In this method, the size of droplets can be precisely controlled by changing the strength of the electric field. Moreover, by using AC, the droplets are generated by electrowetting-on-dielectric (EWOD) effect. The function of the EWOD mechanism is to reduce the contact angle of liquid and the microchannel walls.**[39]** Furthermore, DEP method is used for droplet generation. Due to the electric field gradient created using electric current, an extra force is exerted on the dispersed and continuous phase to facilitate the droplet formation**[40]**.

Magnetic method:

In the magnetic method, nanoscale ferromagnetic particles are suspended in the continuous or dispersed phases to apply the magnetic force to continuous or dispersed phases phase and consequently, they manipulate the size of generated droplets and their formation frequency. Using ferrorfluids, another force is exerted on the dispersed or continuous phases in order to facilitate droplet formation and assist the process of controlling the size and frequency of droplet formation**[41]**. The droplet microfluidic using magnetic forces can be characterized by defining bond number which is the relative strength of magnetic force to interfacial tension.

Thermal method:

Since surface tension is a function of temperature, the capillary number can be affected by changing the temperature inside the microchannel. Therefore, by heating a part or the entire

microchannel, the process of droplet generation can be controlled**[42]**. The flow regime, size of droplets and the frequency of droplet generation can be tuned by heating the microchannel to generate the required temperature gradient.

Mechanical method:

By using pneumatic and hydrodynamics element, mechanical forces can be applied to the droplet microfluidics in order to control the droplet size and generation frequency. In this method, a moving object such as chopper can be used to cut off the droplet with the desired size and frequency**[43]**. Moreover, piezoelectric elements are utilized to generate vibration in the system in order to induce droplet breaking up**[44]**.

2.2.5 Fluid instabilities:

As it was mentioned in the previous section, droplets are pinched off in different breakup modes. Breakup modes occur due to different fluid instabilities. Among breakup modes, squeezing occur because of pressure drop while for other breakup modes, pinch off originates from capillary instabilities.

Pressure drop

When the capillary number is low, the breakup does not occur due to shear stress. In this situation, droplets are pinched off because of pressure perturbation. Since droplets block the channel in the squeezing regime, the pressure difference between back and forth of droplet buildup which causes the droplet to pinch off. The droplets generated in this instability are mostly like slug rather than typical spherical droplets.

Capillary instability:

Contrary to squeezing regime which occurs due to pressure build up between the back and forth of droplets, other breakup modes are initiated because of capillary instability. There are two different instabilities: absolute and convective instability. In absolute instability, the disturbance is propagated to the whole domain and the velocity profile experiences an instability which is called absolute instability. However, if the disturbance is carried only to the downstream, another kind of disturbance called convective disturbance affects the velocity profile. Among those regimes initiated by this instability, dripping and widening occur due to absolute instability,

narrowing jet and tip streaming due to convective instability and tip-multi-breaking due to global instability. The droplets generated in this instability are mostly spherical.

2.3 Multiple emulsions:

In contrast to single emulsions such as water/oil or oil/water droplets where two phases are being used for generation, multiple emulsions are generated from more than two phases which consist of a droplet containing different compartments. In the previous sections, a brief review was presented on the physics and different methods for the formation of single emulsions. In this section, the main focus is on the formation of multiple emulsion formations in microfluidics. The main purpose for approaching multiple emulsion is to fabricate capsules and vesicles for protecting sensitive materials**[45][46][47]** and their target release**[48][49][50]** at the specified time and location. Multiple emulsions are categorized into three main groups: single-cored, multi-cored and Janus. Single-cored emulsions consist of a core surrounded by multi concentric shells. In Fig 16, double, triple, quadruple, and quintuple emulsions consist of one, two, three and four shells, respectively, are illustrated.

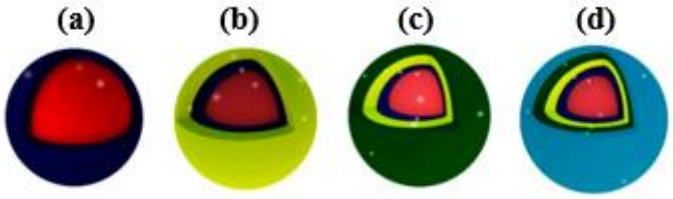

Figure 16 Double (a), triple(b), quadruple(c), and quintuple(d) emulsions**[51]**

In multi-cored emulsions, as illustrated in Fig 17, multiple droplets are encapsulated in a larger droplet.

Figure 17 Multi-cored emulsions**[51]**

As shown in Fig 18, in Janus emulsions, cores or the shells of emulsion compose of two different materials which are physically or chemically distinctive.

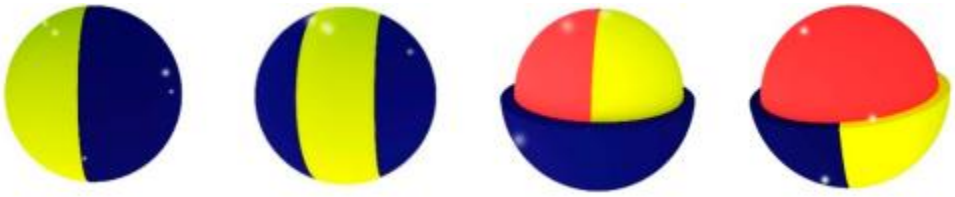

Figure 18 Janus emulsions**[51]**

Since the main purpose of this project is developing a platform for polymersome formation and as discussed in the previous section, polymersomes are generated from double emulsions. In what follows, the literature is more focused on double emulsions. Generally, two different types of double emulsions are generated for the formation of vesicles: water-oil-water or oil-water-oil double emulsions. Glass capillary and lithography-based microfluidics are the most common methods for fabrication of emulsions. In what follows, different geometries and methods used for emulsion fabrication are briefly described.

2.3.1 Double emulsion formation using Microfluidics:

As it was discussed before, two different microfluidic chips are utilized for droplet formation: glass capillary microfluidics and lithography based microfluidics. The methods that each of these microfluidics designs have employed for producing double emulsion can be classified in three distinct categories: 1- single-step double emulsion formation 2- two consecutive double emulsion formation steps 3- double emulsion formation in two separate connected chips. In what follows, first glass capillary microfluidics is compared with lithography-based microfluidics and then, the advantages and disadvantages of different methods for double emulsion formation are thoroughly investigated.

Glass capillary microfluidics:

Glass capillary microfluidics is composed of different round capillary tubes fitted in another capillary tube with square cross section. In Fig 19, a glass capillary microfluidics designed for the production of double emulsions in two steps is illustrated. As shown in the figure, the chip consists of two co-flow drop maker located along each other. In the first co-flow, single droplets are

generated and in the second co-flow drop maker, the first single droplets are encapsulated in the second droplets to form double emulsions.

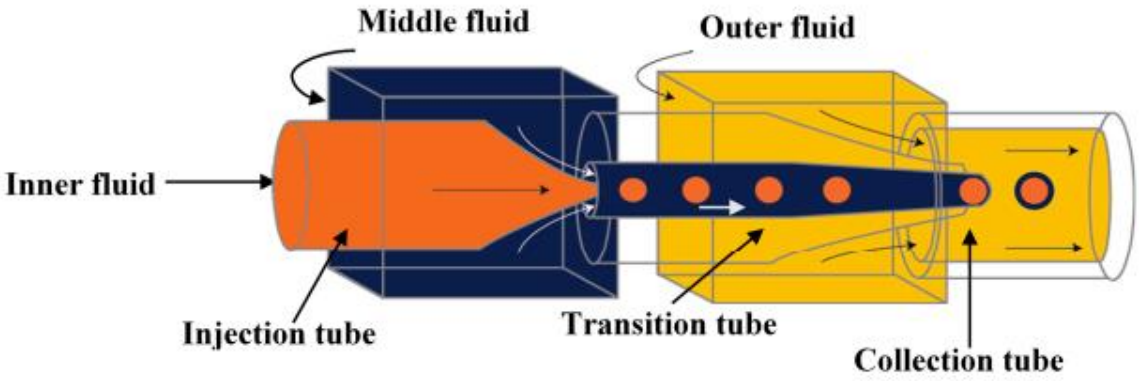

Figure 19 Glass capillary microfluidics for double emulsion formation in two steps**[51][52]**

One step emulsification is another method used for producing double emulsions. In these microchannels, core and the shell of double emulsions are produced simultaneously. In Fig 20, a glass capillary microfluidics designed by Utada et al for double emulsion formation in a single step is illustrated**[53]**.

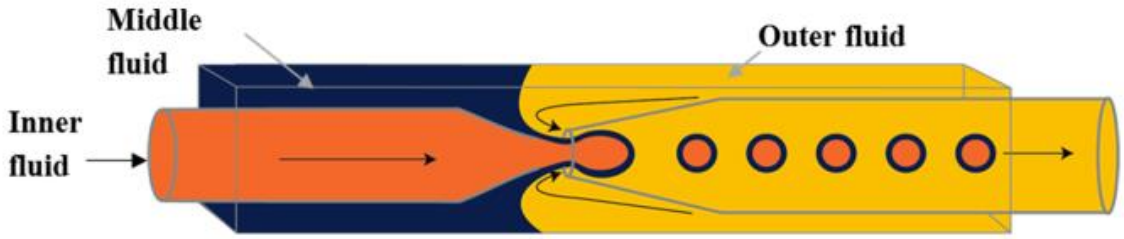

Figure 20 Glass capillary microfluidics for double emulsion formation in a single step**[51][52]**

This glass capillary microfluidic composed of two rounded glass capillaries inserted coaxially inside a squared glass capillary. Each of the glass capillaries is surface treated separately in a way that one of the rounded glass capillaries is wetted by the inner phase and the other one wetted by the outer phase. The outer phase is pumped through the channel in the opposite direction of the inner and middle phase and, by applying shear stress to their interface, double emulsions are generated. The size of double emulsions is a function of flow rates and the surface tension between phases.

As droplet formation in glass capillary microfluidics is in 3D, the dispersed phase is surrounded by the continuous phase and, thus, it does not contact with the orifice surface which should be wetted by the continuous phase. Therefore, droplet formation in glass capillary microfluidics is more stable in comparison with lithography-based microfluidics. Since, for double emulsion formation, the first part of the channel is wetted by the middle phase and the second part by the continuous phase, surface modification is very important for stable production of double emulsion. Since in glass capillary microfluidics, unlike lithography based microfluidics, each part is fabricated separately, controlling the wettability of microchannel is much easier in comparison with lithography-based methods. The other advantage of glass capillary microfluidics is their better optical properties compared with lithography-based methods. However, two draw backs of glass capillary microfluidics inhibit their vast utilization for droplet formation. Each glass capillary should be tapered and manually aligned with the other glass capillaries which slow down the process of microchannel fabrication. Furthermore, these microchannel unlike lithography-based methods is not replicable which limit their adoption for usage in the industry due to their low reproducibility. In this thesis, due to these draw backs, lithography-based methods are employed for double emulsion formation. In the next section, lithography-based methods used for double emulsion formation are described in detail.

Lithography-based microfluidics for double emulsion formation:

In this method, channels are mostly fabricated from PDMS. Microchannels in this method are fabricated by soft lithography in a larger amount compared with glass capillary methods with low cost as it is a replicable method. The main challenge for producing double emulsion in these channels is surface modification. Since, in double emulsion microfluidics, the first part of the channel should be wetted by the middle phase and the second part by outerphase, surface modification should be done very precisely. After bonding PDMS to the glass slide using PLASMA treatment, the surface of the channel is hydrophilic. Afterwards, the fabricated channel is baked overnight to make the channel hydrophobic again. Different solutions are proposed for hydrophilic treatment of the channel. For instance, in 2018, Deshpande et al. used the channel shown in fig to produce double emulsions**[54].** The channels before and after the junction are wetted by the middle and outer phases, respectively. PVA solution is employed to make the second part of the channel (after the junction) hydrophobic. PVA solution was pumped through the

channel from OA inlets and LO and IA inlets were block to prevent PVA solution go to the left side of the junction. Hence, the surfaces were treated to control the wettability of microchannel for double emulsion production.

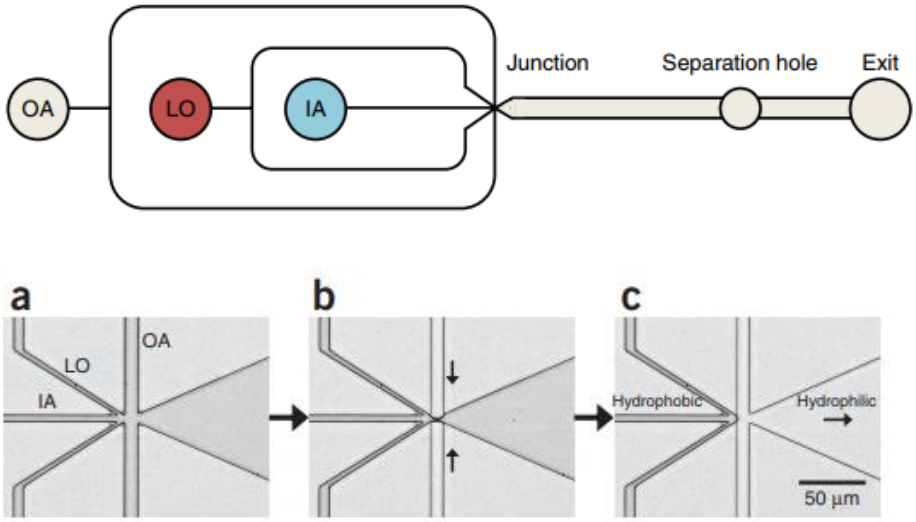

Figure 21 Controlling the wettability of microchannels for double emulsion formation**[54]**

In general, lithography-based microfluidics for double emulsion formation is categorized into three groups:1- single-step 2- two-step 3- tandem. In two-step methods, as illustrated in Fig 22, double emulsion is created in two steps. In the first step, the core of double emulsion is created and, in the second step, a drop-maker with different surface wettability from the first drop-maker generates the shell of the double emulsion. In Fig 22, two flow focusing drop-makers are located in series to produce double emulsion. However, two T-junctions**[55][56][57],** two flow focusing**[58][59]** can be located along each other to form double emulsion in two steps.

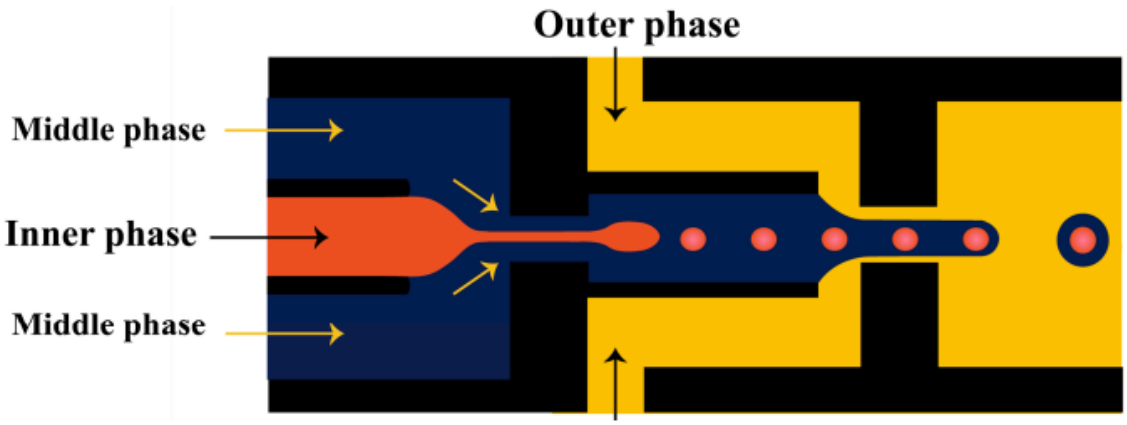

Figure 22 Using lithography-based microfluidics for double emulsion formation in two steps**[51][60]**

As illustrated in Fig 23, Okushima et al. designed two T-junction drop-makers located in series to produce double emulsion**[56].**

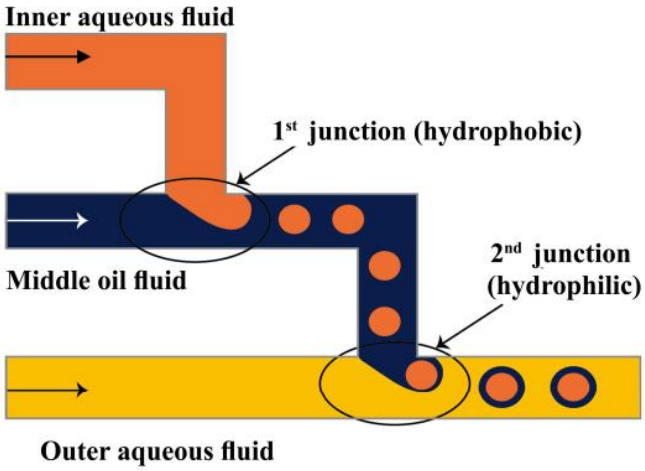

Figure 23 Using two T-junction for double emulsion formation**[51][56]**

In Fig 24, two-step double emulsion microfluidics for producing W/O/W droplets is illustrated. The first part of channel is treated hydrophobic and the second part hydrophilic.

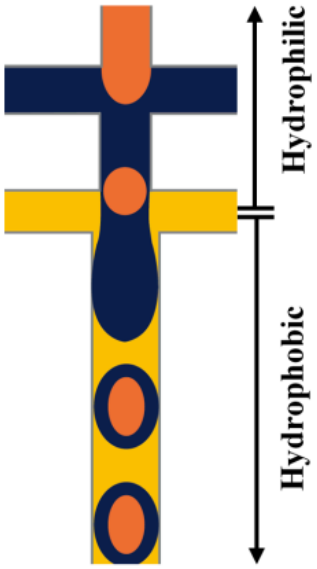

Figure 24 Using two flow focusing for W/O/W double emulsion formation**[51][60]**

The other group of double emulsion microfluidics fabricate core/shell drops in a single step. Two single steps double emulsion microfluidics are illustrated in Fig 25 and 26. In the first design, illustrated in Fig 25, double flow-focusing is fabricated to produce double emulsion in a single step. The size of droplets in the single step method is dependent on the flow rate ratio of phases and the size of orifice. In the second design, as shown in Fig 26, A.P.Lee et al. designed microfluidics composed double flow-focusing unit. Running different experiments, a power relation between the size of inner droplets and ratio between the continuous phase and summation of inner and middle flow rates was found**[61]**.

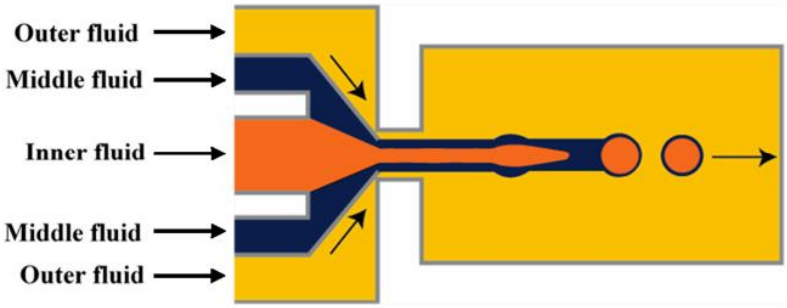

Figure 25 Using lithography-based microfluidics for double emulsion formation in a single step**[62][51]**

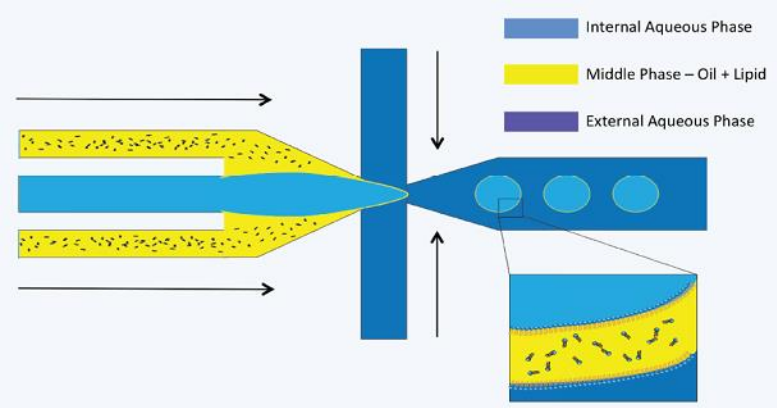

Figure 26 Using lithography-based microfluidics for double emulsion formation in single step**[61]**

The main advantage of two-step double emulsion formation is that the size of the inner and outer droplets is more controllable in comparison with single-step methods. If the first drop-maker is faraway enough from the second drop-maker, two distinct drop-maker can be easily controlled to produce double emulsions with the desired sizes. However, the drawback of both methods is that the wettability of the surface should be controlled very precisely which, otherwise, the stability of double emulsion formation is adversely affected. In 2017, Weitz's group proposed using tandem microfluidics to solve the issue of surface treatment**[63]**. In this method, similar to two step method, the inner droplet is formed in a dropmaker and then the enveloped by the middle phase and produce double emulsion in the second dropmaker. However, in this method the first and second drop makers are located in two distinct chip. Therefore, in the first inner droplet is formed and transported to the second chip for double emulsion formation using tubing. A schematic of this method is shown in Fig 27.

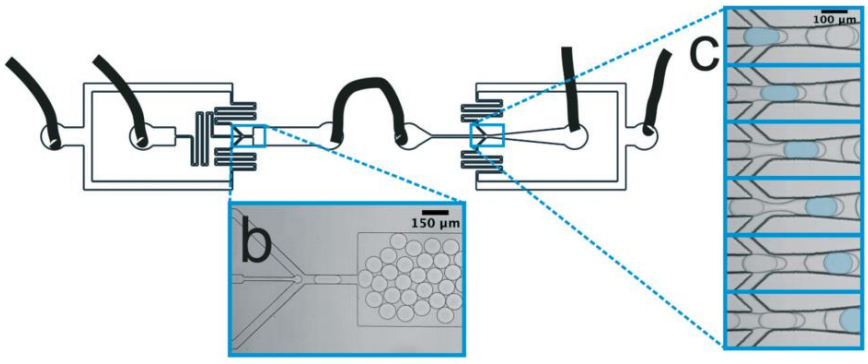

Figure 27 Using tandem microfluidics for double emulsion formation**[63]**

Two main advantage of using tandem microfluidics are avoiding coupling effect between first and second drop makers and selective surface treatment of chip for producing double emulsion. The challenge of using this method for double emulsion is that the spacing between droplets during their transportation from the first chip to the second chip is not uniform which can adversely affect the monodispersity of generated double emulsions. In this thesis, a solution is proposed for solving the issue of non-uniform spacing between droplets during their transportation in order to generate monodispersed double emulsion with thin middle phase.

In order to produce polymersomes, the second step is to extract the middle phase to form the bilayer of polymersomes. In the next section, a review is done on the physics and different methods employed for extraction of the middle phase of double emulsions.

2.4 Dewetting

One of the key steps in formation of polymersomes is the extraction of the organic phase from the bilayer of generated double emulsions. As illustrated in Fig 28, the diblock copolymers are merged and form the bilayer of polymersomes instantly after the dewetting of the organic phase from the middle phase.

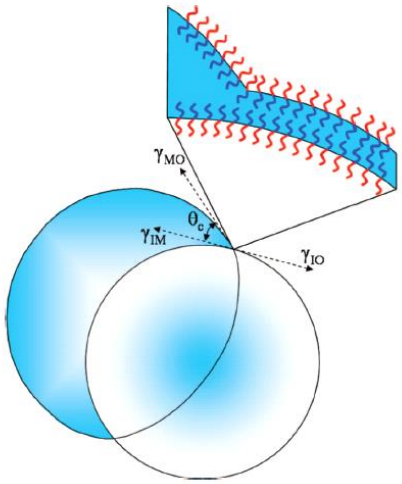

Figure 28 Extraction of middle phase for formation of double emulsion**[64]**

When three immiscible liquids are in contact with each other, the equilibrium morphology of the system can be predicted by calculating the interfacial energy. The energy of an interface can be defined by a parameter called spreading coefficient. Spreading coefficient of an interface between

two liquids is the tendency of a fluid phase to spread on the fluid interface. The spreading coefficient of an interface can be defined as:

$$S_k = \gamma_{ij} - \gamma_{ik} - \gamma_{jk} \quad (2)$$

Where S_k is the spreading coefficient between the interface of fluid i and j and γ_{ij}, γ_{ik}, γ_{jk} are the interfacial tension between i, j and k phases **[65][61][66][67]**. Three possible morphology is possible for a double emulsion suspended in a liquid: complete engulfing (formation of a double emulsion), partial engulfing and non-engulfing. The morphology of the system can be predicted by calculating the spreading coefficient of the system. As illustrated in Fig 29, the dewetting of the middle phase in a double emulsion occurs when the spreading coefficient of the outer phase becomes positive. In this case, the interface of inner and middle phases tends to spread on the fluid interface of inner and middle by extracting the middle phase from the double emulsion. Therefore, by changing the interfacial tension energy of system immiscible liquids, the morphology of the system can be changed. In what follows, two different methods are proposed for extracting the middle phase or reducing the thickness of middle phase by separating a fraction of the middle phase.

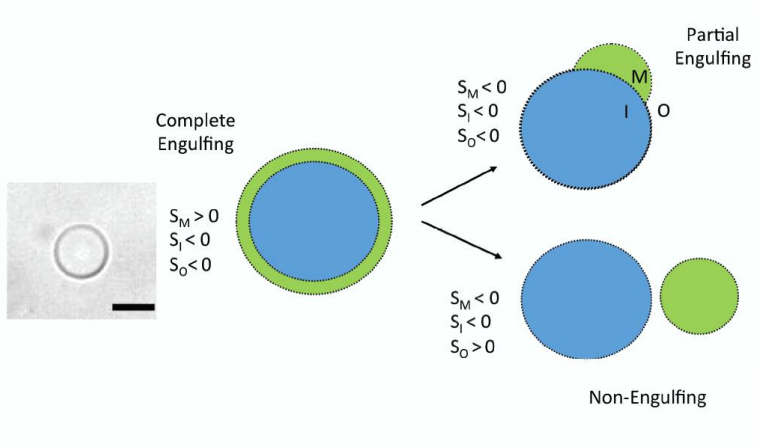

Figure 29 Three possible morphology**[61]**

The conventional method for dewetting is based on dissolving the double emulsion in Ethanol. Ethanol diffuses to the middle phase and, by reacting with the organic phase, facilitates the extraction or evaporation of the middle phase to produce polymersome**[22][5]**. However, as such a bulk method is uncontrollable, it has always been observed that in some portion of double

emulsions, dewetting steps are not done completely. Moreover, conventional methods are very time consuming and mostly the double emulsions should be kept in the solvent for over 10 hours to evaporate all the middle phase**[68]**. The other limitation of conventional method is that the oil phase should be chosen very carefully to be volatile enough to be evaporated after double emulsion formation.

Recently, a lot of effort has been done to do dewetting on-chip by affecting the surface tension between phases in order to speed up the dewetting process and enhance its efficiency as in the microfluidic chips, the process is more controllable in comparison with bulk methods. In 2016, surfactant-assisted method was proposed by T. S. Huck et al. to precisely control the surface tension between inner and middle phases in order to facilitate dewetting by affecting the interfacial tension between phases on chip**[66]**. In Fig 30, it is shown the process of liposome formation using a surfactant. As it was explained previously, the surfactant is added to the phases to satisfy the condition mentioned in Fig 29 the extraction of the middle phase.

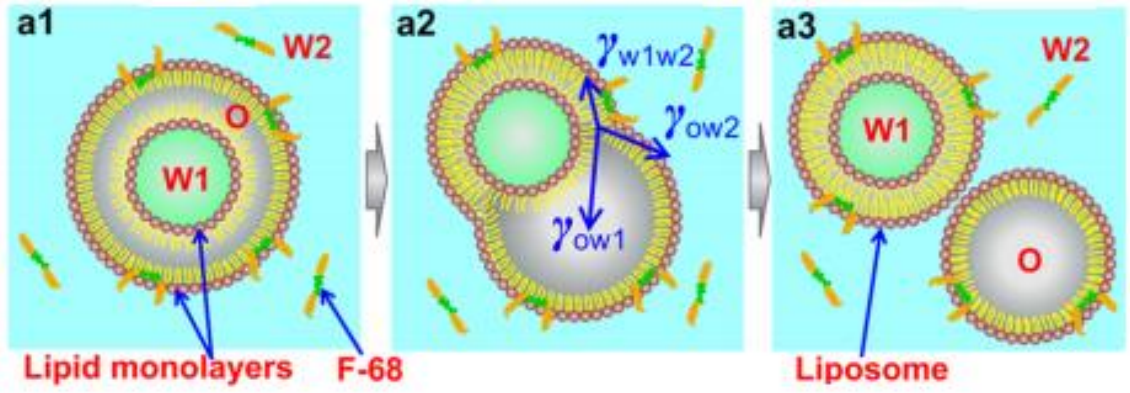

Figure 30 The process of liposome formation using surfactant **[66]**

In 2017, Dekker's group, proposed an on-chip method for liposome production. In this method, as illustrated in Fig 31, Octane was used as the organic phase instead of Oleic acid in order to have the desired surface tension between phases to do dewetting on-chip instantly after the formation of double emulsion**[54].**

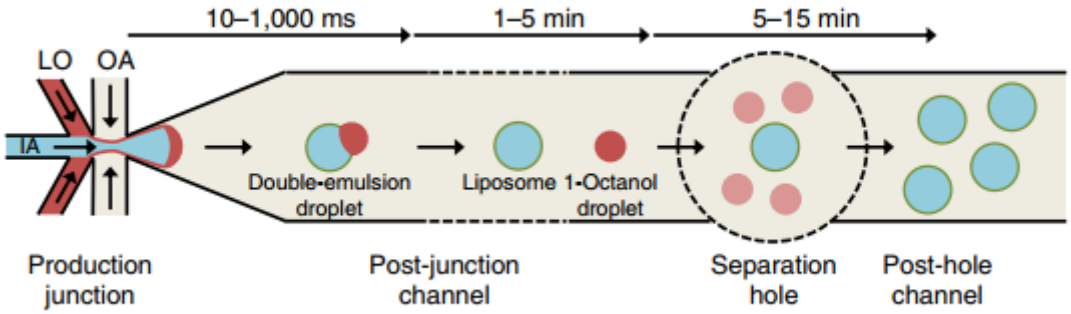

Figure 31 On-chip dewetting using octane as the organic phase**[54]**

In 2016, Peitt et al. used ethanol with concentration 14% wt. [84] in the outerphase of double emulsion in order to extract the oleic acid and generate polymersomes. They observed that oleic acid in double emulsion dissolved in DI water containing ethanol with concentration 14% wt were extracted few hours after the formation of double emulsions. In this project, oleic acid is used as the middle phase to avoid PDMS swelling. Moreover, Peitt et al. method was used to extract the middle phase and formation of polymersomes. [84]

Chapter 3: Materials and fabrication

In this section, experimental methods and protocol and experimental facilities going to be utilized for this thesis are explained.

3.1 Microfabrication

The microchannel is fabricated using soft lithography method. The process is started from designing the photo mask containing the negative image of microchannel. The photomask is designed in AutoCAD software and printed on Mylar films. Different SU-8 types with different viscosities are used for fabrication. Therefore, based on the required thickness, the SU-8 should be determined as the first step of fabrication. UV exposure cross links the SU-8 material by making a chemical reaction on the exposed region. The dose of exposure must be determined very carefully since low dose causing cross-linking does not extend to the substrate and the Su-8 features to lift off. The final step of cross linking is baking the water at 65C and 95C. In this step, the non-exposed SU-8 region is dissolved in order to create the desired microchannel pattern on SU-8. A jar is poured with SU-8 developer. Then, the nitrogen bubbling rod is placed in the jar and turned very slowly until there would be only a little agitation. The wafer is suspended in the SU-8 developer while being held by the wafer dipping holder. The next step is being washed by the isopropanol until no white solute appears and all the non cross-lined SU-8 being removed. The final step is washing the wafer with ultra-pure water and dry with blown air. After finishing fabrication of the master, PDMS replica mold is fabricated from the master and bonded to the glass to create the desired microchannel. PDMS is poured over the master and degassed remove any possible trapped bubbles. Then, the PDMS mold is baked at 95C for 1-1.5h. The inlet and outlet of the microchannel in the PDMS is punched using biopsy punches. The final step is bonding the PDMS mold to the glass slide using plasma cleaner. In Fig 32, a summary of the procedure for fabrication microchannel using soft lithography is presented.

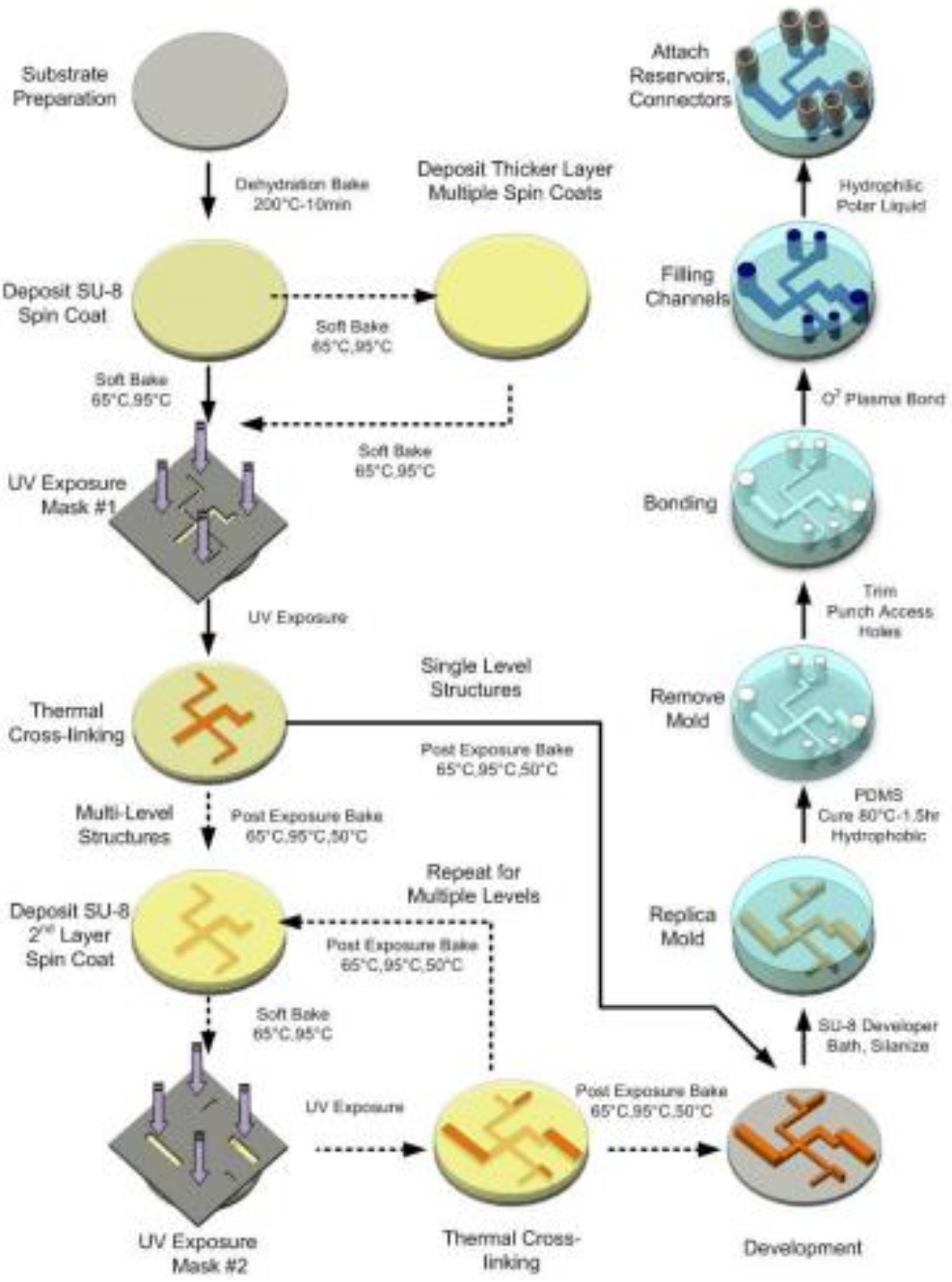

Figure 32 Procedure of microfabrication using soft lithography method [69]

3.2 Materials

3.2.1 Oil phase

As discussed in the previous chapter, the first step of polymersome formation is producing W/O/W double emulsions. Diblock copolymers are dissolved in the oil phase in order that after extraction of oil phase, create the bilayer of polymersome. Diblock copolymers are dissolved in different organic phases such as Toluene, Chloroform and oleic acid. Since, Toluene and Chloroform are strong organic phases, they can swell PDMS. Therefore, glass like coating is used in order to avoid swelling of the PDMS. In this thesis, Oleic acid is utilized in order to prevent the necessity of using glass like coating of the PDMS. Middle phase consists of poly(butadiene)-b-poly(ethylene oxide) or PbD_{40}-b PEO_{34} dissolved in oleic acid with the concentration of 1 mg/ml.

3.2.2 Aqueous phase

The outer phase of double emulsion is created from DI water, Glycerol and ethanol. Glycerol is added to the solution in order to increase the viscosity of outer phase which can facilitate the pinching of droplets in the second drop maker. Moreover, ethanol is added to the solution in order to extract the oleic acid from the middle phase after formation of double emulsion resulting formation of bilayer and polymersome. The concentration of Glycerol and ethanol in the outer phase are 50% wt. and 14 % wt., respectively. Glycerol and ethanol are not added to the inner phase as the inner phase is not responsible for pinching off droplets or extraction of oil phase. Hence, pure DI water is employed as the inner phase.

3.3 Experimental setup

The setup consists of pressure controller system, syringe pump, a TiE-inverted microscope, flow-sensors, a high-speed camera, a CCD camera, a UV light handheld, and a mercury lamp.

Pressure controller system and syringe pump are used for pumping the flow through microchannel. The priority is to use pressure controller pump rather than syringe pump as the flow rate generated by the pressure pump has fluctuation which can adversely affect the droplet formation. At low revolutions, stepper motor generates pulsate flow and at high revolutions, deficiency in the derive screw of the syringe pump make some changes in the flow rate. Therefore, for project that the accuracy of flow rate is very crucial, utilization of pressure controller system is highly recommended. However, as maximum pressure applied to the system by pressure controller is 2 Bas, for project 2 and 3 that high flow rate inside the channel is required, syringe pump is going

to be used. The pressure system used in this project can apply four pressure at the same time. Flow sensor is utilized to measure the flow rate inside the channel when pressure controller system is used. To visualize the channel and video record the droplet formation or middle phase extraction, inverted epifluorescence microscope system and NIS software. Two cameras are installed on the microscope to take image and record video. Phantom V210 high speed camera with the full resolution of 1280×800 with 12-bits image quality take images with the speed of 2190 fps. Moreover, CCD camera is installed on the microscope to take images with high resolution. ImageJ software is utilized to analyzed images and videos.

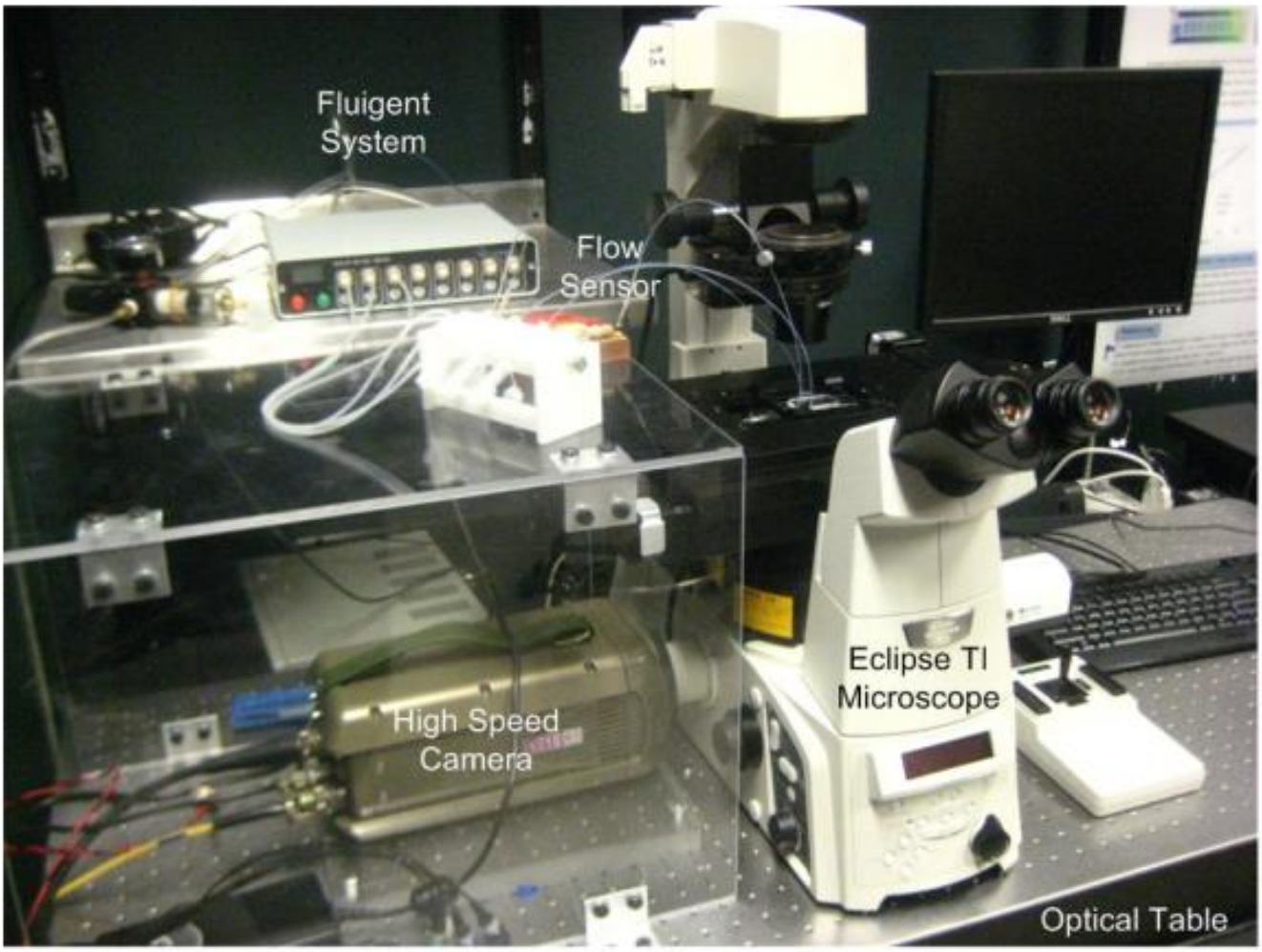

Figure 33 Laboratory facilities**[69]**

Chapter 4: Methodology and circuit analysis

4.1 Methodology

As mentioned in chapter 2, lithography-based microfluidics for double emulsion formation are generally categorized into three groups:1- single-step 2- two-step 3- tandem. The main drawback of single-step and two-step methods is that the wettability of the surface should be managed very precisely. Otherwise, the stability of double emulsion formation is adversely affected. Moreover, as the generation of the inner and outer droplet is not decoupled, two issues are raised: 1- lack of existence of thorough guideline for double emulsion generation due to the high complexity of the system 2- instability in one of the droplet generation can significantly affect the other one. In 2017, Weitz's group proposed using tandem microfluidics to solve the issue of surface treatment **[63]**. In the tandem method, similar to two-step method, inner droplet is formed in the first drop-maker and, then, enveloped by the carrier fluid. The first and second drop-makers are separately fabricated in two microfluidic chips. Therefore, a PEEK tubing acts not only as a bridge to connect both chips together but also as a channel to transport inner droplets from the first drop-maker to the second one. The main challenge for using the tandem microfluidics method is that the spacing between the droplets is not uniform during the transportation. This results in low encapsulation of the inner droplets into outer droplets. Consequently, the fraction of generated droplets without single cores is high. Moreover, to produce small droplets, the flow rate of continuous phase in the first drop-maker is usually much higher than the flow rate of the dispersed phase; so that, production of double emulsions with thin middle phase is limited in this method. Production of double emulsions with thick middle phase is not appropriate for some applications such as the generation of polymersome and liposome as the extraction of a thicker middle phase is more difficult. Therefore, a method should be employed to control the volume of the oil phase in the second chip. In this project, an optimized microfluidics design is proposed to precisely control the spacing between single emulsions coming from the first chip before they are encapsulated into outer droplets. This design will improve the monodispersity of generated double emulsions and enable producing droplets with various sizes, especially small droplets with a thin middle phase. Moreover, by decoupling the first and second drop-makers, instability transfer from the second drop-maker to the first one is limited and controlling the size of the inner and outer droplet is separately achieved. To achieve this, we designed an extraction channel that is embedded in the

second chip to control the spacing between single emulsions by extracting the desired volume of the oil phase. In Fig 34, a schematic of the design is presented.

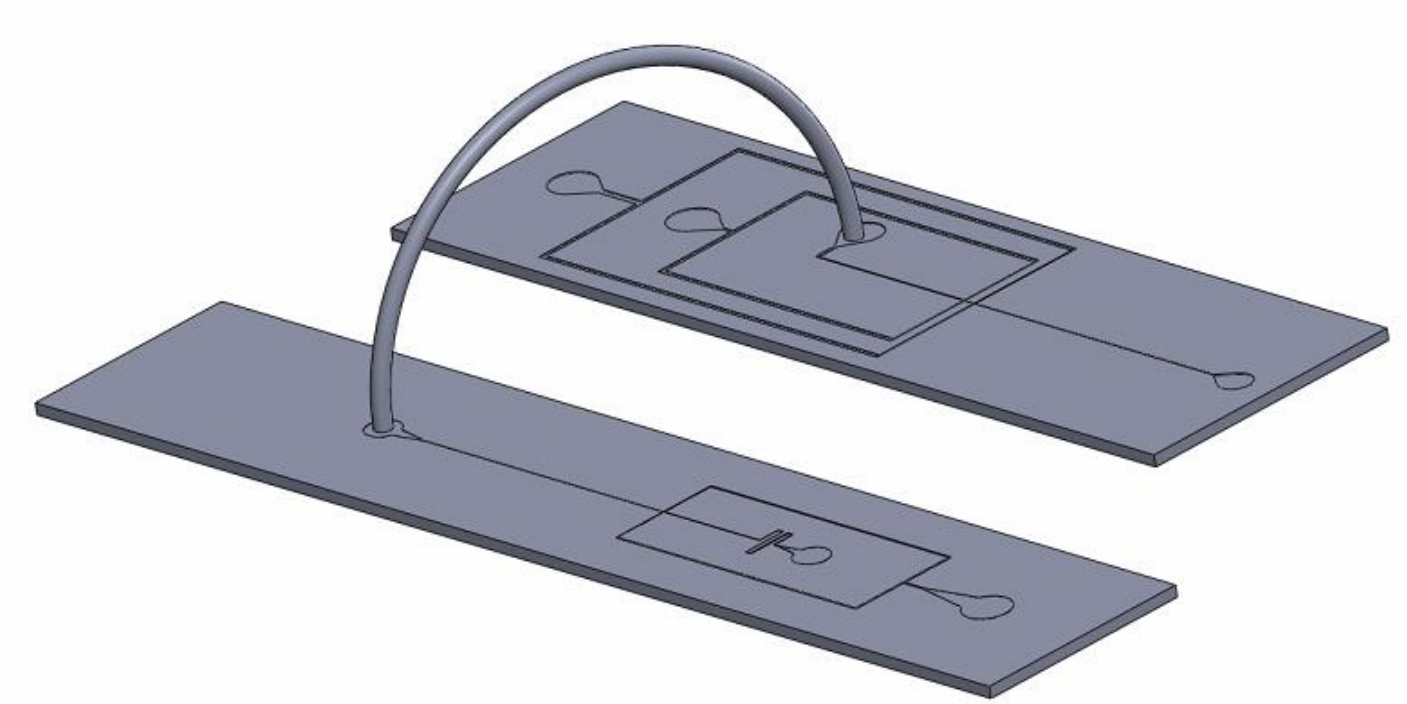

Figure 34 Schematic of the design including first chip, tubing and the second chip

This method composed of three different compartments: 1- first chip responsible for the generation of inner droplet of double emulsion 2- tubing responsible for transportation of single emulsions to the second chip 3- second chip responsible for tuning the volume fraction of single emulsion to the oil phase and generating of double emulsion. In what follows, each compartment is explained in more details.

First Chip:

In the first chip, as illustrated in Fig 34, the inner droplet of the double emulsion is created in order to be transferred to the second chip. To generate a high monodispersed sized single emulsion on the first chip, single emulsions (w/o droplets) are generated using a flow-focusing (cross-junction). The induced symmetric shear during the droplet generation process assists the uniformity of droplet size. In order to have high monodispersity, the flow rates of continuous (Q_c) and dispersed phases (Q_d) are controlled to form the droplets under the squeezing regime. Under the squeezing

regime, as droplets are confined by the microchannel walls, the monodispersity of droplet generation is higher. A schematic of droplet generation in the first drop maker is illustrated in Fig 35.

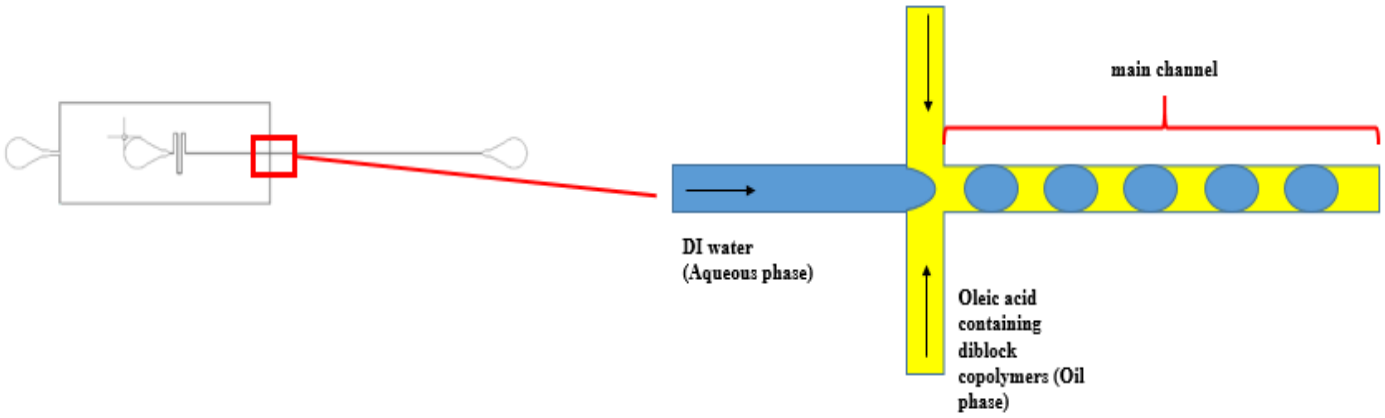

Figure 35 Schematic showing droplet generation in the first chip

In order to produce droplets with the desired size and high monodispersity, the influence of different parameters on the size of droplets is investigated. As shown in equation 3, size of the droplet is a function of flow rate ratio of dispersed phase to continuous phase, viscosity ratio of dispersed phase to continuous phase, the geometry of channel and the interfacial tension between dispersed and continuous phases.

$$V^* = f\left(\frac{Q_{d_1}}{Q_{c_1}}, \frac{\mu_{d_1}}{\mu_{c_1}}, \sigma_{d_1 c_1}, geomtrical\ parameters\right) \quad (3)$$

where V^* is the ratio of volume of droplets to $w_m^2 h$. Therefore, as shown in equation 4, for the designed channel, specified dispersed and continuous phases and diblock copolymer concentration, geometry, interfacial tension and viscosity ratios are constant, the volume of droplet is only a function of flow rate ratio. In the Experimental and Discussion section, the influence of the systematic flow rate ratio on single emulsion size is investigated.

$$V^* = f\left(\frac{Q_d}{Q_c}\right) \quad (4)$$

Tubing:

Single emulsions are delivered to the second microfluidic through a PEEK tubing with an inner diameter less than 0.03 inches. Droplet coalescence, during a transportation stage, is avoided by

adding diblock copolymers and tuning the interfacial tension between single emulsions and continuous phase. In this current study with DI water as the dispersed phase, diblock copolymer (poly(butadiene)-b-poly(ethylene oxide) or PbD_{40}-b PEO_{34}) with the concentration of $1\ mg/ml$ is added to the oleic acid.

Second Chip:

In the second chip, as illustrated in Fig 36, single emulsions coming from the first chip are enveloped by the third phase, and double emulsions are generated. In order to pinch off the oil phase and generate double emulsions, the cross junction is added to the second chip. However, without controlling the spacing between single emulsions and tuning the volume fraction of single emulsions to the oil phase, single oil emulsions are generated, and even the monodispersity of double emulsion is not good. Therefore, an extraction channel, illustrated in Fig 36, is added to the second chip before the junction in order to reduce the volume of the oil phase and force single emulsions to be back to back in contact with each other. This results in controlling the thickness of generated double emulsions and eliminating the generation of single oil emulsions. Therefore, the volume of the oil phase, which can affect the thickness of double emulsions, can be varied by tuning the flow rate ratio of the extraction channel to the continuous phase channel. In order to vary the flow rate ratio of extraction channel to the continuous phase channel, the pressure applied to the inlet of extraction is changed while the pressure applied to the continuous phase channel kept constant. The spacing between single emulsions should be synchronized by the frequency of droplet generation in the junction in order to eliminate single oil generation and generation of double emulsion with different sizes.

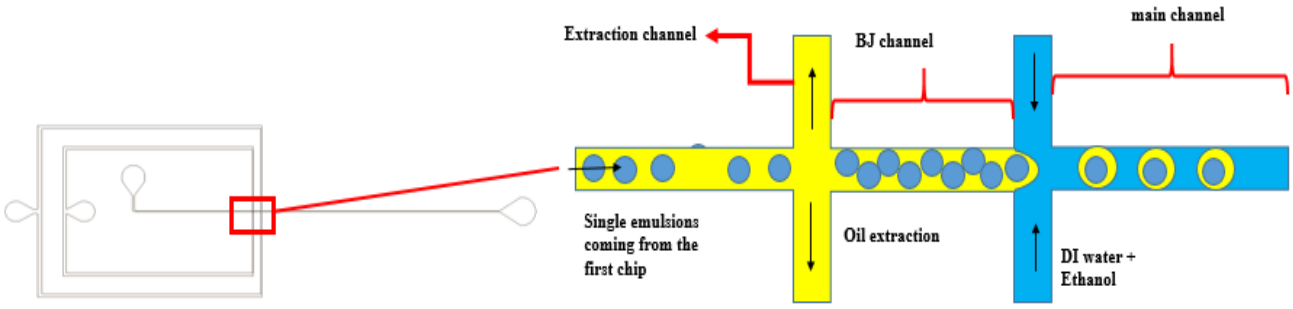

Figure 36 Schematic showing double emulsion generation in the second chip

To show the capability of the designed chip in producing double emulsion with different sizes and middle phase thicknesses, the flow rate ratio of dispersed phase to continuous phase in the first chip is varied. Moreover, the flow rate ratio of the summation of the dispersed phase and continuous phase in the first chip to the flow rate of continuous phase in the second chip and the flow rate ratio of extraction channel to dispersed phase in the second chip are varied. Therefore, the first and second chips are characterized, and the volume and thickness of double emulsion as a function of flow rate ratios are obtained. Moreover, in order to prove the decoupling of the first and second chip, it is important to make sure during changing the pressure applied to the outer phase and extraction channel, the size of generated single emulsions in the first chip is not affected. Therefore, in the next chapter, the effect of applied pressure to the outer phase on the size of the generated single emulsions in the first chip is investigated.

$$T = f\left(\frac{Q_{d1}+Q_{c_1}-Q_{extraction}}{Q_{c_2}}\right) \quad (5)$$

Where T is the thickness of middle phase in double emulsion.

4.2 Design criteria

In 2015, a model was developed by Glawdel et al. for designing a flow-focusing channel for producing monodispersed single emulsions in the squeezing regime. [36, 69] The model is utilized for designing the first and second dropmakers in the first and second chips. In this section, a comprehensive design guideline is provided for designing the extraction channels in the tandem microfluidics. As discussed in the previous section, the whole chip consists of two dropmakers and one extraction channel. The aim of this design is to produce monodispersed double emulsions with the desired size by tuning the flow rate ratios. The core size of double emulsion is specified in the first chip. However, for producing small single emulsions, the flow rate ratio between dispersed and continuous phase in first chip must be very small resulting in high volume fraction of oil phase to the single emulsions in the second chip. Having high volume fraction of the oil phase to the single emulsions in the second chip has two consequences: 1- generation of single oil emulsions 2- production of double emulsions with a thick membrane. Generating single oil emulsions necessitates the separation of double emulsions from the single oil emulsions in the outlet of second chip and adversely affect the monodispersity of generated double emulsions. Moreover, as the main target of this project is to generate polymersomes, producing double

emulsions with a thick membrane makes the production of polymersomes more difficult because of the challenges in oil extraction. Hence, to improve the monodispersity of generated double emulsions, eliminate the generation of single oil emulsions and produce double emulsions with thin middle phase, extraction channel is embedded in the second chip to control the volume ratio of single emulsion to the oil (Fig 36).

The main purpose of adding extraction channel to the second chip is to reduce the volume fraction of oil phase to the single emulsions coming from the first chip by extracting the desired oil phase in order to prevent the formation of single oil emulsions, generate double emulsions with thin middle phase and improve the monodispersity of generated double emulsions.

To successfully generate single and double emulsions in the first and second chips, respectively, design criteria proposed by Glawdel et al. [36, 69], was adopted in this study. Based on that design criteria, in order to minimize the fluctuation of droplet generation, the width of the continuous and dispersed phase was set the same ($w_d = w_c$). Moreover, the hydrodynamic resistance of the dispersed phase was taken two times higher than the continuous phase channel and same as the main channel. Furthermore, in order to eliminate fluctuation in flow rates after droplet generation in the first and second dropmakers, the length of the main channel (name of the channel shown in Fig 35 and 36) in the first and second chip was set high enough to contain 50 droplets. If the length of the main channel was too small, entering and exiting droplets from the main channel would lead to high fluctuation in the flow rates and if it was too long, high enough pressure should be applied to the inlet. Four design criteria are explained about designing the extraction channel. To better consider and understand the criteria used in designing first and second chips, 1D circuit analysis is used. The circuit used for considering the criteria is shown in Fig 37.

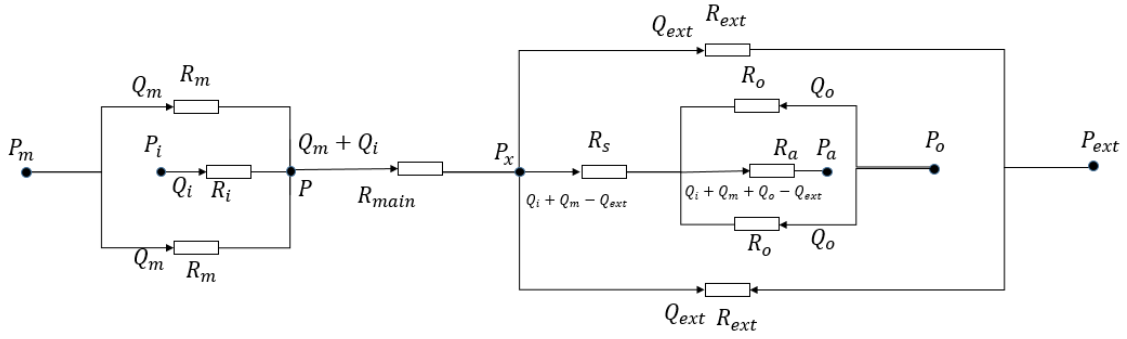

Figure 37 Electric circuit for the first and second chips

As discussed before, to eliminate the formation of single oil emulsions and produce double emulsions with thin middle phase, extraction channel is employed to reduce the volume fraction of oil phase to single emulsions coming from the first chip. The first criterion which should be satisfied is that single emulsions in the BJ channel (name of the channel shown in Fig 36), as illustrated in Fig 36, must be back to back and in contact with each other. Having packed single emulsions in the BJ channel is more challenging when the fraction of the oil phase to the single emulsions is high, resulting the necessitate of extraction more oil phase. Based on the experimental results on the first chip, the maximum volume fraction of the oil phase to the single emulsions is 20, and this belongs to the generation of single emulsion with the size of $50\ \mu m$. Therefore, the first criterion is to extract enough oil phase in order to pack single emulsions in the BJ channel for the volume fraction of 20. The second criterion is that the hydrodynamic resistance of the extraction channel must be large enough to avoid the backflow in the BJ channel. If the hydrodynamic resistance of the extraction channel is too small, the outer phase will enter the BJ channel. Moreover, for large hydrodynamic resistance of the extraction channel, the required oil phase for packing single emulsions in the BJ channel is not extracted. The third criterion is that based on experimental results, when single emulsions are squeezed in BJ channel, they are splitted in the junction, and double emulsions with different core sizes are created. Therefore, in order to eliminate squeezing of single emulsions in the BJ channel, the width of BJ channel should be larger than the size of single emulsions. The last criterion is avoiding single emulsions insertion to the extraction channel using a suitable pillar. In what follows, the first and second chips are designed based on the above criteria.

Chip I:

As discussed before, the first chip is designed based on design criteria developed by Glawdel et al. in 2015. [36, 69] The following conditions should be satisfied by design.

1- In the junction, it is recommended that $1 \leq \Lambda = \frac{W_d}{W_c} < 1/3$ (in flow-focusing design) to reduce the fluctuation caused by Laplace pressure during droplet generation
2- The length of the main channel should be large enough to include at least 50 droplets to eliminate the droplet generation caused by entering and exiting of droplets from the main

channel. Therefore, it was recommended to take the length of the main channel: $L_m = 50 \times 6 \times W_m$

3- In order to eliminate backflow during droplet generation, it is recommended that the hydrodynamic resistance of the dispersed phase and the main channel would be equal and larger than the continuous phase. $R_m \approx R_d \gg R_c$
4- To be in the squeezing regime, as in this regime, the stability and monodispersity of produced droplets are better, the capillary number of continuous phase should be in the range of $0.001 \leq Ca_c \leq 0.1$
5- Based on the pressure pump we are currently using in our lab, P_c and $P_d \leq 1000 - 1500$ mbar
6- It should be noted that If the length of the orifice is short, the required pressure difference between the upstream and downstream in the junction for pinching off the droplet won't be provided. Moreover, the volume of the orifice should be almost the same as the minimum droplet size that should be generated. Therefore, the width of the channel can be estimated.

In order to satisfy the first design criterion, the width of the dispersed and continuous phase was set to be the same ($w_d = w_c = 50\ \mu m$). Moreover, based on the second design criterion, the length of the main channel was set to $1.5\ cm$. The length of dispersed and continuous phase channel, the height of the chip and the width of the main channel were set to satisfy the third design criterion. ($L_d = 4.5\ cm\ and\ L_c = 0.5\ cm, w_m = 50\ \mu m$). Furthermore, based on the sixth design criterion, the width and length of orifice were set to $30\ \mu m$ and $30\ \mu m$, respectively. The CAD design of the first chip is shown in Fig 38.

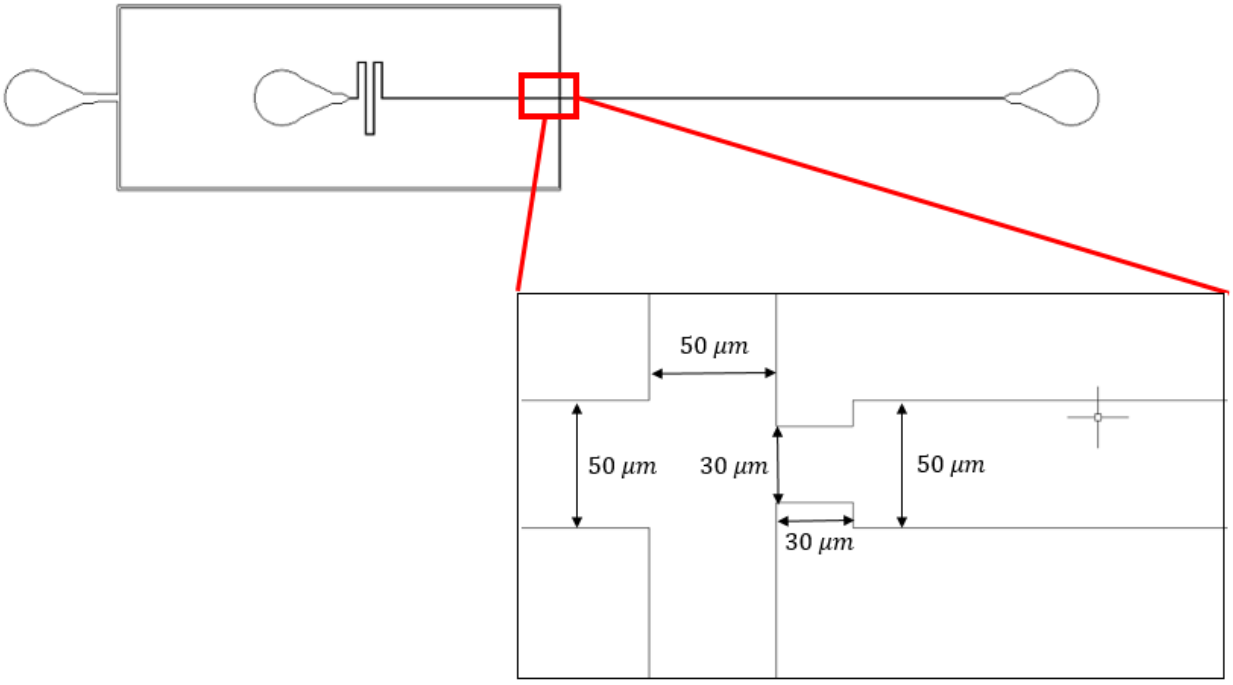

Figure 38 Schematic of the first chip

Second chip:

As illustrated in Fig 36, second chip consists of a flow-focusing dropmaker and an extraction channel in order to control the spacing between single emulsion coming to the second chip. The design criteria used for the designing the dropmaker is the same as criteria mentioned in the previous section. The design criteria for designing the extraction channel are as follows:

1- Single emulsions in the BJ channel, as illustrated in Fig 36, must be back to back and in contact with each other.
2- Hydrodynamic resistance of extraction channel must be large enough to avoid the backflow in the BJ channel and small enough to enable extract the desired fraction of the oil phase mention in the first design criterion.
3- To eliminate single emulsions splition, the width of BJ channel should be at least equal to largest single emulsions generated in the first chip.
4- Single emulsions should be avoided to be inserted to the extraction channel using pillar.

First Criterion:

The first criterion is to extract enough oil so that single emulsions would be back to back in contact with each other in the BJ channel. Based on the experiments ran for the first chip, the minimum volume fraction of single emulsions in the first chip is for droplets with size of $50\ \mu m$ which is 20. Based on Fig 39, for single emulsions with the size of $50\ \mu m$, the volume fraction in BJ channel with this assumption that the width and height of BJ channel were set to $100\ \mu m$, should be 0.261 in order that single emulsions would be back to back in contact with each other.

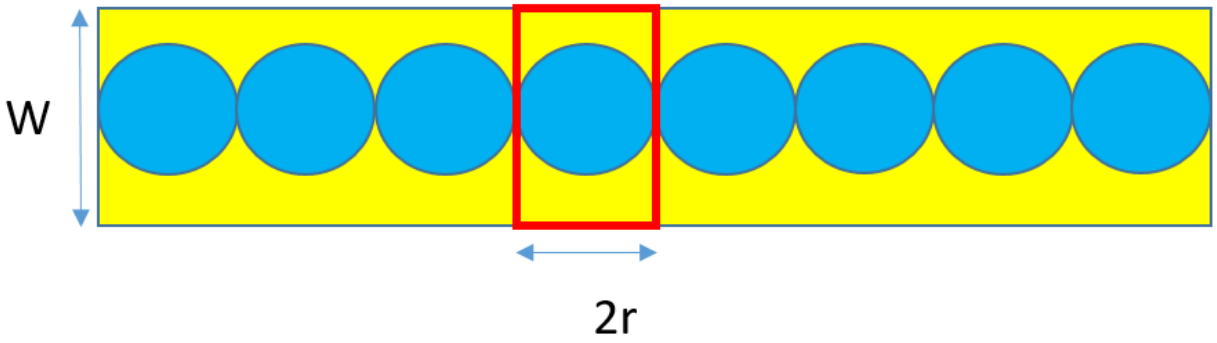

Figure 39 Schematic of single emulsions in the BJ channel

$$\frac{V_{single\ emulsion}}{V_{oil\ phase}} = \frac{\frac{4}{3}\pi r^3}{2r \times W \times h - \frac{4}{3}\pi r^3} = \frac{\frac{4}{3}\pi(25)^3}{2\times 25\times 100\times 100 - \frac{4}{3}\pi(25)^3} = 0.1506 \quad (6)$$

Where h and W are the height of chip and width of BJ channel, respectively. As the volume fraction of single emulsions in the first chip based on the experiments ran on the first chip, is 0.0476, enough oil phase should be extracted to increase the volume fraction to 0.1506. Flow rate ratio is a good approximation of volume fraction. Therefore, as shown in Fig 37, the volume fraction of single emulsions before and after extraction can be calculated using the flow rate of different phases. The volume fraction of single emulsions before extraction channel is calculated as:

$$Volume\ fraction\ (before\ extraction\ channel) = \frac{Q_i}{Q_m} \quad (7)$$

Moreover, with this assumption that the extraction of single emulsion from the extraction channel is almost eliminated by the pillars, the volume fraction in BJ channel is calculated as:

$$\text{Volume fraction (after extraction channel)} = \frac{Q_i}{Q_m - Q_{extraction\ channel}} \quad (8)$$

Therefore, the flow ratios of the inner phase (dispersed phase in the first chip) to the middle phase (continuous phase in the first chip) and extraction channel to the middle phase is estimated as:

$$\frac{Q_i}{Q_m} \sim 0.0476 \quad (9)$$

$$\frac{Q_{extraction\ channel}}{Qm} \sim 0.6839 \quad (10)$$

The maximum oil extracted when the extraction channel is connected to the atmosphere. Therefore, when pressure P_a and P_{ext} are zero in Fig 37, the desired fraction of oil should be extracted. Based on electric circuit drawn in Fig 37, we have:

$$\left.\begin{aligned} P_x &= (Q_i + Q_m - Q_{ext}) \times R_s + (Q_o + Q_i + Q_m - Q_{ext}) \times R_a \quad (11) \\ P_x &= Q_{ext} \times R_{ext} \quad (12) \end{aligned}\right\} \Rightarrow$$

$$Q_{ext} \times (R_s + R_a + R_{ext}) = Q_m \times (R_s + R_a) + Q_i \times (R_s + R_a) + Q_o \times R\_a \quad (13)$$

Q_o is varied by changing the pressure applied to the inlet of outerphase. Based on equation 13, by increasing Q_o, more oil is extracted from the extraction channel. As the target of the third criterion is to design the chip to enable extract enough oil for packing single emulsions in the BJ channel, the worst case scenario is considered. Therefore, by neglecting Q_o minimum flow rate of extraction channel is calculated. Hence, in equation 14. Q_o is neglected, and the other parameters are found in order to extract the desired fraction of the oil phase. Based on equation 10, 11 and 14:

$$0.6839 \times (R_s + R_a + R_{ext}) = 1.1506 \times (R_s + R_a) \Rightarrow \quad (14)$$

$$\frac{R_{ext}}{R_s + R_a} \sim 0.6824 \quad (15)$$

Second Criterion:

The second criterion is to eliminate backflow from the main channel of the second chip into the extraction channel and outer phase channel into the extraction channel. As the dispersed phase channel in the second chip is connected to the first chip, the hydrodynamic resistance of the dispersed phase channel is too high to allow any backflow into the dispersed channel. Therefore, the main concern is the backflow into the extraction channel or continuous channel. As discussed in the third criteria of the first chip, the resistance of the extraction channel and BJ channel was set equal to the main channel and higher than outer phase channel.

$$R_{ext} + R_s \sim R_a > R_o \quad (16)$$

It is concluded from equation 15 and 16 that:

$$R_{ext} \sim 0.72 \times R_a \ \& \ R_s \sim 0.28 \times R_a \quad (17)$$

Third Criterion:

The third criterion is to eliminate squeezing of single emulsions in the BJ channel. In order to satisfy this condition, the width of BJ channel was set to $100\ \mu m$ which is equal to the largest target size for the core of double emulsion in this project.

Fourth criterion

In order to eliminate the entering of single emulsion to the extraction channel, pillar with a distance of $10\ \mu m$ to the wall of the extraction channel is designed. Based on the resolution of printing for the photomask, the minimum allowed distance between the pillar and wall is $10\ \mu m$. The distance is specified based on the minimum target size of the core of double emulsion in this project.

The other design criteria used for designing the second chip is the same as design criteria explain in the first chip for designing a flow focusing. The hydrodynamic resistance of channels is calculated using the following formula:

$$R = \frac{12\mu L}{wh^3} \quad (18)$$

Where L, w and h are length, width and height of the channel, respectively. Moreover, for estimating the resistance of channels containing droplet, the same method used by Glawdel et al., is utilized. [36, 69]

Based on these design criteria, the following chip is designed for the second chip.

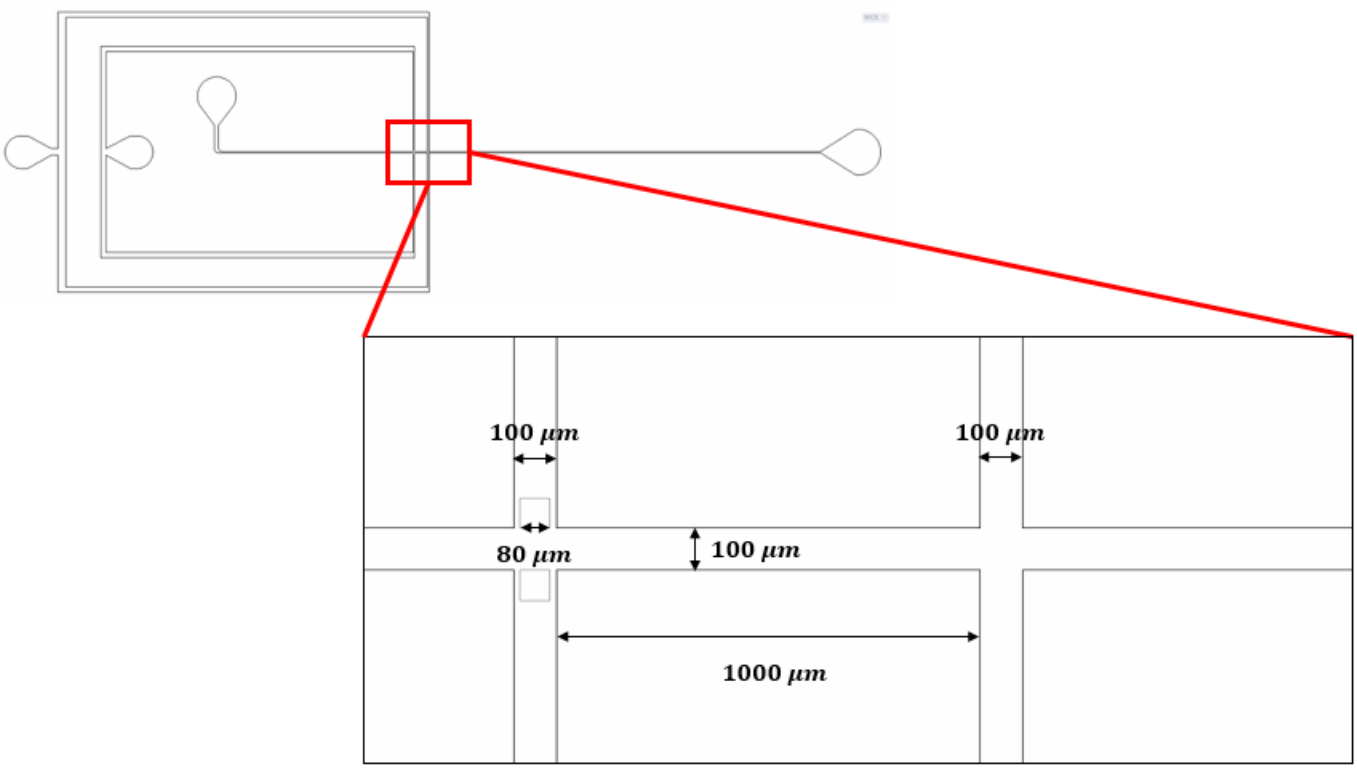

Fig 41 Designed second chip

Chapter 5: Experimental design and results

As discussed in the previous chapter, the first aim of this project is to generate double emulsions with different sizes and reduce their thickness in order to facilitate polymersome formation. Therefore, in this section, the first and second chips are characterized to show the effect of flow rate ratios on the size and monodispersity of generated double emulsions. Then, based on the obtained results, the optimum flow rate ratios for each core size of single emulsions are chosen to generate double emulsions with a minimum thickness of the middle phase and high monodispersity. The last aim of this project is to extract the middle phase of double emulsions in order to form polymersomes. Ethanol with different concentration is used in the outer phase of double emulsions to generate polymersomes. Using different concentration of ethanol, the desired concentration for extraction of the middle phase was specified, and polymersomes are generated. In what follows, at first, experimental procedure and the method used for image analysis and extraction of data from the video and images taken from experiments are explained. Then, the procedure of characterizing the first and second chip are explained, and droplet generation with different sizes and the results of characterizations are presented. At the end, the process of polymersome formation is discussed, and images of generated polymersome are presented.

5.1 Experimental procedure

In these experiments, as discussed before, the two chips are connected via tubing in order to generate double emulsions. First and second chip, as shown in fig 40a, is bonded on a glass and mounted on the microscope stage. A tubing, as shown in fig 40b, connects the first chip to the second chip to transport generated single emulsions in the first chip.

A

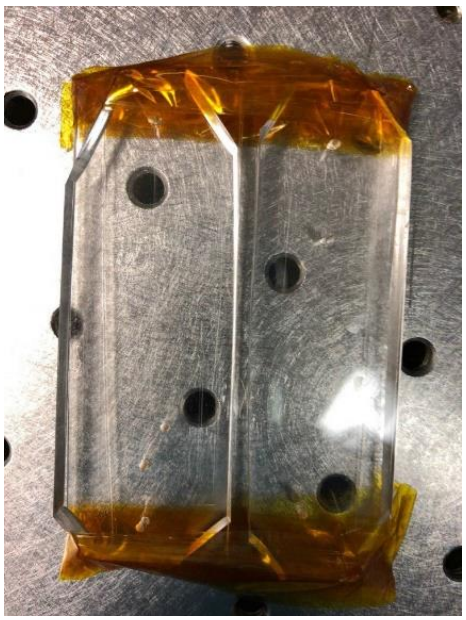

B

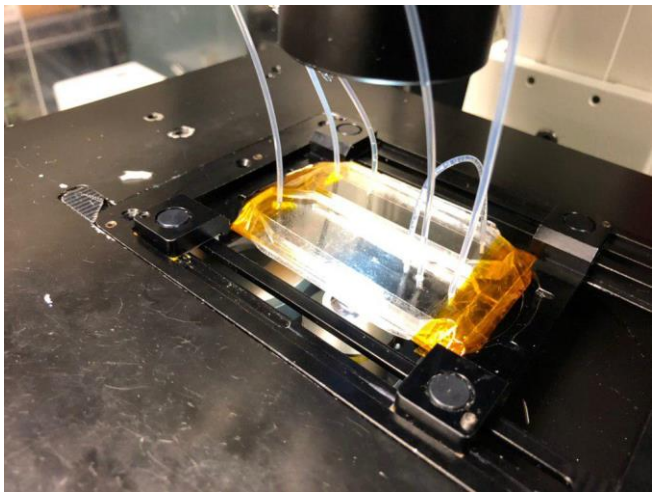

Figure 40 a) first chip and the second chip are mounted on a glass b) first and the second chip are connected via a tubing

Fluigent pressure system is utilized to apply constant pressure to the inlets of first and second chips and extract the oil phase from the second chip. High-speed CMOS camera (Phantom v210, Vision Research) is used to capture droplet generation in the first and second chip with the frame rate of 1000 fps. The maximum possible pressure applied to the system due to the fluigent pressure system

limitation is 1000 mbar. As shown in Fig 37, due to the large hydrodynamic resistance beyond inner and middle phase, the flow rate of the solution containing single emulsions coming from the first chip is low. Hence, the maximum pressure applied to the inlet of the outer phase in the second chip is small. Moreover, based on the experiments, the other limitation for applying high pressure to the outer phase is that for high outer phase flow rate, the shear stress applied to the single emulsions is too high resulting in the splitting of single emulsions in the junction. Some experience of single emulsions splitting due to the high shear stress in the junction of the second chip is presented in Fig 41.

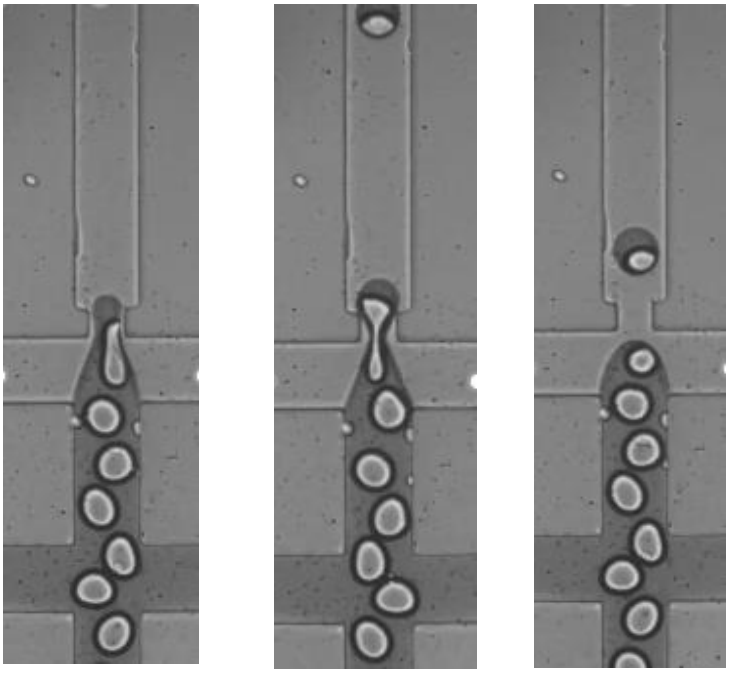

Figure 41 Droplet splitting in the junction of the second chip due to high shear stress

Therefore, due to the limitation of our Fluigent pressure system and to avoid single emulsion splitting, maximum applied pressure to the outer phase inlet is 150 mbar. In this project, the first and second chips are characterized, and the size of generated single emulsions in the first chip and double emulsions in the second chip as a function of flow rate ratio are investigated. Therefore, at first, when the first and second chips are connected, the pressure applied to the inner and middle phase is varied, and the size and flow rate ratios are measured. After characterizing the first chip, the applied pressure to inner and middle phase is set to a constant value, and the second chip is

characterized for two different sizes of single emulsions generated in the first chip. Since the flow rate ratio is important, the pressure applied to outer droplet is kept constant, and the pressure applied to the extraction channel is varied to generate double emulsions with different thickness of the middle phase. Moreover, in order to show the decoupling between first and second chips during experiments, size of single emulsion generated in the first chip is measured at different time in order to show droplet generation in the first chip is not affected by the second chip and the size of single emulsion in the first chip will be always constant if the inner and middle phase pressure is constant. Pressures applied for the first and second experiments are listed in table 2, 3 and 4.

Table 2 Applied pressure to the first and second chip to characterize the first chip

#	P_m (mbar)	P_i(mbar)	P_o(mbar)	P_{ext}(mbar)
1	**860**	**775**	**170**	**130**
2	**860**	**785**	**170**	**130**
3	**860**	**795**	**170**	**130**
4	**860**	**805**	**170**	**130**
5	**860**	**815**	**170**	**130**
6	**860**	**825**	**170**	**130**
7	**860**	**835**	**170**	**130**
8	**860**	**840**	**170**	**130**
9	**860**	**845**	**170**	**130**
10	**860**	**848**	**170**	**130**

Table 3 Applied pressure to characterize the second chip for large inner droplet

#	P_m (mbar)	P_i(mbar)	P_o(mbar)	P_{ext}(mbar)
1	**860**	**845**	**150**	**90**
2	**860**	**845**	**150**	**95**
3	**860**	**845**	**150**	**98**
4	**860**	**845**	**150**	**104**
5	**860**	**845**	**150**	**110**
6	**860**	**845**	**150**	**112**
7	**860**	**845**	**150**	**115**

Table 4 Applied pressure to characterize the second chip for small inner droplet

#	P_m (mbar)	P_i(mbar)	P_o(mbar)	P_{ext}(mbar)
1	**860**	**800**	**125**	**80**
2	**860**	**800**	**125**	**85**
3	**860**	**800**	**125**	**90**
4	**860**	**800**	**125**	**95**
5	**860**	**800**	**125**	**100**
6	**860**	**800**	**125**	**105**
7	**860**	**800**	**125**	**110**

A brief review of the experimental procedure is listed below:

- First chip with the height of $50\ \mu m$ is fabricated and made hydrophobic using aquapel solution. (The procedure is explained in appendix II)
- Second chip with a height of $100\ \mu m$ is fabricated and made hydrophilic using a plasma cleaner machine.
- First chip and the second chip are bonded to a large glass using tape and mounted on the microscope stage
- Oil phase containing diblock copolymers and aqueous phase are prepared
- Tubing are cleaned, and new reservoirs are filled with the prepared solutions
- Fluigent pressure system is connected to the reservoirs and tubing are connected to the first and second chip
- The first chip is run, and single emulsions are generated
- When the tubing connected to the first chip is filled, first and second chip are connected, and the pressure is applied to the outer phase and extraction channel
- During running the experiments, microscope and High-speed CMOS camera (Phantom v210, Vision Research) is used to capture single emulsion and double emulsion generation in the first and second chip, respectively.

5.2 Experimental data

High-speed CMOS camera (Phantom v210, Vision Research) is used to capture images from droplet generation in the first and second chip. Then, image analysis is used to measure flow rates and volume of droplets in each chip. In order to measure the volume and flow rates, ImageJ software is utilized to measure the frequency of droplet generation, the spacing between droplets and length and width of generated droplets. After measuring frequency, spacing, length and width parameters, different procedure is utilized for the first and second chip to estimate the size of generated droplets and flow rates of phases. In what follows, the procedure for each channel is explained.

Chip I:

The first chip consists of a flow-focusing channel to generate single emulsions. To measure the flow rates and volume of generated droplets, the frequency of droplet generation, the spacing between generated single emulsions, and the length and width of generated single emulsions are measured using ImageJ. Different formulas are proposed to calculate the volume of droplets using the width, length of droplets. In 2015, a new formula was proposed to calculate the volume of the droplet in microchannel from a top view image. [83] Based on this formula, the volume of the droplet is:

$$V = \left(hw - (4-\pi)\left(\frac{2}{h} + \frac{2}{W}\right)^{-2} - ch^2\right)\left(L - \frac{w}{3}\right) \quad (19)$$

Where h, w and L are height, width and length of the generated droplet, respectively. Moreover, for microchannels with rectangular cross-section, c is zero. Therefore, after calculating the length and width of generated droplets using ImageJ software, the volume of the droplet is gained from equation 19. The volume ratio of the inner droplet is the nondimensionalized volume of the inner droplet by the height and width of the main channel. The flow rates shown in Fig 42 and the flow rate ratio between the dispersed phase and continuous phase are calculated using the below procedure.

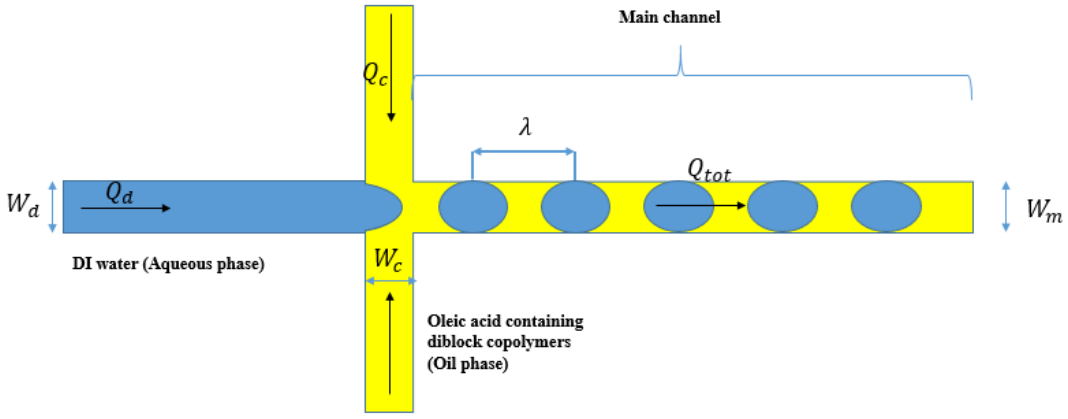

Figure 42 Schematic of droplet generation in chip I

$$Q_d = V_{inner\ droplet} \cdot f \quad (20)$$

$$u_d = \lambda . f \quad (21)$$

$$Q_{total} = u_d . w_m . h/\beta \qquad (\beta = 0.95) \tag{22}$$

$$Q_c = Q_{tatal} - Q_d \tag{23}$$

$$\varphi_1 = Q_d/Q_c \tag{24}$$

where λ and f are spacing between droplets and frequency of droplet generation, respectively. Furthermore, φ is the flow rate ratio between dispersed and continuous phases. Therefore, using ImageJ software and the above equations, volume and flow rates are gained from the images taken from the experiments.

Chip II:

The process of calculating flow rates in the second chip is different from the first chip. A schematic of double emulsion generation and flow rates of extraction channel and outer phase in the second chip is presented in fig 43.

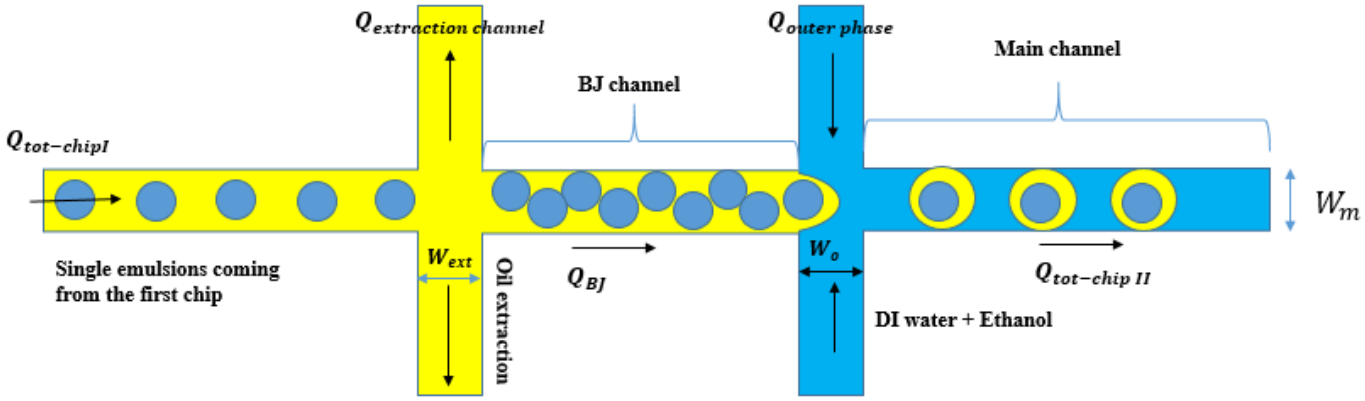

Figure 43 Schematic of double emulsion generation in chip II

In order to calculate the flow rates in chip II, it is important to know the flow rate of solution coming from the first chip. In the next section, it is shown that based on the experiments, chip I and chip II are decoupled. Therefore, during changing the applied pressure to the outer phase in extraction channel in the second chip, if the pressure applied in the first chip is constant, the size of single emulsions and flow rate of solution coming from the first chip will be constant. Hence, the size of single emulsions and flow rate of solution coming from the first chip is calculated from the videos captured from droplet generation in the first chip. Then, by knowing the flow rate

coming from the first chip, the flow rate in the extraction channel and outer phase is calculated. As shown in fig 43, the flow rate in BJ channel is:

$$Q_{BJ} = Q_{tot-chip\ I} - Q_{ext} \tag{25}$$

Then by measuring the frequency of droplet generation and the total volume of double emulsion droplet using the method mention in chip I section, the flow rate of BJ channel is calculated.

$$Q_{BJ} = V_{double\ emulsion} \cdot f \tag{26}$$

By knowing the flow rate of BJ channel and the flow rate of solution coming from the first chip, the flow rate of extraction channel is calculated using equation 25. The procedure of calculating the flow rate of the outer phase is the same as chip I.

$$u_d = \lambda . f \tag{27}$$

$$Q_{BJ} + Q_{outer\ phase} = u_d . w_m . h/\beta \qquad (\beta = 0.95) \tag{28}$$

$$Q_{outer\ phase} = u_d . w_m . h/\beta - Q_{BJ} \tag{29}$$

$$\varphi_2 = (Q_{tot-chipI} - Q_{ext})/Q_{outer\ phase} \tag{30}$$

Moreover, by know the volume of the inner droplet and total volume of double emulsion, the thickness of the middle phase is calculated as follows:

$$thickness = \frac{(V_{double\ emulsion})^{\frac{1}{3}} - (V_{inner\ droplet})^{\frac{1}{3}}}{\left(\frac{4}{3\pi}\right)^{\frac{1}{3}}} \tag{31}$$

Using the thickness and flow rate ratio calculated in equations 31 and 31, the second chip is characterized for two different sizes of the inner droplet.

5.3 Experimental Results and discussions

5.3.1 Characterizing chip I:

The first step to characterize the fabricated chip for double emulsion formation is to characterize the first chip for single emulsion generation. In the next section, it will be shown and proved that

the first and second chips are decoupled, which means during changing the pressure in the second chip, size of single emulsions are almost constant. As shown in fig 44, when the applied pressure in the second chip is changed, the outlet pressure of the first chip, P_x, is changed as well. However, as shown in the next section, the variation in P_x is negligible and does not affect the flow rate ratio and volume of generated droplets in the first chip. Therefore, in this section, the first chip is characterized only based on the flow rate ratio in the first chip. To characterize the first chip, the applied pressure in the second chip and applied pressure to the continuous phase of first chip kept constant, and by varying the applied pressure to the dispersed phase of the first chip, droplets with different size are generated. Then, by using image analysis, the flow rate ratio and the volume ratio of generated droplets are calculated. Volume of droplets is nondimensionalized by $w_m^2 \times h$ (where w_m is the width of the main channel in the first chip and h is the height of first chip). In fig 46, the relationship between the flow rate ratio in the first chip ($\varphi_1 = \frac{Q_d}{Q_c}$) and the nondimensionalized form of volume of droplet $\frac{V_{inner\ droplet}}{w_m^2 \times h}$ is presented.

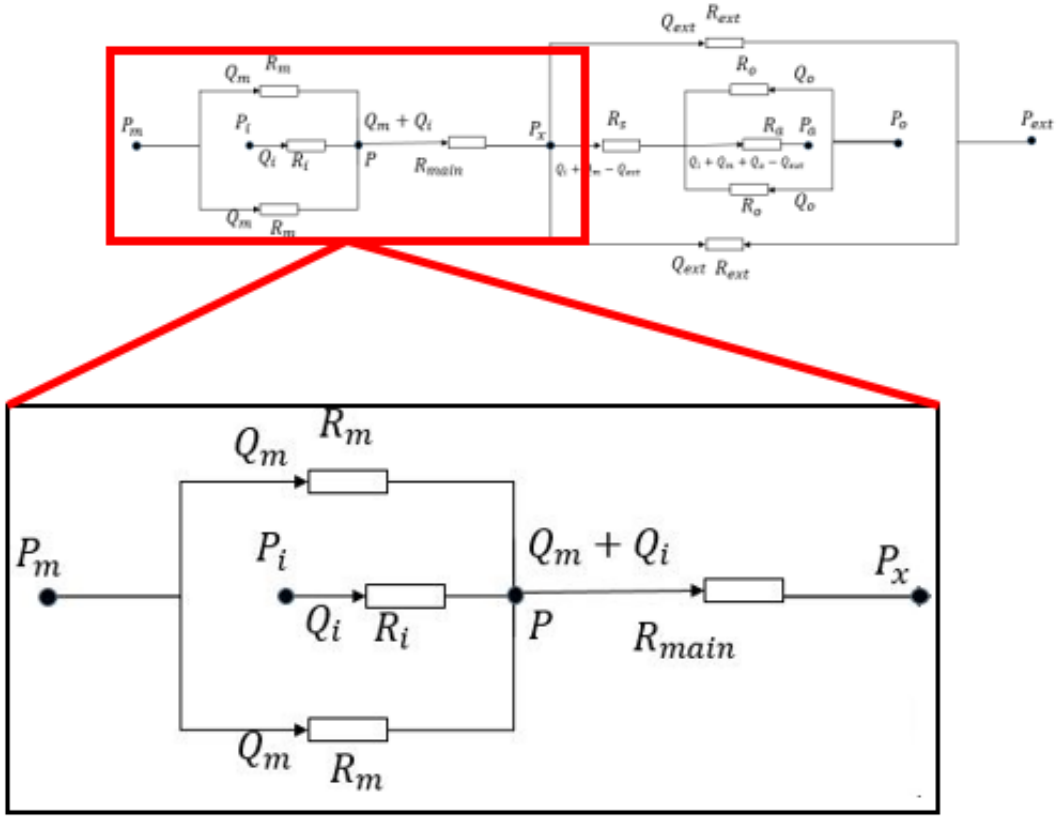

Figure 44 Electric circuit of the first chip

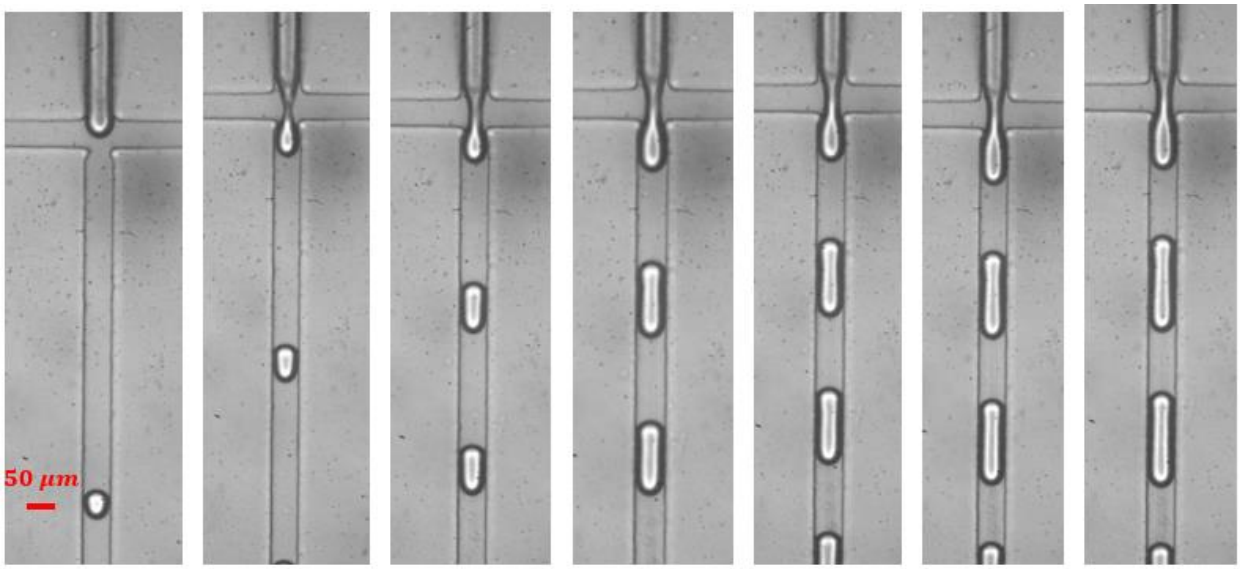

Figure 45 Droplet generation with different sizes in the first chip

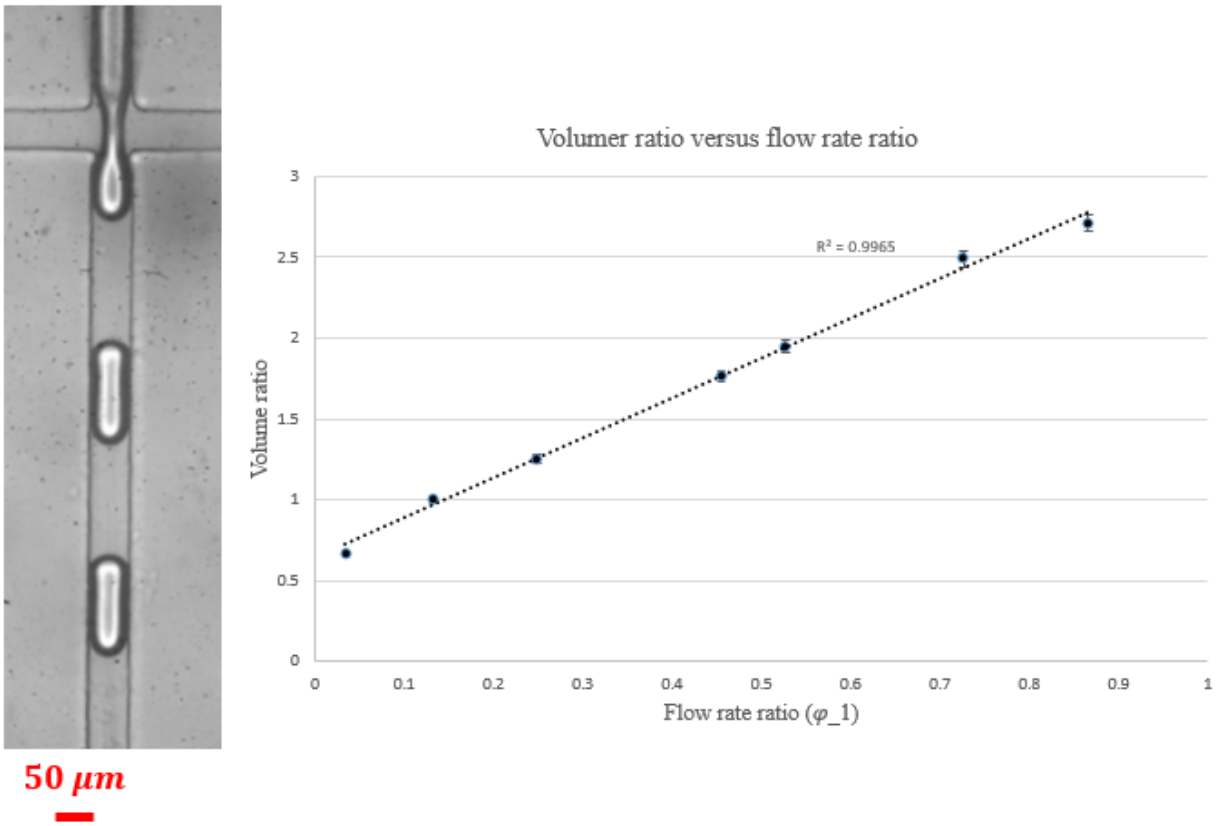

Figure 46 Volume ratio of generated inner droplet vs flow rate ratio in the first chip

Based on the results (fig 46), by increasing the flow rate ratio, the flow rates of continuous phase compared to the dispersed phase increases that result in faster pinching of the dispersed phase and generating smaller single emulsions. Moreover, by reducing the flow rate ratio, it takes more time to pinch off the dispersed phase resulting generation of larger inner droplets. Based on the experimental results, the first chip has the potential to generate droplets in the range of 40 to 85 μm. Therefore, double emulsion with different inner droplet size can be generated in these chips. The next step is to change the flow rate ratio in the second chip in order to control the thickness of the middle phase in the double emulsion.

5.3.2 Investigating decoupling effect:

In order to generate monodispersed double emulsions, it is very important to make sure that the first and second chip are decoupled. As the process of generating double emulsion in Tandem microfluidics is first to generate single emulsion in the first chip and then generate double emulsion in the second chip, it is very important to make sure that when the pressures in the second chip are varied to control the thickness of double emulsion, the size of single emulsion coming from the first chip would be the same. As shown in fig 44, changing the pressure in the second chip can affect the outlet pressure in the first chip. Therefore, in order to investigate the decoupling between the first and second chip, it is required to investigate how the outlet pressure in the first chip is changed during changing the pressure in the first chip and how sensitive the size of generated inner droplets in the first is to the outlet pressure. According to the electric circuit for the first chip shown in fig 47, following equations can be written.

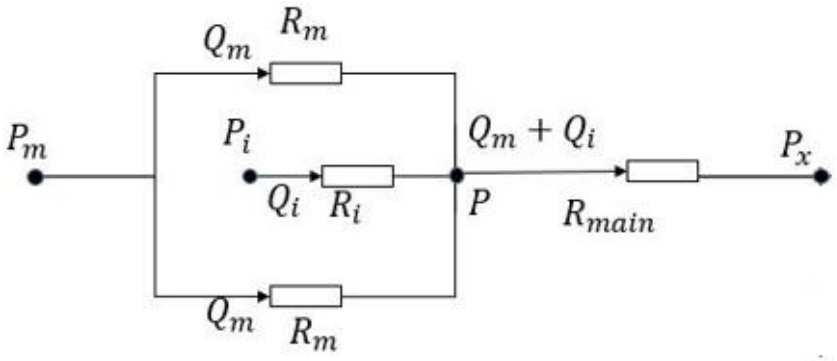

Figure 47 Electric circuit of the first chip

$$P_m - P = Q_m . R_m \quad (32)$$

$$P_i - P = Q_i . R_i \quad (33)$$

$$P - P_x = (Q_i + Q_m) . R_{main} \quad (34)$$

As discussed before, in order to eliminate fluctuation in droplet generation in the first chip, R_i and R_{main} are set equal and, both, two times of R_m.

$$R = \frac{R_i}{2} = \frac{R_{main}}{2} = R_m \quad (35)$$

In this section, the sensitivity of flow rate ratio with respect to outlet pressure is investigated. Therefore, it is assumed P_i and P_m are constant in equations 33-35 and by varying P_x the variation in flow rate ratio is investigated. Equations 33-35 can be written in the following format:

$$Q_m = \frac{2P_m - P_i - P_x}{4R} \quad (36)$$

$$Q_i = \frac{\frac{3}{4}P_i - \frac{P_x}{4} - \frac{P_m}{2}}{2R} \quad (37)$$

Therefore, the flow rate ratio is:

$$\varphi_1 = \frac{Q_i}{Q_m} = \frac{1.5P_i - 0.5P_x - P_m}{2P_m - P_i - P_x} \quad (38)$$

In order to investigate the sensitivity of flow rate ratio to the changes in the outlet pressure when applied pressure to dispersed and continuous phase is constant, the first derivation of flow rate ratio with respect to P_x is calculated.

$$\frac{d\varphi_1}{dP_x} = \frac{2P_i - 2P_m}{(2P_m - P_i - P_x)^2} \quad (39)$$

Based on the pressure applied in this project, as shown in table 2, P_i is in the range of 800-860 mbar and P_m is 860 mbar. Therefore, the maximum absolute value of $\frac{d\varphi_1}{dP_x}$ is:

$$\max\left(\left|\frac{d\varphi_1}{dP_x}\right|\right) = \frac{120}{(860 - P_x)^2} \quad (40)$$

Based on the resistance of channel and the flow rates in the first chip measured by image analysis, P_x is around 300 mbar and dP_x is smaller than 30 mbar. Therefore, the maximum value of $d\varphi_1$is:

$$\max(|d\varphi_1|) = \frac{120}{(860-300)^2} \times 30 = 0.0115 \quad (41)$$

The maximum variation in flow rate ratio during changing the pressure in the second chip is 0.0115. Therefore, based on fig37, the maximum variation of nondimensionalized droplet volume during changing the applied pressure in the second chip is approximately 0.0263. If the same sensitivity analysis done in equation 40, is repeated for nondimensionalized droplet volume and the droplet diameter, it is obtained that the maximum changing in the droplet diameter is 2 μm.

In order to validate this sensitive analysis, figure of volume ratio versus flow rate ratio for two different applied pressure in the second chip is plotted. As shown in fig 48, figures are almost matched.

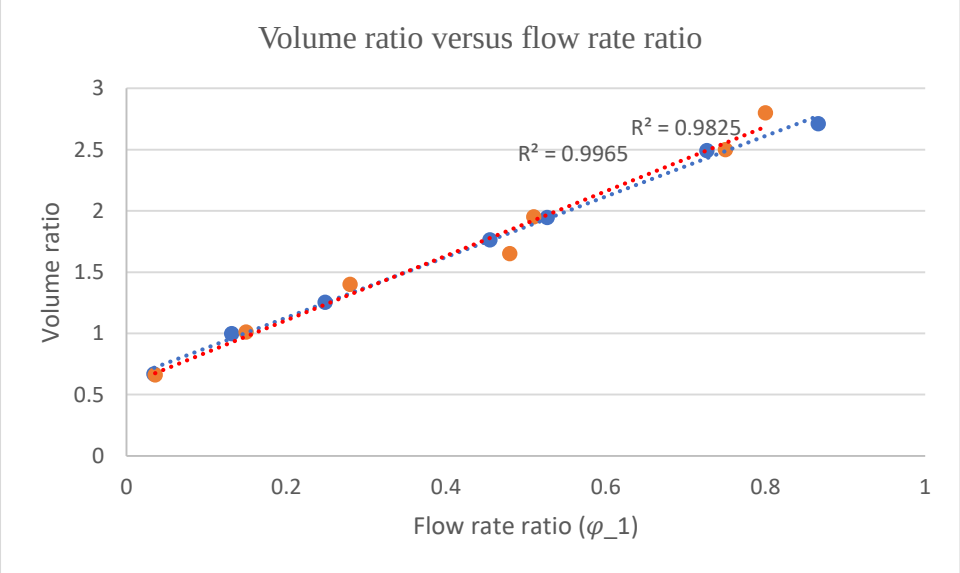

Figure 48 Volume ratio of generated inner droplets versus flow rate ratio for two different sets of applied pressure in the second chip

5.3.3 Characterizing chip II:

The next step is to characterize the second chip and generated double emulsions. As discussed in the methodology section, single emulsions coming from the first chip have different spacing. This spacing is larger when the size of single emulsions is smaller. This is because the flow rate ratio between oil phase (continuous phase) and the aqueous phase (dispersed phase) is very large when generating small single emulsions in the first chip. As shown in fig 48, to generate inner droplets with a size of 50 μm, the flow rate ratio of oil to aqueous phase should be around 20. Therefore,

for small inner droplets, a lot of single oil emulsions or double emulsion with a very thick membrane is generated. To solve this issue, the extraction channel is added to the second chip in order to extract the extra oil from the second chip. In fig 49a, small single emulsions coming from the first chip are shown. As shown, spacing between single emulsions is very large and non-uniform. Therefore, extraction channel assists in improving monodispersity of generated double emulsions, eliminating single oil emulsion and reducing the thickness of generated double emulsions. In fig 49b, it is shown that by using the extraction channel, single emulsions are packed. Therefore, the spacing between single emulsions is lowered to zero, and as shown Fig 53 and 54 and videos taken in the experiments, double emulsions with thin middle phases are generated. Therefore, by adding the extraction channel, the problem of non-uniform spacing is solved by packing the droplets, and when droplets are packed, monodispersed double emulsions with thin middle phase are generated.

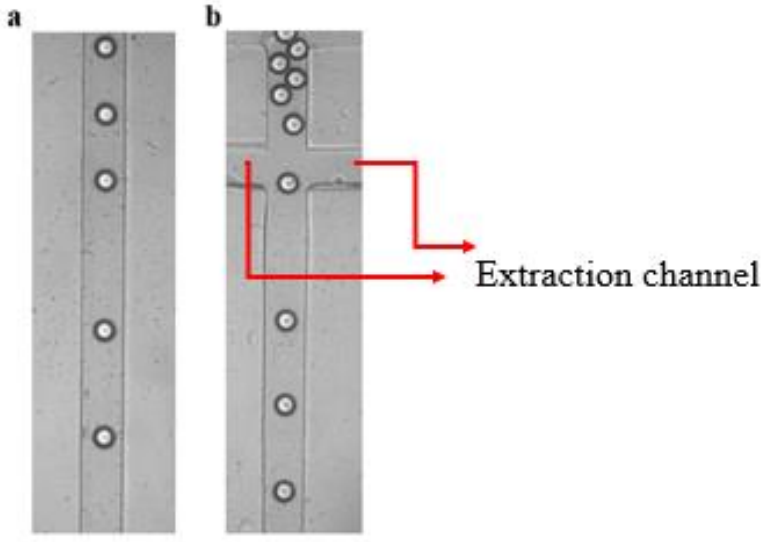

Figure 49 a) single emulsions coming from the first chip with large and non-uniform spacing b) packing single emulsion using extraction channel to improve double emulsion formation

The extraction channel is connected to the pressure pump. Therefore, by changing the pressure applied to the extraction channel, the portion of the oil extracted from the second chip is tuned. By applying lower pressure to the extraction channel, more oil is extracted from the second chip, and double emulsions with lower thickness are generated. However, there is a threshold for reducing the applied pressure to extraction channel, if lower pressure applied to the channel, single oil emulsions are extracted too either with pillar or without. In fig 50, it is shown how single emulsions

are squeezed to pass the pillars. The difference is that by adding the pillar, the minimum allowable applied pressure to the extraction channel without extracting single emulsion is lower.

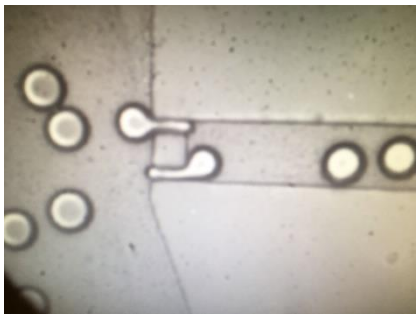

Figure 50 Single emulsions passing pillars when the applied pressure to the extraction channel is very low

Therefore, it is very important to characterize the second chip in order to understand what range of pressure can be applied to the outer phase and extraction channel and the range of thickness can be generated in the second chip. Second chip should be characterized for different size of single emulsions coming from the first chip. To characterize the second chip, two different sizes of single emulsions are generated in the first chip and, then, for each, by changing the applied pressure to the extraction channel and keeping applied pressure to the outer phase, double emulsions with different sizes are generated. After generating double emulsions with different sizes, the flow rates of outer phase and extraction channel and the thickness of generated double emulsions are calculated using the method explained in the previous section. As expected, if single emulsions are not extracted from the first chip, the thickness of double emulsions will be reduced by decreasing the applied pressure to the extraction channel and increasing the flow rate of the extraction channel. Moreover, by increasing the flow rate of the outer phase, as the oil phase containing single emulsions is pinched off faster, the thickness of the middle phase in the double emulsions is smaller. Hence, in order to consider the effect of the flow rate of extraction channel and outer phase on the thickness of generated double emulsions, non-dimensional parameter φ_2, defined in equation 30, is utilized. By increasing the flow rate of the outer phase or extraction channel resulting reducing φ_2, the thickness of generated double emulsions should be reduced. Hence, the thickness of generated double emulsions versus flow rate ratio is plotted for two different sizes of single emulsions (inner droplets).

Inner droplet with a diameter of 60μm :

Fig 53 shows double emulsion generation with different size of the outer droplet by changing the applied pressure to the extraction channel. The flow rates of extraction and outer phase channel are calculated, and the thickness of the middle phase in double emulsions versus flow rate ratio is plotted in Fig 54. Based on the results, although the spacing between single emulsions coming from the first chip before extraction channel is very large and non-uniform, no single emulsion is generated, and the monodispersity of generated double emulsion is around 96 %. Moreover, as shown in Fig 54, the relationship between the flow rate ratio and the thickness of double emulsion is linear. This is consistent with predictions before running the experiments that by increasing the flow rate of outer phase or extraction channel, double emulsions with lower thickness of the middle phase are generated. Therefore, by increasing the flow rate of the continuous phase and extraction channel, the flow rate ratio defined in equation 30 decreases, and the relationship between thickness of middle phase and flow rate ratio is linear and direct. Minimum thickness achieved in this experiment for an inner droplet with a diameter of 60μm is 6.5 μm.

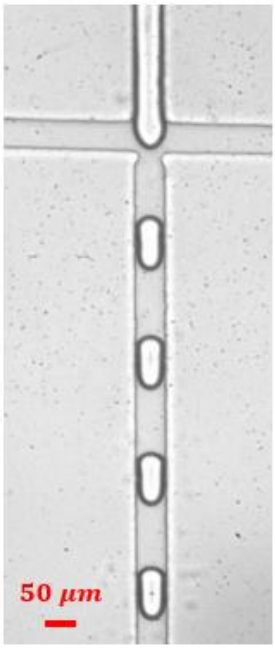

Figure 51 Droplet generation in the first chip

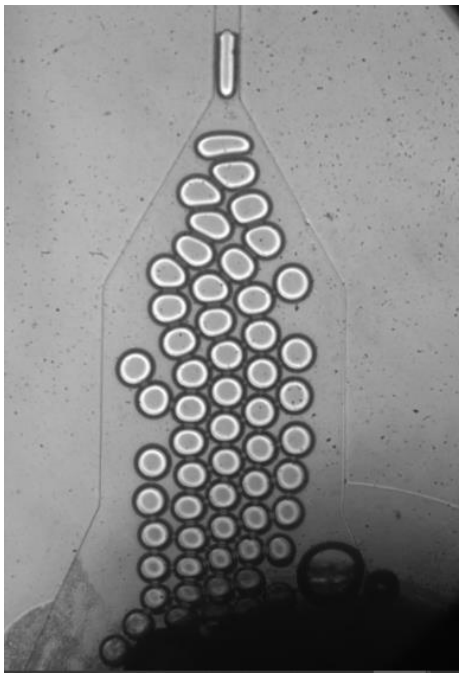

Figure 52 Outlet of the first chip during droplet generation

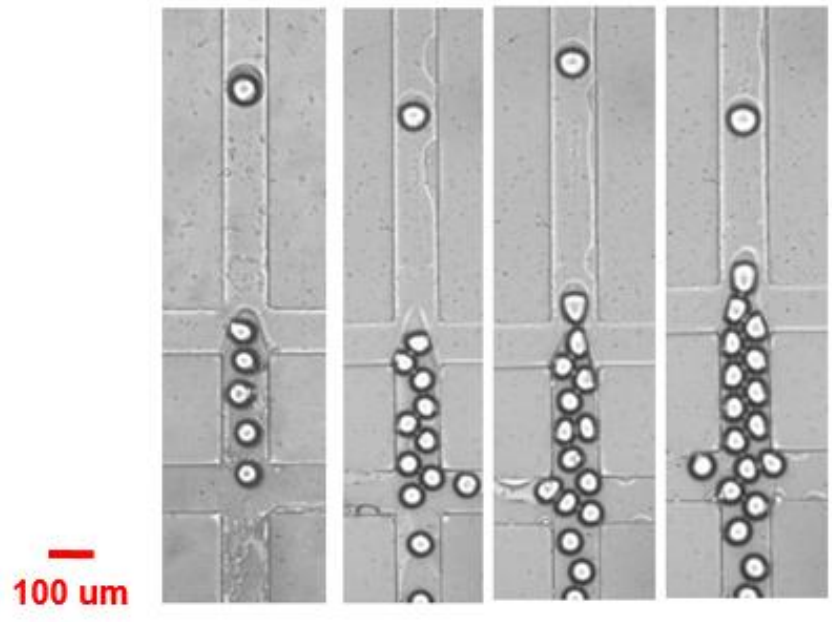

Figure 53 Double emulsion generation with different thickness of the middle phase by changing the applied pressure to the extraction channel

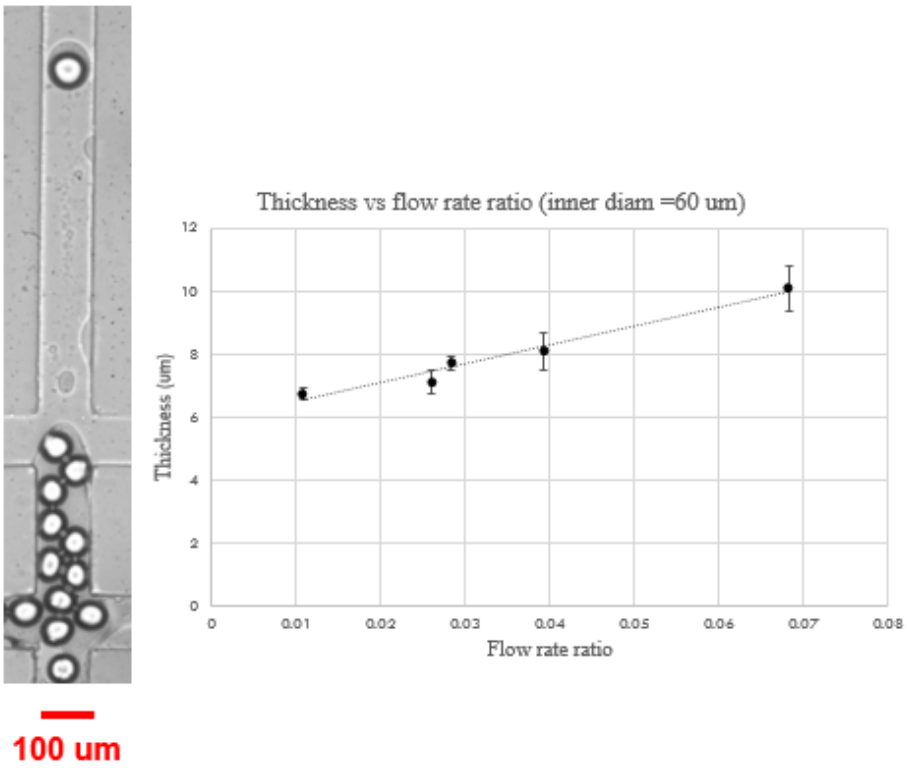

Figure 54 The effect of flow rate ratio on the thickness of the middle phase in generated double emulsions

Inner droplet with a diameter of 85μm :

Next step to characterize the second chip is to generate double emulsions with different thickness of the middle phase when the diameter of the inner droplet is large. To generate single emulsions with a larger diameter in the first chip, the flow rate ratio of the oil phase (continuous phase) to the aqueous phase (dispersed phase) is small. Therefore, as shown in fig 56, spacing between single emulsions in the second chip is smaller, and uniformity of spacing is much better. The relationship between the thickness of middle phase and flow rate ratio, as shown in Fig 60, is inverse for small flow rate ratio and direct for large flow rate ratio. This is different from what observed for double emulsions with the small inner droplet. Therefore, there is a threshold for flow rate ratio, which beyond that threshold, the reverse relationship between thickness and flow rate ratio changes to direct. The reason is that that for double emulsions with large core droplet, due to the high volume fraction between single emulsion and the oil phase, single emulsions are packed in the second chip. Therefore, when the flow rate of the extraction channel is high, some single emulsions are extracted from the extraction channel. This is unlike double emulsions with small core droplet.

Hence, due to the extraction of single oil emulsion from the extraction channel for a large flow rate of extraction channel, by increasing the flow rate of extraction (reducing the flow rate ratio defined in equation 2), the thickness of double emulsion increases. Therefore, for a specific threshold of flow rate ratio, as the extraction of the single emulsion is started, the relationship between the thickness of double emulsion and flow rate ratio is changed from direct to reverse. In fig 55, it is shown how for very low φ_2(large flow rate of extraction channel), single emulsions are extracted.

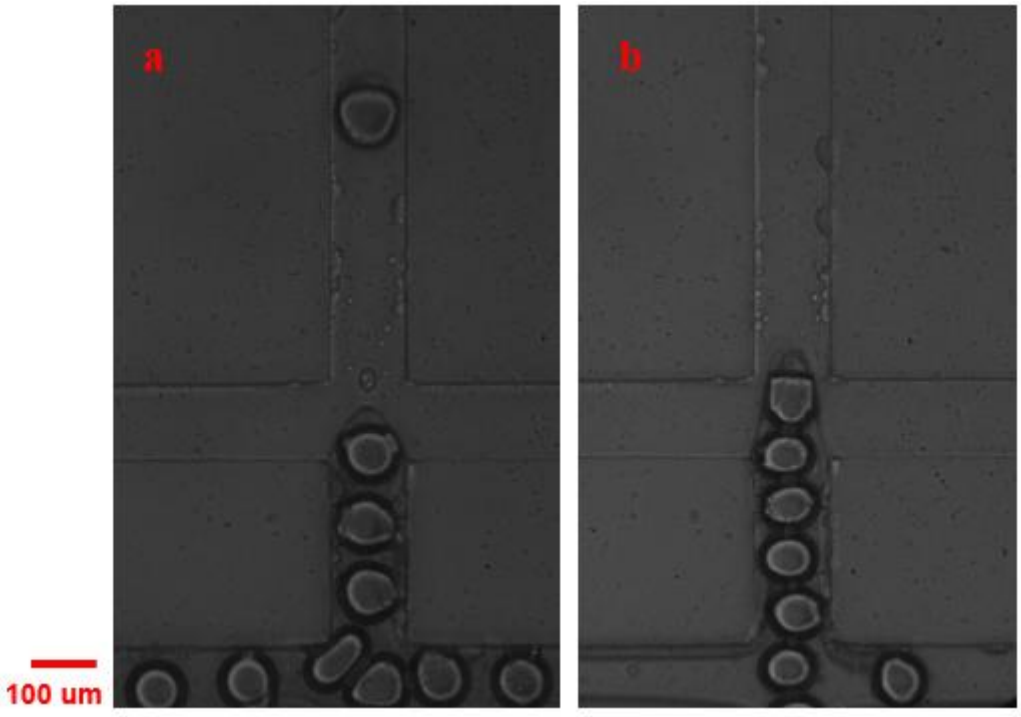

Figure 55 Extraction of single emulsions when the flow rate of the extraction channel is high b) Single emulsions are lined up, and the extraction of single emulsions are eliminated for a low flow rate of the extraction channel

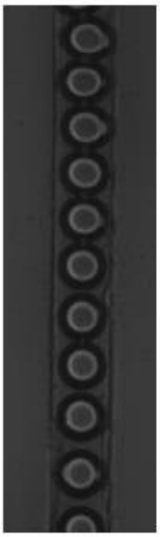

Figure 56 Single emulsions coming from the first chip

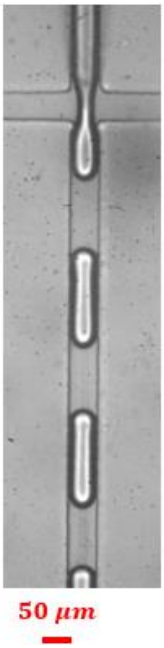

Figure 57 Droplet generation in the first chip

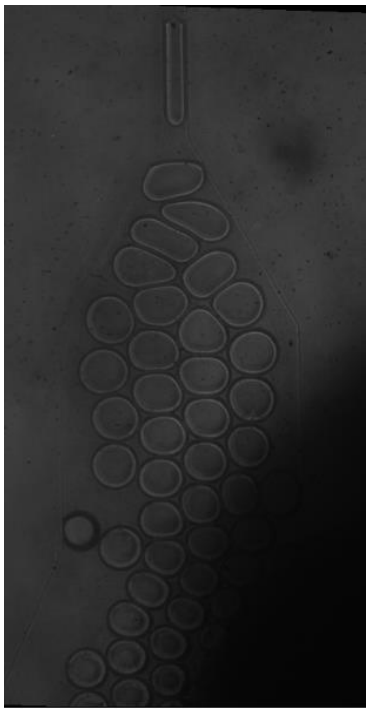

Figure 58 Outlet of the first chip during droplet generation

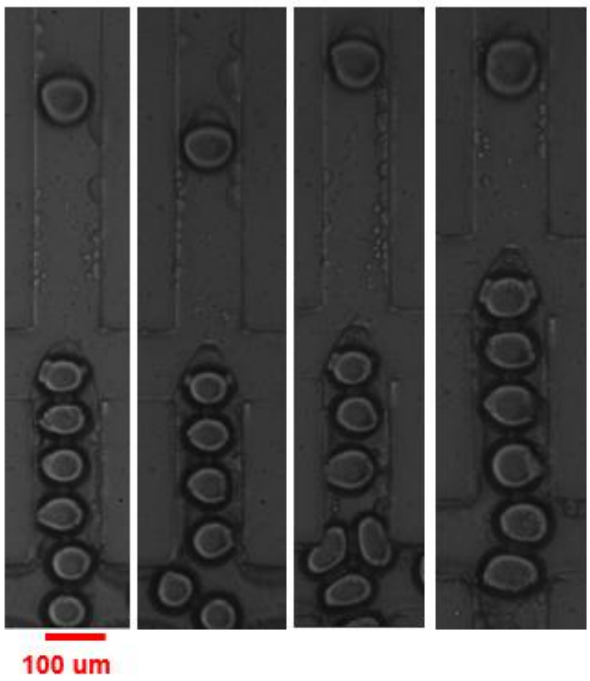

Figure 59 Double emulsion generation with different thickness of the middle phase by changing the applied pressure to the extraction channel

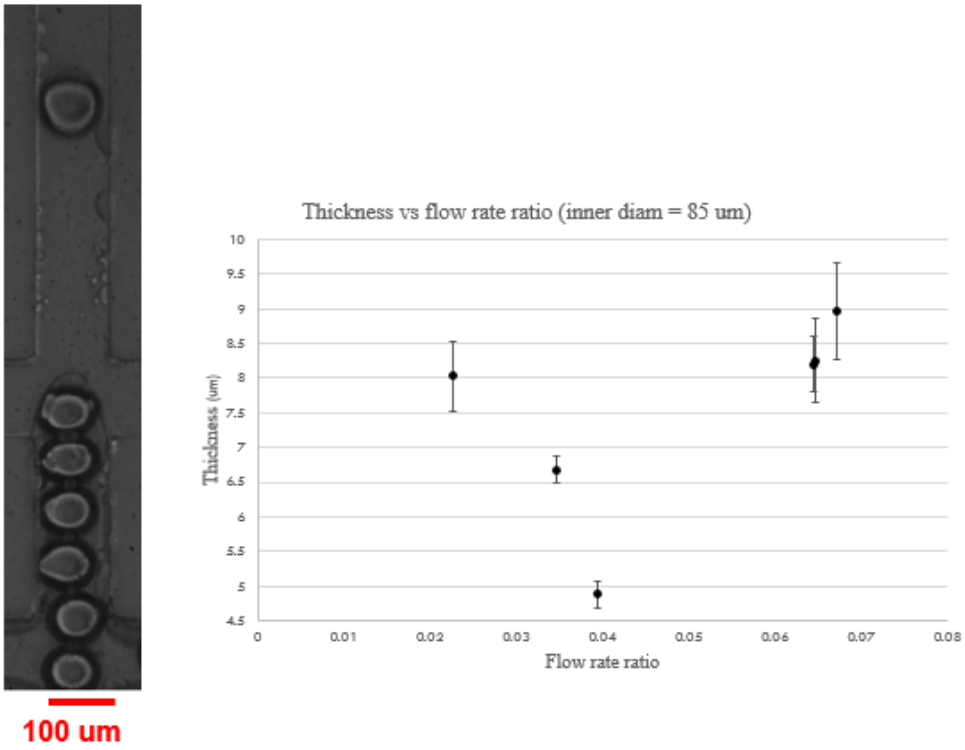

Figure 60 The effect of flow rate ratio on the thickness of the middle phase in generated double emulsions

5.3.4 Dewetting and polymersome formation

The last step for generating polymersome is extraction middle phase. By extracting the middle phase, diblock copolymers dissolved in the middle phase are integrated, and the bilayer is formed. As discussed in the literature review, there are different methods to extract the middle phase. In this project, ethanol with the concentration of 14% w/w in the outer phase is utilized to extract the middle phase. To confirm the formation of polymersome, different techniques are utilized. The most accurate method for recognizing the formation of the bilayer is taking SEM Images. Moreover, in another method, for better visualization of dewetting, Nile red fluorescent dyes are dissolved in the middle phase. In this project, due to lack of accessibility to Nile red fluorescent dyes, the formation of polymersome is confirmed based on the reported observations in the literature. Based on the literature, when the process of dewetting is started, as shown in Fig 61, two possible morphologies are observed: 1- partial dewetting 2- complete dewetting. As illustrated in Fig 61, in partial dewetting, the thickness of the membrane is not uniform. This is the most important feature of dewetting used in this project to confirm the formation of polymersomes. The

double emulsions immediately after formation in the outlet of the second chip are illustrated in Fig 62.

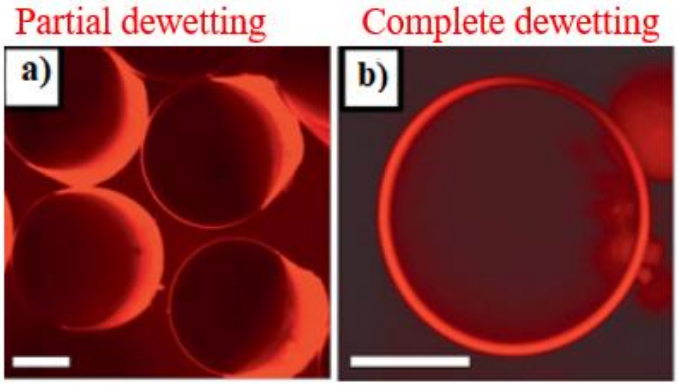

Figure 61 Partially dewetted double emulsions b) complete dewetted double emulsion [82]

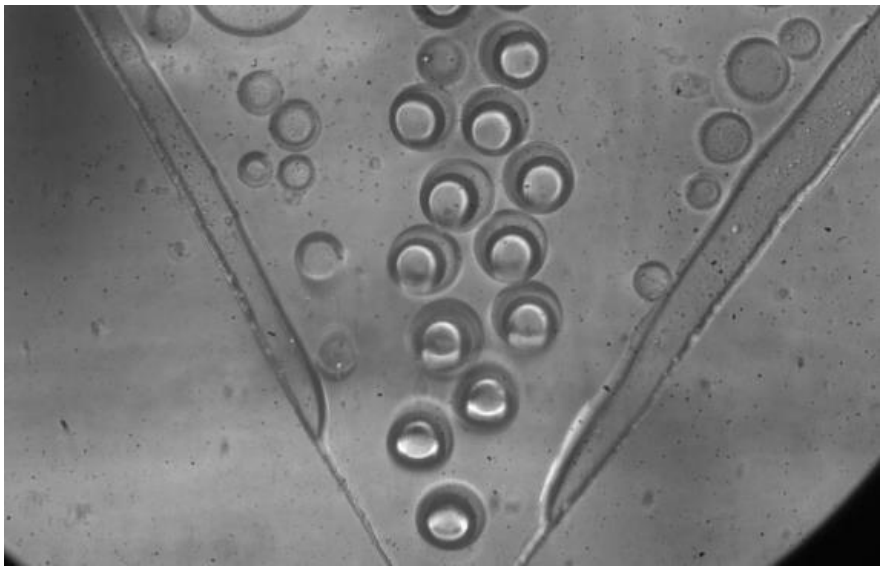

Figure 62 Generated double emulsions in the outlet of the second chip

Then, the solution is transferred to a vial and left under the fume hood for three hours. In Fig 63, double emulsions dissolved in a solution containing ethanol after three hours is presented.

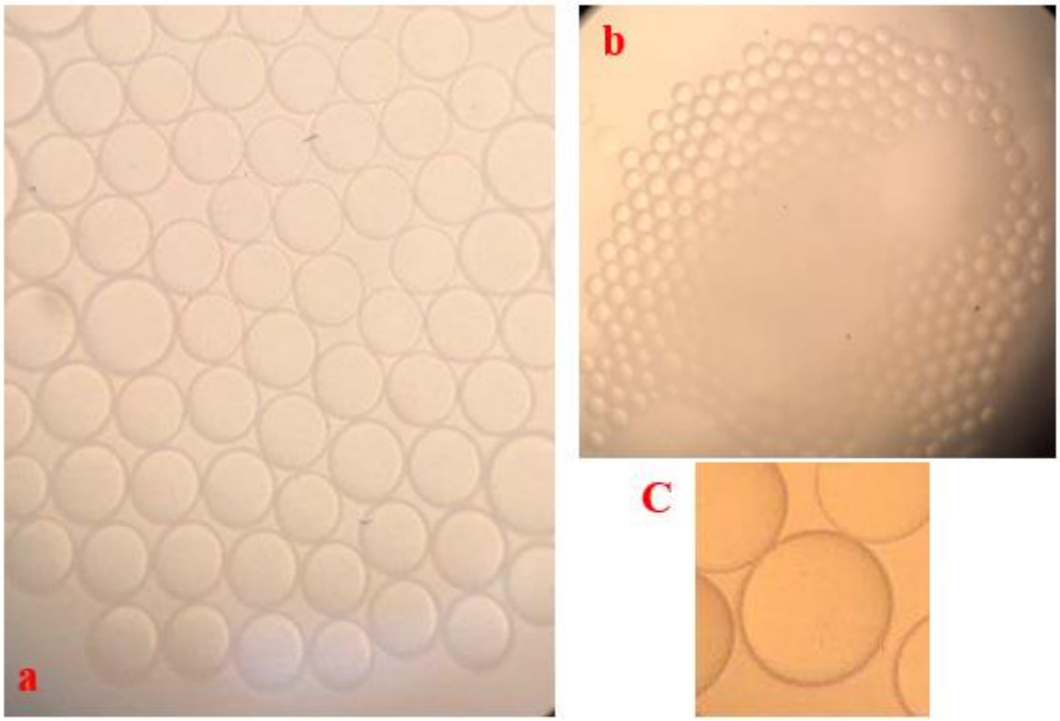

Figure 63 a) and b) generated double emulsions after dewetting c) enlarged image of generated double emulsions after dewetting

Due to the three following reasons, emulsions shown in Fig 63 are polymersome:

1- The color of inner and outer phases is the same and different from the middle phase which shows double emulsions are generated successfully

2- The thickness of the middle phase is much smaller than what produced in the outlet of the second chip shown in Fig 62. Therefore, the process of dewetting is started

3- Since the thickness of the middle phase is uniform, as discussed in literature and shown in Fig 61 and 63, the process of dewetting is completed.

Hence, it is confirmed that the process of polymersome formation is completed successfully.

Chapter 6: Conclusion and recommendations for future works:

6.1 Conclusion

Currently, there are key challenges in the existing droplet microfluidic techniques that limit their applicability in making double emulsions. The need for partial surface modification of micro channels and the lack of thorough guideline to control the size or the thickness of the middle phases are two main challenges of producing double emulsions with the desired size using conventional microfluidics methods. Recently, different methods have been proposed for producing double emulsions. However, except the tandem method, other methods are suffering from the need for selective surface treatment which is very challenging. Moreover, in these methods, since the inner and outer droplets are generated in the same chip, the two generation steps affect each other. Coupling effect between inner and outer droplet generation makes the process of double emulsion generation very complex resulting in inability of providing a thorough guideline for double emulsion generation and high control over the size of inner and outer droplets. Although the main challenge of one step and two step methods mentioned above is solved using the tandem method proposed by Weitz et al. [63], new challenges are raised up. In the tandem method, single emulsions generated in the first chip are transported via tubing to the second chip, and double emulsions are generated in the second chip. First, when single emulsions are transported to the second chip via tubing, non-uniform spacing between single emulsions is created which can significantly affect the monodispersity of generated double emulsions. Secondly, as for generating small single emulsion in the first chip (shown in fig 46), the flow rate ratio between dispersed and continuous phases in the first chip must be very small, thus, volume fraction between single emulsions and oil phase in the second chip is very large. Therefore, for double emulsions with small inner droplet, the thickness of the middle phase in the generated double emulsions would be very high. This thickness of inner droplet with a diameter of $50\ \mu m$, would be equal to the radius of the inner droplet. However, generation of double emulsion with thick middle phase is not desirable for some applications such as polymersome formation because the process of dewetting gets more challenging and time-consuming. Therefore, in this work, a new technique is proposed to resolve the main challenge of the tandem method. Moreover, a guideline is provided that allows researchers to design two chips to generate high monodisperse double emulsions (w/o/w) and manipulate the thickness of the middle phase in a highly controlled manner. In this technique, an

extraction channel is embedded in the second chip in order to reduce and control the thickness of the middle phase in the double emulsion. In this work, first, the decoupling between the first and second chip is proved. Then, the capability of the designed chip in generating double emulsion with different core droplet size and thickness of double emulsions is investigated.

To sum up, this thesis presents a droplet-based microfluidic platform for producing double-emulsion towards polymersome with the following novel or improved features as compared with the literature: i) By adding the extraction channel, the limitation of tandem method in generating double emulsion with core size of larger than 100 μm is lifted, and double emulsion with inner droplet of 60 μm is generated ii) the thickness of middle phase of generated double emulsion is better controlled by the integration of an extraction channel to the second chip; iii) a guideline is provided to design the droplet makers in the first and second chips and the extraction channel.

6.2 Recommendations and future works

As discussed before, the process of polymersome formation consists of two different steps. The first step is double emulsion generation in microfluidics, and the second step is dewetting the middle phase and formation of polymersomes. Despite its lots of improvement compared to the previous methods, the presented method used in this project for double emulsion generation has some drawbacks and challenges. The first challenge is that, when the first chip is connected to the second chip, the hydrodynamic resistance of the first chip increases in a very short time that affects droplet generation in the first chip. This increase in hydrodynamics resistance of the first chip in a short time causes the cessation of droplet generation in the first chip. Consequently, a mixture of aqueous and oil phases is transported to the second chip. The second chip is hydrophilic, and the aqueous phase coming from the first chip wets the wall. Depending on how long it takes that the droplet generation in the first chip is started again, sometimes some part of the second chips are wetted by the inner phase till the end of experiments which adversely affect the functionality of the second chip. This process takes at least two hours. During this time, the oil phase is in contact with the channel walls. Therefore, in some experiments at the end of the experiment, severe wetting issues are raised up. In some papers, it is mentioned that PDADMAC is employed to sustain the channel treatment. [84] Hence, in the future works, it is highly recommended to use PDADMAC, to sustain the treatment of the second chip. The other potential research on the proposed method for double emulsion generation is investigating the effect of adding pillar to the extraction channel

on the thickness of generated double emulsions. As discussed in chapter 5, to eliminate the extraction of single emulsion from the extraction channel, the applied pressure to the extraction channel has some limitation. Although applying low pressure to the extraction channel causes more oil to be extracted from the extraction channel, extraction of single emulsions causes the thickness of double emulsions is not reduced too much. However, adding pillars allow us to apply lower pressure to the extraction channel and extract more oil phases. This results in the generation of double emulsions with a thinner middle phase. Therefore, it is highly recommended to investigate the effect of adding pillars with different sizes to the extraction channel on the lowest achievable thickness of double emulsions.

Extraction of the middle phase from double emulsion is one of the key steps for the formation of polymersomes. The method used in this thesis is based on dissolving double emulsions in Ethanol after their formation**[22]**. However, as such a bulk method is uncontrollable, it has been observed that in some portion of double emulsions, dewetting steps are not done completely. Moreover, conventional methods are very time consuming, and mostly the double emulsions should be kept in the solvent for over 10 hours to evaporate all the middle phase**[68]**. The other limitation of the conventional method is that the middle phase should be chosen very carefully to be volatile enough to be evaporated after double emulsion formation. It is highly recommended to do research on proposing an on-chip dewetting method to speed up the process of dewetting and improve the efficiency of dewetting since in on-chip method, the process is more controllable in comparison with bulk methods.

References:

[1] Sackmann, E. K., Fulton, A. L., & Beebe, D. J. (2014). The present and future role of microfluidics in biomedical research. *Nature*, *507*(7491), 181.

[2] Thorsen, T., Roberts, R. W., Arnold, F. H., & Quake, S. R. (2001). Dynamic pattern formation in a vesicle-generating microfluidic device. *Physical review letters*, *86*(18), 4163.

[3] Huebner, A., Sharma, S., Srisa-Art, M., Hollfelder, F., & Edel, J. B. (2008). Microdroplets: a sea of applications? *Lab on a Chip*, *8*(8), 1244-1254.

[4] Teh, S. Y., Lin, R., Hung, L. H., & Lee, A. P. (2008). Droplet microfluidics. *Lab on a Chip*, *8*(2), 198-220.

[5] Lorenceau, E., Utada, A. S., Link, D. R., Cristobal, G., Joanicot, M., & Weitz, D. A. (2005). Generation of polymerosomes from double-emulsions. *Langmuir*, *21*(20), 9183-9186.

[6] Bleul, R., Thiermann, R., & Maskos, M. (2015). Techniques to control polymersome size. *Macromolecules*, *48*(20), 7396-7409.

[7] Discher, B. M., Won, Y. Y., Ege, D. S., Lee, J. C., Bates, F. S., Discher, D. E., & Hammer, D. A. (1999). Polymersomes: tough vesicles made from diblock copolymers. *Science*, *284*(5417), 1143-1146.

[8] Uneyama, T. (2007). Density functional simulation of spontaneous formation of vesicle in block copolymer solutions. *The Journal of chemical physics*, *126*(11), 114902.

[9] Bernardes, A. T. (1996). Monte Carlo simulation of vesicle self-organisation. *Journal de Physique II*, *6*(2), 169-174.

[10] Leng, J., Egelhaaf, S. U., & Cates, M. E. (2003). Kinetics of the micelle-to-vesicle transition: aqueous lecithin-bile salt mixtures. *Biophysical journal*, *85*(3), 1624-1646.

[11] Israelachvili, J. N., Mitchell, D. J., & Ninham, B. W. (1976). Theory of self-assembly of hydrocarbon amphiphiles into micelles and bilayers. *Journal of the Chemical Society, Faraday Transactions 2: Molecular and Chemical Physics*, *72*, 1525-1568.

[12] Reeves, J. P., & Dowben, R. M. (1969). Formation and properties of thin-walled phospholipid vesicles. *Journal of cellular physiology*, *73*(1), 49-60.

[13] Angelova, M. I., & Dimitrov, D. S. (1986). Liposome electroformation. *Faraday discussions of the Chemical Society*, *81*, 303-311.

[14] Sun, B., & Chiu, D. T. (2005). Determination of the encapsulation efficiency of individual vesicles using single-vesicle photolysis and confocal single-molecule detection. *Analytical chemistry*, *77*(9), 2770-2776.

[15] Lee, J. C. M., Bermudez, H., Discher, B. M., Sheehan, M. A., Won, Y. Y., Bates, F. S., & Discher, D. E. (2001). Preparation, stability, and in vitro performance of vesicles made with diblock copolymers. *Biotechnology and bioengineering*, *73*(2), 135-145.

[16] Ghoroghchian, P. P., Frail, P. R., Susumu, K., Blessington, D., Brannan, A. K., Bates, F. S., ... & Therien, M. J. (2005). Near-infrared-emissive polymersomes: self-assembled soft matter for in vivo optical imaging. *Proceedings of the National Academy of Sciences*, *102*(8), 2922-2927.

[17] LoPresti, C., Lomas, H., Massignani, M., Smart, T., & Battaglia, G. (2009). Polymersomes: nature inspired nanometer sized compartments. *Journal of Materials Chemistry*, *19*(22), 3576-3590.

[18] Howse, J. R., Jones, R. A., Battaglia, G., Ducker, R. E., Leggett, G. J., & Ryan, A. J. (2009). Templated formation of giant polymer vesicles with controlled size distributions. *Nature materials*, *8*(6), 507.

[19] Hauschild, S., Lipprandt, U., Rumplecker, A., Borchert, U., Rank, A., Schubert, R., & Förster, S. (2005). Direct preparation and loading of lipid and polymer vesicles using inkjets. *Small*, *1*(12), 1177-1180.

[20] Müller, W., Maskos, M., Metzke, D., & Löb, P. (2009). Synthesis of block copolymer vesicles in a micromixer. *La Houille Blanche*, (6), 125-128.

[21] Lorenceau, E., Utada, A. S., Link, D. R., Cristobal, G., Joanicot, M., & Weitz, D. A. (2005). Generation of polymerosomes from double-emulsions. *Langmuir*, *21*(20), 9183-9186.

[22] Hayward, R. C., Utada, A. S., Dan, N., & Weitz, D. A. (2006). Dewetting instability during the formation of polymersomes from block-copolymer-stabilized double emulsions. *Langmuir*, *22*(10), 4457-4461.

[23] Shum, H. C., Kim, J. W., & Weitz, D. A. (2008). Microfluidic fabrication of monodisperse biocompatible and biodegradable polymersomes with controlled permeability. *Journal of the American Chemical Society*, *130*(29), 9543-9549.

[24] Christopher, G. F., & Anna, S. L. (2007). Microfluidic methods for generating continuous droplet streams. *Journal of Physics D: Applied Physics*, *40*(19), R319.

[25] Cramer, C., Fischer, P., & Windhab, E. J. (2004). Drop formation in a co-flowing ambient fluid. *Chemical Engineering Science*, *59*(15), 3045-3058.

[26] Cramer, C., Fischer, P., & Windhab, E. J. (2004). Drop formation in a co-flowing ambient fluid. *Chemical Engineering Science*, *59*(15), 3045-3058.

[27] Umbanhowar, P. B., Prasad, V., & Weitz, D. A. (2000). Monodisperse emulsion generation via drop break off in a coflowing stream. *Langmuir*, *16*(2), 347-351.

[28] Utada, A. S., Fernandez-Nieves, A., Stone, H. A., & Weitz, D. A. (2007). Dripping to jetting transitions in coflowing liquid streams. *Physical review letters*, *99*(9), 094502.

[29] Anna, S. L., Bontoux, N., & Stone, H. A. (2003). Formation of dispersions using "flow focusing" in microchannels. *Applied physics letters*, *82*(3), 364-366.

[30] Cubaud, T., & Mason, T. G. (2008). Capillary threads and viscous droplets in square microchannels. *Physics of Fluids*, *20*(5), 053302.

[31] Lee, W., Walker, L. M., & Anna, S. L. (2009). Role of geometry and fluid properties in droplet and thread formation processes in planar flow focusing. *Physics of Fluids*, *21*(3), 032103.

[32] Anna, S. L. (2016). Droplets and bubbles in microfluidic devices. *Annual Review of Fluid Mechanics*, *48*, 285-309.

[33] Garstecki, P., Fuerstman, M. J., Stone, H. A., & Whitesides, G. M. (2006). Formation of droplets and bubbles in a microfluidic T-junction—scaling and mechanism of break-up. *Lab on a Chip*, *6*(3), 437-446.

[34] Guillot, P., & Colin, A. (2005). Stability of parallel flows in a microchannel after a T junction. *Physical Review E*, *72*(6), 066301.

[35] Gordillo, J. M., Sevilla, A., & Campo-Cortés, F. (2014). Global stability of stretched jets: conditions for the generation of monodisperse micro-emulsions using coflows. *Journal of Fluid Mechanics*, *738*, 335-357.

[36] Glawdel, T., Elbuken, C., & Ren, C. L. (2012). Droplet formation in microfluidic T-junction generators operating in the transitional regime. I. Experimental observations. *Physical Review E*, *85*(1), 016322.

[37] Nunes, J. K., Tsai, S. S. H., Wan, J., & Stone, H. A. (2013). Dripping and jetting in microfluidic multiphase flows applied to particle and fibre synthesis. *Journal of physics D: Applied physics*, *46*(11), 114002.

[38] Utada, A. S., Fernandez-Nieves, A., Stone, H. A., & Weitz, D. A. (2007). Dripping to jetting transitions in coflowing liquid streams. *Physical review letters*, *99*(9), 094502.

[39] Nelson, W. C., & Kim, C. J. C. (2012). Droplet actuation by electrowetting-on-dielectric (EWOD): A review. *Journal of Adhesion Science and Technology*, *26*(12-17), 1747-1771.

[40] Kim, H., Luo, D., Link, D., Weitz, D. A., Marquez, M., & Cheng, Z. (2007). Controlled production of emulsion drops using an electric field in a flow-focusing microfluidic device. *Applied Physics Letters*, *91*(13), 133106.

[41] Wu, Y., Fu, T., Ma, Y., & Li, H. Z. (2015). Active control of ferrofluid droplet breakup dynamics in a microfluidic T-junction. *Microfluidics and Nanofluidics*, *18*(1), 19-27.

[42] Stan, C. A., Tang, S. K., & Whitesides, G. M. (2009). Independent control of drop size and velocity in microfluidic flow-focusing generators using variable temperature and flow rate. *Analytical chemistry*, *81*(6), 2399-2402.

[43] Chen, C. T., & Lee, G. B. (2006). Formation of microdroplets in liquids utilizing active pneumatic choppers on a microfluidic chip. *Journal of microelectromechanical systems*, *15*(6), 1492-1498.

[44] Bransky, A., Korin, N., Khoury, M., & Levenberg, S. (2009). A microfluidic droplet generator based on a piezoelectric actuator. *Lab on a Chip*, *9*(4), 516-520.

[45] Lifesciences, C., Coulter, B., Biosciences, A., Nanosciences, B., Elmer, P., & Biosciences, B. D. (2006). Microfluidics in commercial applications; an industry perspective. *Lab Chip*, *6*, 1118-1121.

[46] Whitesides, G. M. (2006). The origins and the future of microfluidics. *Nature*, *442*(7101), 368.

[47] De Rose, R., Zelikin, A. N., Johnston, A. P., Sexton, A., Chong, S. F., Cortez, C., ... & Kent, S. J. (2008). Binding, internalization, and antigen presentation of vaccine-loaded nanoengineered capsules in blood. *Advanced Materials*, *20*(24), 4698-4703.

[48] Pessi, J., Santos, H. A., Miroshnyk, I., Weitz, D. A., & Mirza, S. (2014). Microfluidics-assisted engineering of polymeric microcapsules with high encapsulation efficiency for protein drug delivery. *International journal of pharmaceutics*, *472*(1-2), 82-87.

[49] Huang, J., Li, W., Li, Y., Luo, C., Zeng, Y., Xu, Y., & Zhou, J. (2014). Generation of uniform polymer eccentric and core-centered hollow microcapsules for ultrasound-regulated drug release. *Journal of Materials Chemistry B*, *2*(39), 6848-6854.

[50] Patravale, V. B., & Mandawgade, S. D. (2008). Novel cosmetic delivery systems: an application update. *International journal of cosmetic science*, *30*(1), 19-33.

[51] Vladisavljević, G., Al Nuumani, R., & Nabavi, S. (2017). Microfluidic production of multiple emulsions. *Micromachines*, *8*(3), 75.

[52] Chu, L. Y., Utada, A. S., Shah, R. K., Kim, J. W., & Weitz, D. A. (2007). Controllable monodisperse multiple emulsions. *Angewandte Chemie*, *119*(47), 9128-9132.

[53] Utada, A. S., Lorenceau, E. L., Link, D. R., Kaplan, P. D., Stone, H. A., & Weitz, D. A. (2005). Monodisperse double emulsions generated from a microcapillay device. *Science*, *308*(5721), 537-541.

[54] Deshpande, S., & Dekker, C. (2018). On-chip microfluidic production of cell-sized liposomes. *Nature protocols*, *13*(5), 856.

[55] Nisisako, T., Okushima, S., & Torii, T. (2005). Controlled formulation of monodisperse double emulsions in a multiple-phase microfluidic system. *Soft Matter*, *1*(1), 23-27.

[56] Okushima, S., Nisisako, T., Torii, T., & Higuchi, T. (2004). Controlled production of monodisperse double emulsions by two-step droplet breakup in microfluidic devices. *Langmuir*, *20*(23), 9905-9908.

[57] Barbier, V., Tatoulian, M., Li, H., Arefi-Khonsari, F., Ajdari, A., & Tabeling, P. (2006). Stable modification of PDMS surface properties by plasma polymerization: application to the formation of double emulsions in microfluidic systems. *Langmuir*, *22*(12), 5230-5232.

[58] Seo, M., Paquet, C., Nie, Z., Xu, S., & Kumacheva, E. (2007). Microfluidic consecutive flow-focusing droplet generators. *Soft Matter*, *3*(8), 986-992.

[59] Abate, A. R., Krummel, A. T., Lee, D., Marquez, M., Holtze, C., & Weitz, D. A. (2008). Photoreactive coating for high-contrast spatial patterning of microfluidic device wettability. *Lab on a Chip*, *8*(12), 2157-2160.

[60] Abate, A. R., Thiele, J., & Weitz, D. A. (2011). One-step formation of multiple emulsions in microfluidics. *Lab on a Chip*, *11*(2), 253-258.

[61] Vallejo, D., Lee, S. H., Lee, D., Zhang, C., Rapier, C., Chessler, S. D., & Lee, A. P. (2017). Cell-sized lipid vesicles for cell-cell synaptic therapies. *Technology*, *5*(04), 201-213.

[62] Nie, Z., Xu, S., Seo, M., Lewis, P. C., & Kumacheva, E. (2005). Polymer particles with various shapes and morphologies produced in continuous microfluidic reactors. *Journal of the American chemical society*, *127*(22), 8058-8063.

[63] Eggersdorfer, M. L., Zheng, W., Nawar, S., Mercandetti, C., Ofner, A., Leibacher, I., ... & Weitz, D. A. (2017). Tandem emulsification for high-throughput production of double emulsions. *Lab on a Chip*, *17*(5), 936-942.

[64] Shum, H. C., Kim, J. W., & Weitz, D. A. (2008). Microfluidic fabrication of monodisperse biocompatible and biodegradable polymersomes with controlled permeability. *Journal of the American Chemical Society*, *130*(29), 9543-9549.

[65] Deng, N. N., Wang, W., Ju, X. J., Xie, R., Weitz, D. A., & Chu, L. Y. (2013). Wetting-induced formation of controllable monodisperse multiple emulsions in microfluidics. *Lab on a Chip*, *13*(20), 4047-4052.

[66] Deng, N. N., Yelleswarapu, M., & Huck, W. T. (2016). Monodisperse uni-and multicompartment liposomes. *Journal of the American Chemical Society*, *138*(24), 7584-7591.

[67] Torza, S., & Mason, S. G. (1970). Three-phase interactions in shear and electrical fields. *Journal of colloid and interface science*, *33*(1), 67-83.

[68] Teh, S. Y., Khnouf, R., Fan, H., & Lee, A. P. (2011). Stable, biocompatible lipid vesicle generation by solvent extraction-based droplet microfluidics. *Biomicrofluidics*, *5*(4), 044113.

[69] T Glawdel, (2012). Droplet Production and Transport in Microfluidic Networks with Pressure Driven Flow Control (Doctoral dissertation). Retrieved from University of Waterloo Database

[70] Gao, M., Gui, L., & Liu, J. (2013). Study of liquid-metal based heating method for temperature gradient focusing purpose. *Journal of Heat Transfer*, *135*(9), 091402.

[71] Shameli, S. M., Glawdel, T., Liu, Z., & Ren, C. L. (2012). Bilinear temperature gradient focusing in a hybrid PDMS/glass microfluidic chip integrated with planar heaters for generating temperature gradients. *Analytical chemistry*, *84*(6), 2968-2973.

[72] Ge, X. H., Huang, J. P., Xu, J. H., & Luo, G. S. (2014). Controlled stimulation-burst targeted release by smart decentered core–shell microcapsules in gravity and magnetic field. *Lab on a chip*, *14*(23), 4451-4454.

[73] Datta, S. S., Kim, S. H., Paulose, J., Abbaspourrad, A., Nelson, D. R., & Weitz, D. A. (2012). Delayed buckling and guided folding of inhomogeneous capsules. *Physical review letters*, *109*(13), 134302.

[74] Vian, A., Favrod, V., & Amstad, E. (2016). Reducing the shell thickness of double emulsions using microfluidics. *Microfluidics and Nanofluidics*, *20*(12), 159.

[75] Zhao, C. X., Chen, D., Hui, Y., Weitz, D. A., & Middelberg, A. P. (2017). Controlled Generation of Ultrathin-Shell Double Emulsions and Studies on Their Stability. *ChemPhysChem*, *18*(10), 1393-1399.

[76] Bei, Z. M., Jones, T. B., & Tucker-Schwartz, A. (2009). Forming concentric double-emulsion droplets using electric fields. *Journal of Electrostatics*, *67*(2-3), 173-177.

[77] Reeves, J. P., & Dowben, R. M. (1969). Formation and properties of thin-walled phospholipid vesicles. *Journal of cellular physiology*, *73*(1), 49-60.

[78] Angelova, M. I., & Dimitrov, D. S. (1986). Liposome electroformation. *Faraday discussions of the Chemical Society*, *81*, 303-311.

[79] Sun, B., & Chiu, D. T. (2005). Determination of the encapsulation efficiency of individual vesicles using single-vesicle photolysis and confocal single-molecule detection. *Analytical chemistry*, *77*(9), 2770-2776.

[80] Berry, J. D., Neeson, M. J., Dagastine, R. R., Chan, D. Y., & Tabor, R. F. (2015). Measurement of surface and interfacial tension using pendant drop tensiometry. *Journal of colloid and interface science*, *454*, 226-237.

[81] Shameli, S. M., Glawdel, T., Liu, Z., & Ren, C. L. (2012). Bilinear temperature gradient focusing in a hybrid PDMS/glass microfluidic chip integrated with planar heaters for generating temperature gradients. *Analytical chemistry*, *84*(6), 2968-2973.

[82] Thiele, J., Abate, A. R., Shum, H. C., Bachtler, S., Förster, S., & Weitz, D. A. (2010). Fabrication of polymersomes using double-emulsion templates in glass-coated stamped microfluidic devices. *Small*, *6*(16), 1723-1727.

[83] Musterd, M., van Steijn, V., Kleijn, C. R., & Kreutzer, M. T. (2015). Calculating the volume of elongated bubbles and droplets in microchannels from a top view image. *RSC Advances*, *5*(21), 16042-16049.

[84] Petit, Julien, et al. "Vesicles-on-a-chip: A universal microfluidic platform for the assembly of liposomes and polymersomes." The European Physical Journal E 39.6 (2016): 59.